



UPPSALA  
UNIVERSITET

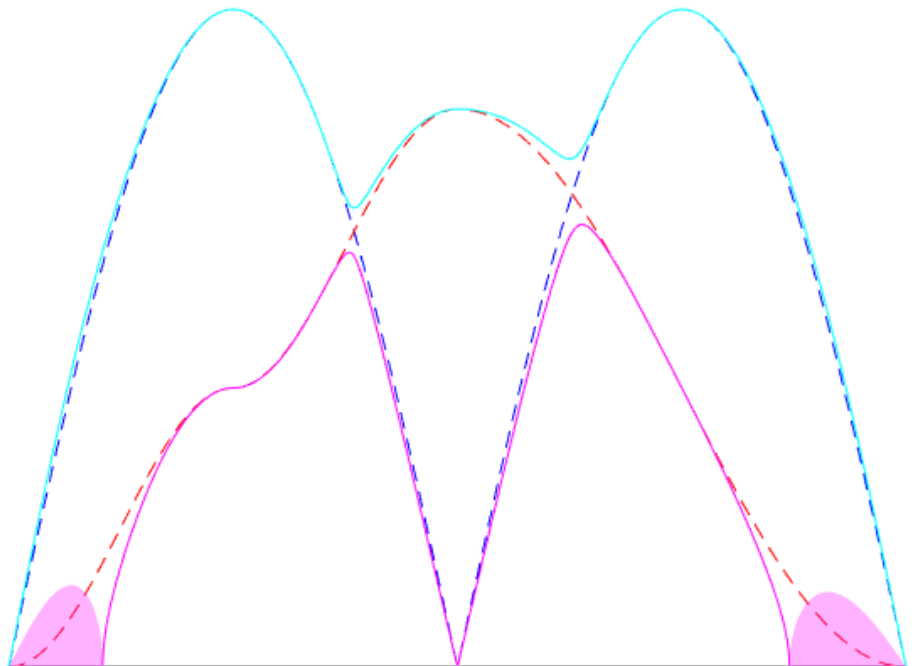
FYSAST; FYSMAS1087  
Degree Project E in Physics, 30 c  
February 2019

# Magnon-Phonon Coupling

Jacob Persson

Department of Physics and Astronomy,  
Uppsala University, Uppsala, Sweden

18 February 2019



Supervisor:	Jonas Fransson, Materials Theory*
Subject reader:	Lars Nordström, Materials Theory*
Examiner:	Andreas Korn, Astronomy and Space Physics*

\*Department of Physics and Astronomy, Uppsala University, Uppsala

Department of  
Physics and Astronomy  
Uppsala University  
P.O. Box 516  
751 20 Uppsala  
Sweden

URN: [urn:nbn:se:uu:diva-377297](https://nbn-resolving.org/urn:nbn:se:uu:diva-377297)

## **Abstract**

Recent experimental and theoretical studies have found evidence of coupled interactions between magnons and phonons. The aim of this study is to construct a model of coupled magnons and phonons, as well as analysing their frequency spectrum. The model is derived by quantizing spin and lattice degrees of freedom, and the frequency spectrum is derived by solving the equations of motion. We found that both the strength and the composition of the coupled interactions affect the frequencies of magnons and phonons, with emphasis on the magnons. Their frequencies are imaginary close to the center of the Brillouin zone, which opens questions for future research.

## Acknowledgements

Foremost, I would like to thank my supervisor *Jonas Fransson* for his invaluable guidance and expertise.

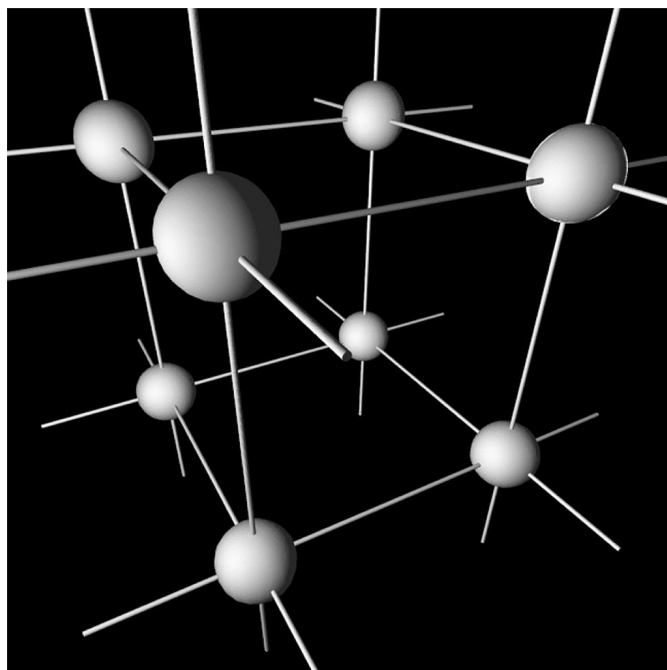
I would also like to thank my subject reader *Lars Nordström* for his feedback.

Finally, I am grateful to my family for their support.

# Popular Science Summary [Swedish]

## Atomernas Främmande Värld

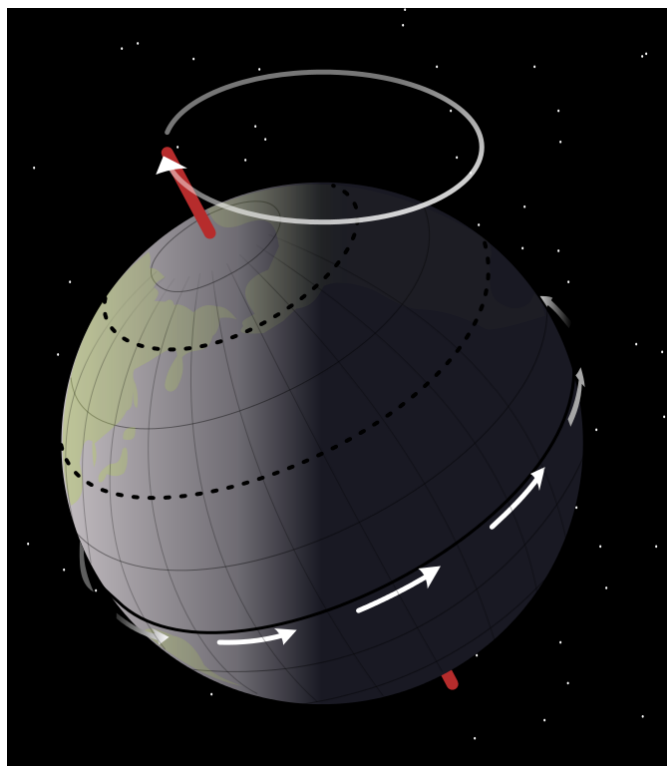
Atomer finns nästan överallt: i marken du går på, i luften du andas, i maten du äter, i maten du inte äter och i all annan materia som du kan se och ta på. Atomerna är mycket små men tillsammans kan de bilda stora objekt. Vissa material innehåller atomer av olika slag, ordnade på olika sätt. Det finns också material som bara innehåller en typ av atomer, exempelvis koppar.



Bilden visar atomer i ett kubiskt mönster [1].

Föreställ dig en kopparplåt, där atomerna är ordnade i ett kubiskt mönster och där alla atomer är kopparatomer. Kopparatomer vill gärna hålla ett lagom avstånd sinsemellan, varken för nära eller för långt ifrån varandra. Om en atom flyttar lite på sig kommer alla dess grannatomer att flytta lite på sig åt samma håll, eftersom de strävar efter att hålla samma avstånd till varandra. Detta medför att närliggande atomer till grannarna också flyttar på sig och så vidare. En atom som flyttar på sig leder alltså till en våg av förflyttningar som går genom alla andra atomer i kopparplåten. En sådan våg av förflyttning kallas för en *fonon*. Men det slutar inte här.

Atomerna förflyttar sig inte bara fram och tillbaka i vågor i kopparplåten. De snurrar också runt sin egen axel på ett liknande sätt som jorden roterar runt jordaxeln. I atomernas värld kallas denna rotation för *spinn*: de spinner runt sin egen axel så att säga. Spinnets är inte alltid i samma riktning, det vinglar lite, vilken närmast liknas vid jordaxeln som vinglar fram och tillbaka i en cirkelrörelse.



Bilden visar hur jordaxeln vinglar. Atomers spinn vinglar på ett liknande sätt. I båda fallen kallas fenomenet precession. [2]

Inte nog med att atomerna vill hålla samma avstånd till varandra, de vill dessutom spinna i takt med sina grannar. Det vill säga atomernas spinn strävar efter att vingla på ett liknande sätt som närliggande atomers spinn. Om en atom ändrar sitt spinn, kommer det att påverka spinnets hos närliggande atomer, vilket i sin tur kommer att påverka närliggande atomers spinn och så vidare. En atom som ändrar sitt spinn leder alltså till en spinnvåg som går genom alla atomer i kopparplåten. En sådan spinnvåg kallas för en *magnon*.

Nu börjar det intressanta. Hur nära två atomer befinner sig varandra påverkar också deras spinn. Dessutom, atomers spinn påverkar hur nära de vill vara sina grannar. Detta får konsekvenser för magnonerna och fononerna. När en atom närmar sig en annan atom leder det till att den andra atomen ändrar sitt spinn. Detta

leder till att grannarna till den andra atomen också ändrar sina spinn, eftersom de vill spinna i takt. Alltså, en förflyttning av en kopparatom påverkar spinnvågorna i kopparplåten. På ett liknande sett kan en atoms spinn påverka vågorna av förflyttning som går genom kopparplåten. Vi kallar detta för att magnonerna och fononerna är *kopplade*.

I den här studien har jag skapat en modell som beskriver kopplade magnoner och fononer. Modellen visar alltså hur atomernas spinn- och förflyttningsvågor påverkar varandra. Jag har också undersökt hur snabba och starka vågorna är. Syftet med studien är helt enkelt att bättre förstå atomernas främmande värld. En av mina slutsatser är att magnonerna är känsligare än fononerna. Det är lättare för en fonon att ändra på en magnon än tvärtom, det vill säga det är lättare för en förflyttningsvåg att ändra på en spinnvåg än tvärtom. En annan slutsats är att såväl kopplingens styrka mellan magnonerna och fononerna som sättet dessa är kopplade på, påverkar deras fart och styrka. Ytterligare en slutsats är att långsamma magnoner beter sig märkligt — de verkar inte ha en bestämd styrka. Min studie har inte lyckats förklara varför det är så. Förhoppningsvis kan framtida studier göra det.

# Contents

<b>1</b>	<b>Introduction</b>	<b>1</b>
<b>2</b>	<b>Model</b>	<b>2</b>
2.1	Free Phonons . . . . .	2
2.2	Free Magnons . . . . .	3
2.3	Coupled Hamiltonian . . . . .	5
<b>3</b>	<b>Frequency Spectrum</b>	<b>10</b>
3.1	Equations of Motion & Green's Function . . . . .	10
3.2	Analytical Solution . . . . .	11
3.3	Numerical Examples . . . . .	14
<b>4</b>	<b>Conclusions</b>	<b>24</b>
	<b>References</b>	<b>25</b>
<b>A</b>	<b>Derivations</b>	<b>27</b>
A.1	Heisenberg Hamiltonian . . . . .	27
A.2	Dzyaloshinskii-Moriya Hamiltonian . . . . .	28
A.3	Scalar Contribution . . . . .	30
A.4	Vector Contribution . . . . .	31
A.5	Coupled Hamiltonian . . . . .	33
A.6	Green's Functions . . . . .	35
A.7	Coupled Phonons . . . . .	37
A.8	Coupled Magnons . . . . .	39
<b>B</b>	<b>Numerical Script</b>	<b>44</b>

# 1. Introduction

Ions in solid materials interact with each other. The most relevant interactions occur between nearest neighbouring ions and are mediated by the underlying electronic structure. Although these interactions are local, they give rise to waves that propagate through the material. The quantized modes of these waves are called *phonons*. In many solid materials, phonons can be approximated by harmonic oscillators. Another property of ions is spin. Similarly to the translational interactions, there are spin-spin interactions between ions that give rise to spin-waves. The quantized modes of these waves are called *magnons* and they can also be approximated by harmonic oscillators. At least in homogeneous magnetic materials with a very large ion-magnon ratio and with small fluctuations in the spin. [3]

There are also *coupled* interactions between magnons and phonons. Evidence of this is found in body-centered cubic iron [4, 5] and in Europium Oxide [6]. Additionally, a recently published theoretical paper derives, from first principles, a framework for the dynamics of coupled magnetizations and lattice degrees of freedom [7]. To gain more insight, this study aims to develop a model of coupled magnons and phonons by quantizing the magnetization and lattice degrees of freedom. Further, the frequency spectrum of the developed model should be investigated. This theoretical study might lead to a better understanding of experimental results concerning the frequencies of magnons and phonons in solid materials.

Here, it is assumed that the material is a solid with crystal structure, that is, it can be represented by a lattice. Further assumptions and approximations for the development of the model are as follows: localized electrons at the same positions in different unit cells, localized spin-moments, one spin at each lattice site, same spin-spin interaction for each unit cell and the spin-spin interaction tensor is neglected. The coupled interactions between magnons and phonons are evaluated in the static limit, assumed to be equal for each unit cell and the symmetric tensor contribution of the coupled interactions between magnons and phonons is neglected. For the derivation of the frequency spectrum, it is assumed that the system is in thermodynamic equilibrium. Numerical calculations are made with a specific choice of parameters described in section 3.3. Moreover, the word *ion* does not necessarily imply a charged system in this thesis: atoms are considered special cases of ions. Vectors are written in bold text and natural units are used throughout the thesis: the speed of light, the reduced Planck constant and the Boltzmann constant are all dimensionless and equal to one.

## 2. Model

### 2.1. Free Phonons

Phonons are quantized vibrational modes of ions. Free phonons can be approximated by harmonic oscillators:

$$H_0 = \sum_{\mathbf{k}, \lambda} \omega_{\mathbf{k}, \lambda} \left( a_{\mathbf{k}, \lambda}^\dagger a_{\mathbf{k}, \lambda} + \frac{1}{2} \right), \quad (2.1)$$

where  $\omega_{\mathbf{k}, \lambda}$  is the frequency of a phonon with crystal momentum  $\mathbf{k}$  and mode number  $\lambda$ . Let  $\mathbf{a} = (a_x, a_y, a_z)$  denote the lattice constant,  $m$  the mass of each ion and  $K_\lambda$  the force constant. Then, the phonon frequency is

$$\omega_{\mathbf{k}, \lambda} = \sqrt{\frac{4K_\lambda}{m} \sin^2 \left( \frac{\mathbf{k} \cdot \mathbf{a}}{2} \right)}. \quad (2.2)$$

We can note that  $\omega_{-\mathbf{k}, \lambda} = \omega_{\mathbf{k}, \lambda}$ . The phonon creation  $a_{\mathbf{k}, \lambda}^\dagger$  and destruction  $a_{\mathbf{k}, \lambda}$  operators obey bosonic commutation relations:

$$\begin{aligned} [a_{\mathbf{k}, \lambda}, a_{\mathbf{k}', \lambda'}^\dagger] &= a_{\mathbf{k}, \lambda} a_{\mathbf{k}', \lambda'}^\dagger - a_{\mathbf{k}', \lambda'}^\dagger a_{\mathbf{k}, \lambda} = \delta_{\mathbf{k}, \mathbf{k}'} \delta_{\lambda, \lambda'}, \\ [a_{\mathbf{k}, \lambda}, a_{\mathbf{k}', \lambda'}] &= 0, \quad [a_{\mathbf{k}, \lambda}^\dagger, a_{\mathbf{k}', \lambda'}^\dagger] = 0. \end{aligned} \quad (2.3)$$

Further, the phonon destruction operator acting on the state of no phonons is equal to zero:  $a_{\mathbf{k}, \lambda} |0\rangle_p = 0$ . [3]

The ions also interact with surrounding electrons, causing an electron-phonon interaction. Here, I assume that the electrons are localized: they cannot recoil, and their kinetic energy is neglected. Thus, the Hamiltonian for the electron-phonon interaction is

$$H_{ep} = \sum_{j, \mathbf{k}, \lambda} \left( a_{\mathbf{k}, \lambda} + a_{-\mathbf{k}, \lambda}^\dagger \right) e^{i\mathbf{k} \cdot \mathbf{r}_j} F_{\mathbf{k}, \lambda}(\mathbf{r}_j), \quad (2.4)$$

where  $F_{\mathbf{k}, \lambda}(\mathbf{r}_j)$  is the effective matrix element of the electron-phonon interaction at the position of electron  $j$   $\mathbf{r}_j$ . The Hamiltonian of phonons and electrons if no other interactions are present is  $H_p = H_0 + H_{ep}$ . [3]

## 2.2. Free Magnons

A homogeneous magnetic system with the same spin on each site can be described by the Heisenberg model. I will only consider nearest neighbour interactions. However, the strength of the spin-spin interactions in one direction might be different than in the other two directions. Such a system can be described by the anisotropic Heisenberg Hamiltonian:

$$H_{he} = -J_{\parallel} \sum_{j,\delta} S_j^{(z)} S_{j+\delta}^{(z)} - J_{\perp} \sum_{j,\delta} S_j^{(-)} S_{j+\delta}^{(+)}, \quad (2.5)$$

where  $J_{\parallel}$  denotes the coupling constant in the  $z$ -direction and  $J_{\perp}$  denotes the coupling constant in the  $xy$ -plane. The spin vector at site  $j$  is denoted by  $\mathbf{S}_j = (S_j^{(x)}, S_j^{(y)}, S_j^{(z)})$ ; the first, second and third components correspond to its spin in the  $x$ -,  $y$ - and  $z$ -directions, respectively.  $S_j^{(+)} = S_j^{(x)} + iS_j^{(y)}$  and  $S_j^{(-)} = S_j^{(x)} - iS_j^{(y)}$  are the spin raising and lowering operators, respectively. The subscript notation  $j+\delta$  means nearest neighbour  $\delta$  of site  $j$ , and  $\sum_{\delta}$  is the summation over all nearest neighbours. [3]

To rewrite the model in terms of bosonic magnon operators, I start by using the Holstein-Primakoff transformation [8]:

$$\begin{aligned} S_j^+ &= \sqrt{2S} \sqrt{1 - \frac{b_j^\dagger b_j}{2S}} b_j, \\ S_j^- &= \sqrt{2S} b_j^\dagger \sqrt{1 - \frac{b_j^\dagger b_j}{2S}}, \\ S_j^z &= S - b_j^\dagger b_j, \end{aligned} \quad (2.6)$$

where  $S$  denotes spin, which is the same for all spin sites:  $S = |\mathbf{S}_j|$ . The magnon creation  $b_j^\dagger$  and destruction  $b_j$  operators obey bosonic commutation relations:

$$\begin{aligned} [b_j, b_l^\dagger] &= \delta_{j,l}, \\ [b_j, b_l] &= 0, \\ [b_j^\dagger, b_l^\dagger] &= 0. \end{aligned} \quad (2.7)$$

Additionally, the destruction operator acting on the state of no magnons is equal to zero:  $b_j|0\rangle_m = 0$ . Note that  $\delta_{j,l}$  is the Kronecker delta of  $j$  and  $l$ :

$$\delta_{j,l} = \begin{cases} 1 & \text{if } j = l, \\ 0 & \text{if } j \neq l. \end{cases} \quad (2.8)$$

Later, in this thesis, the  $\delta$ -symbol will have a third meaning, namely the Dirac delta function:

$$\int_{\mathbb{R}^n} f(\mathbf{x})\delta(\mathbf{x})d\mathbf{x} = f(\mathbf{0}), \quad (2.9)$$

where  $n \in \mathbb{Z}^+$  and  $f$  is a compactly supported continuous function [9]. To clarify, the  $\delta$  notations have three different meanings depending on their context:

- Nearest neighbour if  $\delta$  is in the subscript,
- Kronecker delta if  $\delta_{jl}$  has two subscripts  $j$  and  $l$ ,
- Dirac delta function if  $\delta(\mathbf{x})$  is a function of an  $n$ -dimensional real vector  $\mathbf{x}$ .

By assuming that the fluctuations from the ground state are small:  $b_j^\dagger b_j \ll S$ , for all lattice sites  $j$ , the Holstein-Primakoff transformation (2.6) becomes

$$\begin{aligned} S_j^+ &= \sqrt{2S}b_j, \\ S_j^- &= \sqrt{2S}b_j^\dagger, \\ S_j^z &= S - b_j^\dagger b_j. \end{aligned} \quad (2.10)$$

With the aim of expressing the model in reciprocal space, the magnon operators are Fourier transformed:

$$\begin{aligned} b_j &= \frac{1}{\sqrt{N}} \sum_{\mathbf{k}} e^{-i\mathbf{k} \cdot \mathbf{R}_j} b_{\mathbf{k}}, \\ b_j^\dagger &= \frac{1}{\sqrt{N}} \sum_{\mathbf{k}} e^{i\mathbf{k} \cdot \mathbf{R}_j} b_{\mathbf{k}}^\dagger, \end{aligned} \quad (2.11)$$

where  $N$  is the number of lattice sites and  $\mathbf{R}_j$  is the position of site  $j$ . In appendix A.1, it is shown that the anisotropic Heisenberg Hamiltonian (2.5) can be rewritten in terms of magnon operators in reciprocal space:

$$H_{he} = -J_{\parallel} N S^2 Z + 2S \sum_{\mathbf{k}} (J_{\parallel} Z - J_{\perp} C_{\mathbf{k}}) b_{\mathbf{k}}^\dagger b_{\mathbf{k}} - \frac{J_{\parallel}}{N} \sum_{\mathbf{k}, \mathbf{k}', \mathbf{k}''} C_{\mathbf{k}-\mathbf{k}'} b_{\mathbf{k}}^\dagger b_{\mathbf{k}'} b_{\mathbf{k}''}^\dagger b_{\mathbf{k}-\mathbf{k}'+\mathbf{k}''}, \quad (2.12)$$

where  $Z$  is the number of nearest neighbours. The structure constant is defined by  $C_{\mathbf{k}} = \sum_{\delta} e^{-i\mathbf{k} \cdot \mathbf{R}_{\delta}}$ , where  $\mathbf{R}_{\delta}$  is the vector from any lattice site to its nearest neighbour site  $\delta$ .

The ions are also influenced by spin-orbit coupling. This coupling induces an antisymmetric exchange interaction between neighbouring ions, called the anisotropic Dzyaloshinskii-Moriya interaction:

$$H_{DM} = \sum_{j, \delta} \mathbf{D}_{j, j+\delta} \cdot (\mathbf{S}_j \times \mathbf{S}_{j+\delta}), \quad (2.13)$$

where  $\mathbf{D}_{j,j+\delta} = (D_{j,j+\delta}^{(x)}, D_{j,j+\delta}^{(y)}, D_{j,j+\delta}^{(z)})$  is the Dzyaloshinskii-Moriya coupling vector between site  $j$  and nearest neighbours  $\delta$  of  $j$ . The first, second and third components correspond to the Dzyaloshinskii-Moriya coupling in the  $x$ -,  $y$ - and  $z$ -directions, respectively. [10]

Under the assumption that the Dzyaloshinskii-Moriya interaction is equal for all unit cells, I can make the following definitions:  $\mathbf{D}_{\mathbf{k}} = \frac{1}{Z} \sum_{\delta} \mathbf{D}_{j,j+\delta} e^{-i\mathbf{k} \cdot \mathbf{R}_{\delta}}$  and  $\mathbf{D}_0 = \frac{1}{Z} \sum_{\delta} \mathbf{D}_{j,j+\delta}$ . Now, as is shown in appendix A.2, the Hamiltonian in equation (2.13) can be written in terms of magnon operators in reciprocal space:

$$\begin{aligned} H_{DM} = & -\sqrt{2S^3N}Z \left[ \left( iD_0^{(x)} + D_0^{(y)} \right) b_0 + \left( -iD_0^{(x)} + D_0^{(y)} \right) b_0^{\dagger} \right] - \sqrt{2}iSZ \sum_{\mathbf{k}} D_{\mathbf{k}}^{(z)} b_{\mathbf{k}}^{\dagger} b_{\mathbf{k}} \\ & + \sqrt{\frac{S}{2N}}Z \sum_{\mathbf{k}, \mathbf{k}'} \left[ \left( iD_{-\mathbf{k}}^{(x)} + D_{-\mathbf{k}}^{(y)} \right) b_{\mathbf{k}} b_{\mathbf{k}'}^{\dagger} b_{-\mathbf{k}+\mathbf{k}'} - \left( iD_{\mathbf{k}-\mathbf{k}'}^{(x)} + D_{\mathbf{k}-\mathbf{k}'}^{(y)} \right) b_{\mathbf{k}}^{\dagger} b_{\mathbf{k}'} b_{\mathbf{k}-\mathbf{k}'} \right. \\ & \left. + \left( -iD_{\mathbf{k}}^{(x)} + D_{\mathbf{k}}^{(y)} \right) b_{\mathbf{k}}^{\dagger} b_{\mathbf{k}'}^{\dagger} b_{\mathbf{k}+\mathbf{k}'} - \left( -iD_{\mathbf{k}-\mathbf{k}'}^{(x)} + D_{\mathbf{k}-\mathbf{k}'}^{(y)} \right) b_{\mathbf{k}}^{\dagger} b_{\mathbf{k}'} b_{-\mathbf{k}+\mathbf{k}'}^{\dagger} \right], \end{aligned} \quad (2.14)$$

where  $\mathbf{0}$  denotes the vector with all elements equal to zero.

### 2.3. Coupled Hamiltonian

The effective model for coupled magnetization and lattice dynamics is taken from reference [7] where it is defined as

$$H_{MQ} = -\frac{1}{2} \sum_{i,j} \left[ \mathbf{Q}_j \cdot \left( T_{i,j}^{(cc)} \cdot \mathbf{Q}_j + T_{i,j}^{(cs)} \cdot \mathbf{M}_j \right) + \mathbf{M}_i \cdot \left( T_{i,j}^{(sc)} \cdot \mathbf{Q}_j + T_{i,j}^{(ss)} \cdot \mathbf{M}_j \right) \right]. \quad (2.15)$$

The lattice displacement vector of ion  $j$  is defined by  $\mathbf{Q}_j = \mathbf{R}_j - \mathbf{R}_j^{(0)}$ , where  $\mathbf{R}_j^{(0)}$  is the equilibrium position of ion  $j$ . The localized spin moment of ion  $j$  is denoted by  $\mathbf{M}_j$ . The interactions tensor  $T_{i,j}^{(cc)}$  defines the electron-phonon interaction between ions  $i$  and  $j$ , which I reviewed in section 2.1.  $T_{i,j}^{(ss)}$  defines the spin-spin interaction. The scalar and vector contributions to the spin-spin interaction are covered in section 2.2. The tensor contribution to the spin-spin interaction, however, is not considered in this thesis.  $T_{i,j}^{(cs)}$  and  $T_{i,j}^{(sc)}$  are the lattice-spin and spin-lattice interaction tensors, respectively. These interactions will be examined in this section.

In the static limit is  $T_{i,j}^{(sc)}$  related to  $T_{i,j}^{(cs)}$  by the transpose:  $\{T_{ij}^{(sc)}\}^{\mu\nu} = \{T_{ij}^{(cs)}\}^{\nu\mu}$ , where  $\mu$  and  $\nu$  are explicit Cartesian tensor components. Thus, the

spin-lattice part of the Hamiltonian can be rewritten as

$$\begin{aligned}
H_{MQ}^{sl} &= -\frac{1}{2} \sum_{i,j} \left( \mathbf{Q}_i \cdot T_{i,j}^{(cs)} \cdot \mathbf{M}_j + \mathbf{M}_i \cdot T_{i,j}^{(sc)} \cdot \mathbf{Q}_j \right) \\
&= -\sum_{i,j} \left( T_{i,j} \mathbf{Q}_j \cdot \mathbf{M}_j + \mathbf{T}_{i,j} \cdot \mathbf{Q}_i \times \mathbf{M}_j + \mathbf{Q}_i \cdot T_{i,j}^{(2)} \cdot \mathbf{M}_j \right),
\end{aligned} \tag{2.16}$$

where  $T_{i,j}$ ,  $\mathbf{T}_{i,j} = (T_{i,j}^{(x)}, T_{i,j}^{(y)}, T_{i,j}^{(z)})$  and  $T_{i,j}^{(2)}$  are the scalar, vector and symmetric second-rank tensor decompositions of  $T_{i,j}^{(cs)}$ , respectively. I will only consider the scalar and vector contributions to the lattice-spin interactions in the following calculations. [7]

The aim is to rewrite the Hamiltonian from equation (2.16) in terms of magnon and phonon operators in reciprocal space. Hence, the lattice displacement vector is evaluated in reciprocal space through the following expansion:

$$\mathbf{Q}_j = i \sum_{\mathbf{k},\lambda} \sqrt{\frac{1}{2mN\omega_{\mathbf{k},\lambda}}} \boldsymbol{\xi}_{\mathbf{k},\lambda} \left( a_{\mathbf{k},\lambda} + a_{-\mathbf{k},\lambda}^\dagger \right) e^{i\mathbf{k} \cdot \mathbf{R}_j}. \tag{2.17}$$

The phonon polarization vector  $\boldsymbol{\xi}_{\mathbf{k},\lambda} = (\xi_{\mathbf{k},\lambda}^{(x)}, \xi_{\mathbf{k},\lambda}^{(y)}, \xi_{\mathbf{k},\lambda}^{(z)})$ , is antisymmetric with respect to the crystal momentum of phonons:  $\boldsymbol{\xi}_{\mathbf{k},\lambda} = -\boldsymbol{\xi}_{-\mathbf{k},\lambda}$ , and it is assumed to approach zero faster than the square root of the free phonon frequency when the crystal momentum approaches zero:

$$\lim_{\mathbf{k} \rightarrow \mathbf{0}} \frac{\boldsymbol{\xi}_{\mathbf{k},\lambda}}{\sqrt{\omega_{\mathbf{k},\lambda}}} = \mathbf{0}. \tag{2.18}$$

The first, second and third components of the polarization vector are the phonon polarizations in the  $x$ -,  $y$ - and  $z$ -directions, respectively. The localized spin moment relates to the spin vector through the Gyromagnetic ratio:  $\mathbf{M}_j = \gamma \mathbf{S}_j$  [11].

Now, I can express the scalar decomposition of the spin-lattice Hamiltonian (2.16) in terms of magnon and phonon operators in reciprocal space:

$$\begin{aligned}
H_{SQ}^{(S)} &= \frac{\gamma Z}{\sqrt{2m}} \left( \sum_{\mathbf{k},\lambda} \frac{T_{\mathbf{k}}}{\sqrt{\omega_{\mathbf{k},\lambda}}} \left( a_{\mathbf{k},\lambda} + a_{-\mathbf{k},\lambda}^\dagger \right) \left\{ \sqrt{\frac{S}{2}} \left[ -i \xi_{\mathbf{k},\lambda}^{(x)} (b_{\mathbf{k}} + b_{-\mathbf{k}}^\dagger) \right. \right. \right. \\
&\quad \left. \left. \left. + \xi_{\mathbf{k},\lambda}^{(y)} (b_{\mathbf{k}} - b_{-\mathbf{k}}^\dagger) \right] + \frac{i}{\sqrt{N}} \sum_{\mathbf{k}'} \xi_{\mathbf{k},\lambda}^{(z)} b_{\mathbf{k}'}^\dagger b_{\mathbf{k}+\mathbf{k}'} \right\} \right),
\end{aligned} \tag{2.19}$$

where it is assumed that the scalar decomposition of the lattice-spin interaction tensor is equal for all unit cells:  $T_{\mathbf{k}} = \frac{1}{Z} \sum_{\delta} T_{j,j+\delta} e^{-i\mathbf{k} \cdot \mathbf{R}_\delta}$  and  $T_0 = \frac{1}{Z} \sum_{\delta} T_{j,j+\delta}$ . The derivation can be found in appendix A.3.

I can also express the vector decomposition of the spin-lattice Hamiltonian (2.16) in terms of magnon and phonon operators in reciprocal space:

$$\begin{aligned}
H_{SQ}^{(V)} = & \frac{\gamma Z}{\sqrt{2m}} \sum_{\lambda, \mathbf{k}} \frac{1}{\sqrt{\omega_{\mathbf{k}, \lambda}}} \left( a_{\mathbf{k}, \lambda} + a_{-\mathbf{k}, \lambda}^\dagger \right) \\
& \times \left\{ \sqrt{\frac{S}{2}} \left[ T_{\mathbf{k}}^{(x)} \xi_{\mathbf{k}, \lambda}^{(z)} \left( b_{\mathbf{k}} - b_{-\mathbf{k}}^\dagger \right) - iT_{\mathbf{k}}^{(y)} \xi_{\mathbf{k}, \lambda}^{(z)} \left( b_{\mathbf{k}} + b_{-\mathbf{k}}^\dagger \right) \right. \right. \\
& \quad \left. \left. - T_{\mathbf{k}}^{(z)} \xi_{\mathbf{k}, \lambda}^{(x)} \left( b_{\mathbf{k}} - b_{-\mathbf{k}}^\dagger \right) + iT_{\mathbf{k}}^{(z)} \xi_{\mathbf{k}, \lambda}^{(y)} \left( b_{\mathbf{k}} + b_{-\mathbf{k}}^\dagger \right) \right] \right. \\
& \quad \left. + \frac{i}{\sqrt{N}} \sum_{\mathbf{k}'} \left( T_{\mathbf{k}}^{(x)} \xi_{\mathbf{k}, \lambda}^{(y)} b_{\mathbf{k}'}^\dagger b_{\mathbf{k}+\mathbf{k}'} - T_{\mathbf{k}}^{(y)} \xi_{\mathbf{k}, \lambda}^{(x)} b_{\mathbf{k}'}^\dagger b_{\mathbf{k}+\mathbf{k}'} \right) \right\}, \tag{2.20}
\end{aligned}$$

where it is assumed that the vector decomposition of the lattice-spin interaction tensor is equal for all unit cells:  $\mathbf{T}_{\mathbf{k}} = \frac{1}{Z} \sum_{\delta} \mathbf{T}_{j, j+\delta} e^{-i\mathbf{k} \cdot \mathbf{R}_{\delta}}$  and  $\mathbf{T}_0 = \frac{1}{Z} \sum_{\delta} \mathbf{T}_{j, j+\delta}$ .  $T_{i,j}^{(x)}$ ,  $T_{i,j}^{(y)}$ ,  $T_{i,j}^{(z)}$  are the first, second and third components of the vector decomposition of the lattice-spin interaction tensor. This derivation can be found in appendix A.4.

The total Hamiltonian of coupled magnons and phonons is

$$\begin{aligned}
H_T = & H_p + H_{he} + H_{DM} + H_{SQ}^{(S)} + H_{SQ}^{(V)} \\
= & -J_{\parallel} N S^2 Z + \sum_{\mathbf{k}, \lambda} \frac{\omega_{\mathbf{k}, \lambda}}{2} + \sum_{\mathbf{k}, \lambda} F'_{\mathbf{k}, \lambda} \left( a_{\mathbf{k}, \lambda} + a_{-\mathbf{k}, \lambda}^\dagger \right) + \sum_{\mathbf{k}} \left( G_{\mathbf{k}} b_{\mathbf{k}} + G_{-\mathbf{k}}^* b_{-\mathbf{k}}^\dagger \right) \\
& + \sum_{\mathbf{k}, \lambda} \omega_{\mathbf{k}, \lambda} a_{\mathbf{k}, \lambda}^\dagger a_{\mathbf{k}, \lambda} + \sum_{\mathbf{k}} \epsilon_{\mathbf{k}} b_{\mathbf{k}}^\dagger b_{\mathbf{k}} + \sum_{\mathbf{k}, \lambda} \left( a_{\mathbf{k}, \lambda} + a_{-\mathbf{k}, \lambda}^\dagger \right) \left( E_{\mathbf{k}, \lambda} b_{\mathbf{k}} + E_{-\mathbf{k}, \lambda}^* b_{-\mathbf{k}}^\dagger \right) \\
& + \sqrt{\frac{S}{2N}} Z \sum_{\mathbf{k}, \mathbf{k}'} \left[ \left( iD_{-\mathbf{k}}^{(x)} + D_{-\mathbf{k}}^{(y)} \right) b_{\mathbf{k}} b_{\mathbf{k}'}^\dagger b_{\mathbf{k}-\mathbf{k}'} - \left( iD_{\mathbf{k}-\mathbf{k}'}^{(x)} + D_{\mathbf{k}-\mathbf{k}'}^{(y)} \right) b_{\mathbf{k}}^\dagger b_{\mathbf{k}'} b_{\mathbf{k}-\mathbf{k}'} \right. \\
& \quad \left. + \left( -iD_{\mathbf{k}}^{(x)} + D_{\mathbf{k}}^{(y)} \right) b_{\mathbf{k}}^\dagger b_{\mathbf{k}'}^\dagger b_{\mathbf{k}+\mathbf{k}'} - \left( -iD_{\mathbf{k}-\mathbf{k}'}^{(x)} + D_{\mathbf{k}-\mathbf{k}'}^{(y)} \right) b_{\mathbf{k}}^\dagger b_{\mathbf{k}'} b_{-\mathbf{k}+\mathbf{k}'}^\dagger \right] \\
& + i \frac{\gamma Z}{\sqrt{2mN}} \sum_{\mathbf{k}, \mathbf{k}', \lambda} \frac{1}{\sqrt{\omega_{\mathbf{k}, \lambda}}} \left( a_{\mathbf{k}, \lambda} + a_{-\mathbf{k}, \lambda}^\dagger \right) \left( T_{\mathbf{k}} \xi_{\mathbf{k}, \lambda}^{(z)} + T_{\mathbf{k}}^{(x)} \xi_{\mathbf{k}, \lambda}^{(y)} - T_{\mathbf{k}}^{(y)} \xi_{\mathbf{k}, \lambda}^{(x)} \right) b_{\mathbf{k}'}^\dagger b_{\mathbf{k}+\mathbf{k}'} \\
& - \frac{J_{\parallel}}{N} \sum_{\mathbf{k}, \mathbf{k}', \mathbf{k}''} C_{\mathbf{k}-\mathbf{k}'} b_{\mathbf{k}}^\dagger b_{\mathbf{k}'} b_{\mathbf{k}''}^\dagger b_{\mathbf{k}-\mathbf{k}'+\mathbf{k}''} \tag{2.21}
\end{aligned}$$

with

$$\epsilon_{\mathbf{k}} = 2SJ_{\parallel} Z - 2SJ_{\perp} C_{\mathbf{k}} - \sqrt{2}iSZD_{\mathbf{k}}^{(z)}, \tag{2.22}$$

$$F'_{\mathbf{k}, \lambda} = \sum_j F_{\mathbf{k}, \lambda}(\mathbf{r}_j) e^{i\mathbf{k} \cdot \mathbf{r}_j}, \tag{2.23}$$

$$G_{\mathbf{k}} = -\sqrt{2NS^3Z} \left( iD_0^{(x)} + D_0^{(y)} \right) \delta_{\mathbf{k},\mathbf{0}} \quad (2.24)$$

and

$$E_{\mathbf{k},\lambda} = \frac{\gamma\sqrt{SZ}}{2\sqrt{m\omega_{\mathbf{k},\lambda}}} \left( T_{\mathbf{k}} \left[ -i\xi_{\mathbf{k},\lambda}^{(x)} + \xi_{\mathbf{k},\lambda}^{(y)} \right] + \left[ T_{\mathbf{k}}^{(x)} \xi_{\mathbf{k},\lambda}^{(z)} - iT_{\mathbf{k}}^{(y)} \xi_{\mathbf{k},\lambda}^{(z)} - T_{\mathbf{k}}^{(z)} \xi_{\mathbf{k},\lambda}^{(x)} + iT_{\mathbf{k}}^{(z)} \xi_{\mathbf{k},\lambda}^{(y)} \right] \right). \quad (2.25)$$

Again, this Hamiltonian is valid given a material with crystal structure with one spin at each lattice site. It is also assumed that all interactions are between nearest neighbours and of equal strength for all unit cells. The electrons and the ionic spin moments are assumed to be localized, where the localized electrons are assumed to be at the same positions in all different unit cells. The spin fluctuations are assumed to be small and the tensor contribution of the spin-spin interaction is neglected. Moreover, the coupled interactions between magnons and phonons are considered in the static limit and their symmetric tensor decomposition is neglected.

The Hamiltonian can be simplified by making two more assumptions. Firstly, it is assumed that the square root of the number of lattice sites is much larger than the number of magnons:  $\sqrt{N} \gg \sum_{\mathbf{k}} b_{\mathbf{k}}^\dagger b_{\mathbf{k}}$ . Secondly, it is assumed that all localized electrons are at the same positions within different unit cell, implying that  $\sum_j F_{\mathbf{k}}(\mathbf{r}_j) e^{i\mathbf{k}\cdot\mathbf{r}_j} = \sum_j F_{-\mathbf{k}}^*(\mathbf{r}_j) e^{i\mathbf{k}\cdot\mathbf{r}_j}$  [3]. The final Hamiltonian is

$$H = \sum_{\mathbf{k},\lambda} \omega_{\mathbf{k},\lambda} \alpha_{\mathbf{k},\lambda}^\dagger \alpha_{\mathbf{k},\lambda} + \epsilon_{\mathbf{k},\lambda} \beta_{\mathbf{k},\lambda}^\dagger \beta_{\mathbf{k},\lambda} + \left( \alpha_{\mathbf{k},\lambda} + \alpha_{-\mathbf{k},\lambda}^\dagger \right) \left( E_{\mathbf{k},\lambda} \beta_{\mathbf{k},\lambda} + E_{-\mathbf{k},\lambda}^* \beta_{-\mathbf{k},\lambda}^\dagger \right) + K_{\mathbf{k},\lambda}, \quad (2.26)$$

with

$$\alpha_{\mathbf{k},\lambda} = a_{\mathbf{k},\lambda} + I_{\mathbf{k},\lambda} \quad \text{and} \quad \beta_{\mathbf{k},\lambda} = b_{\mathbf{k}} + J_{\mathbf{k},\lambda}, \quad (2.27)$$

where

$$I_{\mathbf{k},\lambda} = \begin{cases} 0 & \text{if } \mathbf{k} = \mathbf{0}, \\ \frac{-F_{\mathbf{k},\lambda}^* \epsilon_{\mathbf{k},\lambda} \epsilon_{-\mathbf{k},\lambda} E_{\mathbf{k},\lambda}^*}{-\omega_{\mathbf{k},\lambda} \epsilon_{\mathbf{k},\lambda} \epsilon_{-\mathbf{k},\lambda} E_{\mathbf{k},\lambda} + 2E_{\mathbf{k},\lambda}^* |E_{\mathbf{k},\lambda}|^2 (\epsilon_{-\mathbf{k},\lambda} - \epsilon_{\mathbf{k},\lambda})} & \text{if } \mathbf{k} \neq \mathbf{0} \end{cases}, \quad (2.28)$$

$$J_{\mathbf{k},\lambda} = \begin{cases} \frac{\sqrt{2NS^3Z}}{\epsilon_{\mathbf{k}}} \left( iD_0^{(x)} - D_0^{(y)} \right) & \text{if } \mathbf{k} \rightarrow \mathbf{0}, \\ \frac{2F_{\mathbf{k},\lambda} \epsilon_{-\mathbf{k},\lambda} E_{\mathbf{k},\lambda}}{-\omega_{\mathbf{k},\lambda} \epsilon_{\mathbf{k},\lambda} \epsilon_{-\mathbf{k},\lambda} + 2E_{\mathbf{k},\lambda}^2 (\epsilon_{-\mathbf{k},\lambda} - \epsilon_{\mathbf{k},\lambda})} & \text{if } \mathbf{k} \neq \mathbf{0} \end{cases}, \quad (2.29)$$

$$K_{\mathbf{k},\lambda} = -\frac{J_{\parallel} S^2 Z}{L} + \omega_{\mathbf{k},\lambda} \left( \frac{1}{2} - |I_{\mathbf{k},\lambda}|^2 \right) - \epsilon_{\mathbf{k},\lambda} |J_{\mathbf{k},\lambda}|^2 - 2I_{\mathbf{k}} \left( E_{\mathbf{k},\lambda} J_{\mathbf{k},\lambda} + E_{-\mathbf{k},\lambda}^* J_{-\mathbf{k},\lambda}^* \right) \quad (2.30)$$

and  $\epsilon_{\mathbf{k},\lambda} = \frac{\epsilon_{\mathbf{k}}}{L}$ .  $L$  denotes the number of phonon modes:  $L = \sum_{\lambda} 1$ . The equations above are derived in appendix A.5.

We will call the new operators  $\alpha_{\mathbf{k},\lambda}$ ,  $\alpha_{\mathbf{k},\lambda}^{\dagger}$ ,  $\beta_{\mathbf{k},\lambda}$  and  $\beta_{\mathbf{k},\lambda}^{\dagger}$  the shifted phonon destruction, shifted phonon creation, shifted magnon destruction and shifted magnon creation operators, respectively. These new operators have a shifted equilibrium point but oscillates with the same frequency as the original operators. The shifted operators are bosonic:

$$\begin{aligned} & \left[ \alpha_{\mathbf{k},\lambda}, \alpha_{\mathbf{k}',\lambda'}^{\dagger} \right] = \delta_{\mathbf{k},\mathbf{k}'} \delta_{\lambda,\lambda'}, \quad \left[ \beta_{\mathbf{k},\lambda}, \beta_{\mathbf{k}',\lambda'}^{\dagger} \right] = \delta_{\mathbf{k},\mathbf{k}'} \\ \text{and} \quad & \left[ \alpha_{\mathbf{k},\lambda}, \alpha_{\mathbf{k}',\lambda'} \right] = \left[ \alpha_{\mathbf{k},\lambda}^{\dagger}, \alpha_{\mathbf{k}',\lambda'}^{\dagger} \right] = \left[ \beta_{\mathbf{k},\lambda}, \beta_{\mathbf{k}',\lambda'} \right] = \left[ \beta_{\mathbf{k},\lambda}^{\dagger}, \beta_{\mathbf{k}',\lambda'}^{\dagger} \right] = 0. \end{aligned} \quad (2.31)$$

We can note that the Hamiltonian in equation (2.26) approaches the Hamiltonian of free magnons and phonons  $H_p + H_{he} + H_{DM}$  in the limit of zero coupling,  $E_{\mathbf{k},\lambda} \rightarrow 0$ . Also, the Hamiltonian is Hermitian  $H^{\dagger} = H$ . These properties are to be expected.

With a coupling  $E_{\mathbf{k},\lambda} \neq 0$ , we can observe that there are terms that mix shifted magnon and phonon operators. The terms that mix destruction and creation operators ( $E_{-\mathbf{k},\lambda}^* \alpha_{\mathbf{k},\lambda} \beta_{-\mathbf{k},\lambda}^{\dagger}$  and  $E_{\mathbf{k},\lambda} \alpha_{-\mathbf{k},\lambda}^{\dagger} \beta_{\mathbf{k},\lambda}$ ) behave as harmonic oscillators. We know this because it is possible to introduce a new bosonic operator  $c_{\mathbf{k},\lambda}$ , such that  $E'_{\mathbf{k},\lambda} c_{\mathbf{k},\lambda}^{\dagger} c_{\mathbf{k},\lambda} = E_{-\mathbf{k},\lambda}^* \alpha_{\mathbf{k},\lambda} \beta_{-\mathbf{k},\lambda}^{\dagger} + E_{\mathbf{k},\lambda} \alpha_{-\mathbf{k},\lambda}^{\dagger} \beta_{\mathbf{k},\lambda}$ , where  $E'_{\mathbf{k},\lambda} \in \{\mathbb{R}^+, 0\}$ . However, the terms that mix two destruction or two creation operators indicate that the Hamiltonian does not behave as a harmonic oscillator. The frequency spectrum of the Hamiltonian in equation (2.26) is examined in the following chapter.

### 3. Frequency Spectrum

#### 3.1. Equations of Motion & Green's Function

Applying Heisenberg's equation of motion [11] to the new operators  $\alpha_{\mathbf{k},\lambda}$ ,  $\alpha_{\mathbf{k},\lambda}^\dagger$ ,  $\beta_{\mathbf{k},\lambda}$  and  $\beta_{\mathbf{k},\lambda}^\dagger$  yields:

$$i\partial_t \alpha_{\mathbf{k},\lambda} = [\alpha_{\mathbf{k},\lambda}, H] = \omega_{\mathbf{k},\lambda} \alpha_{\mathbf{k},\lambda} + E_{-\mathbf{k},\lambda} \beta_{-\mathbf{k},\lambda} + E_{\mathbf{k},\lambda}^* \beta_{\mathbf{k},\lambda}^\dagger, \quad (3.1)$$

$$i\partial_t \alpha_{-\mathbf{k},\lambda}^\dagger = [\alpha_{-\mathbf{k},\lambda}^\dagger, H] = -\omega_{-\mathbf{k},\lambda} \alpha_{-\mathbf{k},\lambda}^\dagger - E_{-\mathbf{k},\lambda} \beta_{-\mathbf{k},\lambda} - E_{\mathbf{k},\lambda}^* \beta_{\mathbf{k},\lambda}^\dagger, \quad (3.2)$$

$$\begin{aligned} i\partial_t \beta_{\mathbf{k},\lambda} &= [\beta_{\mathbf{k},\lambda}, H] = \sum_{\lambda'} \left( \epsilon_{\mathbf{k},\lambda'} \beta_{\mathbf{k},\lambda'} + E_{\mathbf{k},\lambda'}^* \alpha_{-\mathbf{k},\lambda'} + E_{\mathbf{k},\lambda'}^* \alpha_{\mathbf{k},\lambda'}^\dagger \right) \\ &= \epsilon_{\mathbf{k},\lambda} \beta_{\mathbf{k},\lambda} - \epsilon_{\mathbf{k},\lambda} J_{\mathbf{k},\lambda} + \sum_{\lambda'} \left( \epsilon_{\mathbf{k},\lambda'} J_{\mathbf{k},\lambda'} + E_{\mathbf{k},\lambda'}^* \alpha_{-\mathbf{k},\lambda'} + E_{\mathbf{k},\lambda'}^* \alpha_{\mathbf{k},\lambda'}^\dagger \right) \end{aligned} \quad (3.3)$$

and

$$\begin{aligned} i\partial_t \beta_{-\mathbf{k},\lambda}^\dagger &= [\beta_{-\mathbf{k},\lambda}^\dagger, H] = \sum_{\lambda'} \left( -\epsilon_{-\mathbf{k},\lambda'} \beta_{-\mathbf{k},\lambda'}^\dagger - E_{-\mathbf{k},\lambda'} \alpha_{-\mathbf{k},\lambda'} - E_{-\mathbf{k},\lambda'} \alpha_{\mathbf{k},\lambda'}^\dagger \right) \\ &= -\epsilon_{-\mathbf{k},\lambda} \beta_{-\mathbf{k},\lambda}^\dagger + \epsilon_{-\mathbf{k},\lambda} J_{-\mathbf{k},\lambda}^* - \sum_{\lambda'} \left( \epsilon_{-\mathbf{k},\lambda'} J_{-\mathbf{k},\lambda'}^* + E_{-\mathbf{k},\lambda'} \alpha_{-\mathbf{k},\lambda'} + E_{-\mathbf{k},\lambda'} \alpha_{\mathbf{k},\lambda'}^\dagger \right), \end{aligned} \quad (3.4)$$

respectively.  $\partial_t$  denotes the partial derivative with respect to time  $t$ .

With the aim of calculating the frequency spectrum of the coupled model (2.26), it is useful to introduce Green's functions of the new operators  $\alpha_{\mathbf{k},\lambda}$ ,  $\alpha_{\mathbf{k},\lambda}^\dagger$ ,  $\beta_{\mathbf{k},\lambda}$  and  $\beta_{\mathbf{k},\lambda}^\dagger$ :

$$\begin{aligned} g_{\alpha_{\mathbf{k},\lambda}}(t-t') &= -i \frac{e^{-\beta H} \text{tr} \left[ T_t \alpha_{\mathbf{k},\lambda}(t) \alpha_{\mathbf{k},\lambda}^\dagger(t') \right]}{\text{tr}(e^{-\beta H})} \\ &= -i \left\langle T_t \alpha_{\mathbf{k},\lambda}(t) \alpha_{\mathbf{k},\lambda}^\dagger(t') \right\rangle, \end{aligned} \quad (3.5)$$

$$g_{\alpha_{\mathbf{k},\lambda}^\dagger}(t-t') = -i \left\langle T_t \alpha_{\mathbf{k},\lambda}^\dagger(t) \alpha_{\mathbf{k},\lambda}(t') \right\rangle, \quad (3.6)$$

$$g_{\beta_{\mathbf{k},\lambda}}(t-t') = -\frac{i}{L} \sum_{\lambda'} \left\langle T_t \beta_{\mathbf{k},\lambda}(t) \beta_{\mathbf{k},\lambda'}^\dagger(t') \right\rangle \quad (3.7)$$

and

$$g_{\beta^\dagger \mathbf{k}, \lambda}(t - t') = -\frac{i}{L} \sum_{\lambda'} \left\langle T_t \beta_{\mathbf{k}, \lambda}^\dagger(t) \beta_{\mathbf{k}, \lambda'}(t') \right\rangle, \quad (3.8)$$

respectively.  $T_t$  denotes the time ordering operator and  $\text{tr}$  denotes the trace.  $\beta$  (without subscripts) is the thermodynamic beta. The angle bracket notation is used to denote thermodynamic average; its mathematical definition is implied by equation (3.5). These equations (3.5)-(3.8), are valid when the system is in thermodynamic equilibrium [3].

The expression for Green's functions of the shifted phonon destruction, phonon creation, magnon destruction and magnon creation operators, in reciprocal space, are derived in appendix A.6 and are found to be as follows:

$$\begin{aligned} g_{\alpha \mathbf{k}, \lambda; z} &= \frac{1}{z - \omega_{\mathbf{k}, \lambda}}, & g_{\alpha^\dagger \mathbf{k}, \lambda; z} &= \frac{1}{z + \omega_{\mathbf{k}, \lambda}}, \\ g_{\beta \mathbf{k}, \lambda; z} &= \frac{1}{z - \epsilon_{\mathbf{k}}} \quad \text{and} \quad g_{\beta^\dagger \mathbf{k}, \lambda; z} &= \frac{1}{z + \epsilon_{\mathbf{k}}}, \end{aligned} \quad (3.9)$$

respectively. By using these functions, the equations of motion (3.1)-(3.4) can be rewritten as

$$\alpha_{\mathbf{k}, \lambda} = g_{\alpha \mathbf{k}, \lambda; z} \left( E_{-\mathbf{k}, \lambda} \beta_{-\mathbf{k}, \lambda} + E_{\mathbf{k}, \lambda}^* \beta_{\mathbf{k}, \lambda}^\dagger \right), \quad (3.10)$$

$$\alpha_{-\mathbf{k}, \lambda}^\dagger = -g_{\alpha^\dagger -\mathbf{k}, \lambda; z} \left( E_{-\mathbf{k}, \lambda} \beta_{-\mathbf{k}, \lambda} + E_{\mathbf{k}, \lambda}^* \beta_{\mathbf{k}, \lambda}^\dagger \right), \quad (3.11)$$

$$\beta_{\mathbf{k}, \lambda} = g_{\beta \mathbf{k}, \lambda; z} \left[ \sum_{\lambda'} \left( E_{\mathbf{k}, \lambda'}^* \alpha_{-\mathbf{k}, \lambda'} + E_{\mathbf{k}, \lambda'}^* \alpha_{\mathbf{k}, \lambda'}^\dagger \right) + \sum_{\lambda' \neq \lambda} (\epsilon_{\mathbf{k}, \lambda'} J_{\mathbf{k}, \lambda'}) \right] \quad (3.12)$$

and

$$\beta_{-\mathbf{k}, \lambda}^\dagger = -g_{\beta^\dagger -\mathbf{k}, \lambda; z} \left[ \sum_{\lambda'} \left( E_{-\mathbf{k}, \lambda'} \alpha_{-\mathbf{k}, \lambda'} + E_{-\mathbf{k}, \lambda'} \alpha_{\mathbf{k}, \lambda'}^\dagger \right) + \sum_{\lambda' \neq \lambda} (\epsilon_{-\mathbf{k}, \lambda'} J_{-\mathbf{k}, \lambda'}^*) \right], \quad (3.13)$$

respectively.

### 3.2. Analytical Solution

The frequencies of the coupled system can be derived by focusing on the phonon operators (see appendix A.7) or the magnon operators (see appendix A.8). Here, I'll outline the main points and results of the derivation with focus on the phonon operators.

Inserting equations (3.12) and (3.13) into equations (3.10) and (3.11) yields

$$\sum_{\lambda'} \begin{pmatrix} g_{\alpha}^{-1} \mathbf{k}, \lambda; z \delta_{\lambda, \lambda'} - A_{\mathbf{k}, \lambda, \lambda'; z} & -A_{\mathbf{k}, \lambda, \lambda'; z} \\ -A_{\mathbf{k}, \lambda, \lambda'; z} & g_{\alpha^\dagger}^{-1} -\mathbf{k}, \lambda; z \delta_{\lambda, \lambda'} - A_{\mathbf{k}, \lambda, \lambda'; z} \end{pmatrix} \begin{pmatrix} \alpha_{\mathbf{k}, \lambda'} \\ \alpha_{-\mathbf{k}, \lambda'}^\dagger \end{pmatrix} = \begin{pmatrix} J'_{\mathbf{k}, \lambda} \\ J'_{\mathbf{k}, \lambda} \end{pmatrix} \quad (3.14)$$

with

$$A_{\mathbf{k}, \lambda, \lambda'; z} = \frac{E_{\mathbf{k}, \lambda, \lambda'}^{(-)} z + E_{\mathbf{k}, \lambda, \lambda'}^{(\epsilon)}}{(z - \epsilon_{-\mathbf{k}})(z + \epsilon_{\mathbf{k}})} \quad (3.15)$$

and

$$J'_{\mathbf{k}, \lambda} = E_{-\mathbf{k}, \lambda} g_{\beta -\mathbf{k}, \lambda; z} \sum_{\lambda' \neq \lambda} (\epsilon_{-\mathbf{k}, \lambda'} J_{-\mathbf{k}, \lambda'}) - E_{\mathbf{k}, \lambda}^* g_{\beta^\dagger \mathbf{k}, \lambda; z} \sum_{\lambda' \neq \lambda} (\epsilon_{\mathbf{k}, \lambda'} J_{\mathbf{k}, \lambda'}^*), \quad (3.16)$$

where

$$E_{\mathbf{k}, \lambda, \lambda'}^{(-)} = E_{\mathbf{k}, \lambda} E_{\mathbf{k}, \lambda'}^* - E_{\mathbf{k}, \lambda}^* E_{\mathbf{k}, \lambda'} \quad (3.17)$$

and

$$E_{\mathbf{k}, \lambda, \lambda'}^{(\epsilon)} = E_{\mathbf{k}, \lambda} E_{\mathbf{k}, \lambda'}^* \epsilon_{\mathbf{k}} + E_{\mathbf{k}, \lambda}^* E_{\mathbf{k}, \lambda'} \epsilon_{-\mathbf{k}}. \quad (3.18)$$

Let us now introduce Green's function for coupled phonons:

$$\mathbb{G}_{A\mathbf{k}, \lambda; z} = \left\langle \left\langle \begin{pmatrix} \alpha_{\mathbf{k}, \lambda} \alpha_{\mathbf{k}, \lambda}^\dagger & \alpha_{\mathbf{k}, \lambda} \alpha_{-\mathbf{k}, \lambda} \\ \alpha_{\mathbf{k}, \lambda}^\dagger \alpha_{-\mathbf{k}, \lambda}^\dagger & \alpha_{-\mathbf{k}, \lambda}^\dagger \alpha_{-\mathbf{k}, \lambda} \end{pmatrix} \right\rangle \right\rangle (z). \quad (3.19)$$

The trace of this function is

$$\text{tr} \mathbb{G}_{A\mathbf{k}, \lambda; z} = \frac{2z(z - \epsilon_{-\mathbf{k}})(z + \epsilon_{\mathbf{k}})}{(z^2 - \omega_{\mathbf{k}, \lambda}^2)(z - \epsilon_{-\mathbf{k}})(z + \epsilon_{\mathbf{k}}) - 2\omega_{\mathbf{k}, \lambda} \left( \sum_{\lambda'} E_{\mathbf{k}, \lambda, \lambda'}^{(-)} z + E_{\mathbf{k}, \lambda, \lambda'}^{(\epsilon)} \right)}. \quad (3.20)$$

The poles of equation (3.20) are the solutions to following equation:

$$\begin{aligned} 0 &= (z^2 - \omega_{\mathbf{k}, \lambda}^2)(z - \epsilon_{-\mathbf{k}})(z + \epsilon_{\mathbf{k}}) - 2\omega_{\mathbf{k}, \lambda} \left( \sum_{\lambda'} E_{\mathbf{k}, \lambda, \lambda'}^{(-)} z + E_{\mathbf{k}, \lambda, \lambda'}^{(\epsilon)} \right) \\ &= z^4 + (\epsilon_{\mathbf{k}} - \epsilon_{-\mathbf{k}}) z^3 - (\omega_{\mathbf{k}, \lambda}^2 + \epsilon_{\mathbf{k}} \epsilon_{-\mathbf{k}}) z^2 \\ &\quad - \left( \omega_{\mathbf{k}, \lambda}^2 [\epsilon_{\mathbf{k}} - \epsilon_{-\mathbf{k}}] + 2\omega_{\mathbf{k}, \lambda} \sum_{\lambda'} E_{\mathbf{k}, \lambda, \lambda'}^{(-)} \right) z + \omega_{\mathbf{k}, \lambda}^2 \epsilon_{\mathbf{k}} \epsilon_{-\mathbf{k}} - 2\omega_{\mathbf{k}, \lambda} \sum_{\lambda'} E_{\mathbf{k}, \lambda, \lambda'}^{(\epsilon)}, \end{aligned} \quad (3.21)$$

such that  $z \neq \epsilon_{\mathbf{k}}$  and  $z \neq \epsilon_{-\mathbf{k}}$ . The frequencies of coupled phonons are the real part of the branch cut that converge to  $\omega_{\mathbf{k}, \lambda}$  when  $E_{\mathbf{k}, \lambda} \rightarrow 0$  and solve the equation

above. The imaginary part of that branch cut is the decay width of coupled phonons. Similarly, the frequencies and decay widths of coupled magnons are the real and imaginary parts, respectively, of the branch cut that converge to  $\epsilon_{\mathbf{k}}$  when  $E_{\mathbf{k},\lambda} \rightarrow 0$  and solve equation (3.21).

The coefficients of equation (3.21) are

$$\begin{aligned} a_{0\mathbf{k},\lambda} &= \omega_{\mathbf{k},\lambda}^2 \epsilon_{\mathbf{k}} \epsilon_{-\mathbf{k}} - 2\omega_{\mathbf{k},\lambda} \sum_{\lambda'} E_{\mathbf{k},\lambda,\lambda'}^{(\epsilon)}, \\ a_{1\mathbf{k},\lambda} &= -\omega_{\mathbf{k},\lambda}^2 [\epsilon_{\mathbf{k}} - \epsilon_{-\mathbf{k}}] - 2\omega_{\mathbf{k},\lambda} \sum_{\lambda'} E_{\mathbf{k},\lambda,\lambda'}^{(-)}, \\ a_{2\mathbf{k},\lambda} &= -\omega_{\mathbf{k},\lambda}^2 - \epsilon_{\mathbf{k}} \epsilon_{-\mathbf{k}} \quad \text{and} \quad a_{3\mathbf{k},\lambda} = \epsilon_{\mathbf{k}} - \epsilon_{-\mathbf{k}}. \end{aligned} \quad (3.22)$$

The branch cuts that solve equation (3.21) are

$$z_{1\mathbf{k},\lambda} = -\frac{1}{4}a_{3\mathbf{k},\lambda} + S_{\mathbf{k},\lambda} + \frac{1}{2}\sqrt{-4S_{\mathbf{k},\lambda}^2 - 2p_{\mathbf{k},\lambda} - \frac{q_{\mathbf{k},\lambda}}{S_{\mathbf{k},\lambda}}}, \quad (3.23)$$

$$z_{2\mathbf{k},\lambda} = -\frac{1}{4}a_{3\mathbf{k},\lambda} + S_{\mathbf{k},\lambda} - \frac{1}{2}\sqrt{-4S_{\mathbf{k},\lambda}^2 - 2p_{\mathbf{k},\lambda} - \frac{q_{\mathbf{k},\lambda}}{S_{\mathbf{k},\lambda}}}, \quad (3.24)$$

$$z_{3\mathbf{k},\lambda} = -\frac{1}{4}a_{3\mathbf{k},\lambda} - S_{\mathbf{k},\lambda} + \frac{1}{2}\sqrt{-4S_{\mathbf{k},\lambda}^2 - 2p_{\mathbf{k},\lambda} + \frac{q_{\mathbf{k},\lambda}}{S_{\mathbf{k},\lambda}}} \quad (3.25)$$

and

$$z_{4\mathbf{k},\lambda} = -\frac{1}{4}a_{3\mathbf{k},\lambda} - S_{\mathbf{k},\lambda} - \frac{1}{2}\sqrt{-4S_{\mathbf{k},\lambda}^2 - 2p_{\mathbf{k},\lambda} + \frac{q_{\mathbf{k},\lambda}}{S_{\mathbf{k},\lambda}}} \quad (3.26)$$

with

$$p_{\mathbf{k},\lambda} = a_{2\mathbf{k},\lambda} - \frac{3}{8}a_{3\mathbf{k},\lambda}^2, \quad (3.27)$$

$$q_{\mathbf{k},\lambda} = \frac{1}{8}a_{3\mathbf{k},\lambda}^3 - \frac{1}{2}a_{3\mathbf{k},\lambda}a_{2\mathbf{k},\lambda} + a_{1\mathbf{k},\lambda}, \quad (3.28)$$

$$\Delta_{0\mathbf{k},\lambda} = a_{2\mathbf{k},\lambda}^2 - 3a_{3\mathbf{k},\lambda}a_{1\mathbf{k},\lambda} + 12a_{0\mathbf{k},\lambda}, \quad (3.29)$$

$$\Delta_{1\mathbf{k},\lambda} = 2a_{2\mathbf{k},\lambda}^3 - 9a_{3\mathbf{k},\lambda}a_{2\mathbf{k},\lambda}a_{1\mathbf{k},\lambda} + 27a_{3\mathbf{k},\lambda}^2a_{0\mathbf{k},\lambda} + 27a_{1\mathbf{k},\lambda}^2 - 72a_{2\mathbf{k},\lambda}a_{0\mathbf{k},\lambda}, \quad (3.30)$$

$$Q_{\mathbf{k},\lambda} = \sqrt[3]{\frac{\Delta_{1\mathbf{k},\lambda} + \sqrt{\Delta_{1\mathbf{k},\lambda}^2 - 4\Delta_{0\mathbf{k},\lambda}^3}}{2}} \quad (3.31)$$

and

$$S_{\mathbf{k},\lambda} = \frac{1}{2}\sqrt{-\frac{2}{3}p_{\mathbf{k},\lambda} + \frac{1}{3}\left(Q_{\mathbf{k},\lambda} + \frac{\Delta_{0\mathbf{k},\lambda}}{Q_{\mathbf{k},\lambda}}\right)}. \quad (3.32)$$

The solutions above hold if  $Q_{\mathbf{k},\lambda} \neq 0$  and  $S_{\mathbf{k},\lambda} \neq 0$ . [12, 13]

If  $E_{\mathbf{k},\lambda,\lambda'}^{(-)} = 0$  and  $\epsilon_{\mathbf{k}} - \epsilon_{-\mathbf{k}} = 0$  for all  $\mathbf{k}$ , we can observe that  $z_{1\mathbf{k},\lambda} = -z_{4\mathbf{k},\lambda}$  and  $z_{2\mathbf{k},\lambda} = -z_{3\mathbf{k},\lambda}$ . Hence, in this case, are  $x_{1\mathbf{k},\lambda} = |\text{Re}(z_{1\mathbf{k},\lambda})|$  and  $x_{2\mathbf{k},\lambda} = |\text{Re}(z_{2\mathbf{k},\lambda})|$  the physical frequencies with  $y_{1\mathbf{k},\lambda} = |\text{Im}(z_{1\mathbf{k},\lambda})|$  and  $y_{2\mathbf{k},\lambda} = |\text{Im}(z_{2\mathbf{k},\lambda})|$  as the corresponding decay widths, respectively.

### 3.3. Numerical Examples

The physical solutions to equation (3.21) are plotted in the numerical computing environment *Matlab R2018b* [14]. The script can be found in appendix B.

In this section, the crystal structure is chosen to be a two-dimensional square lattice with one ion at each lattice site. The parameters that are varied for the different plots are the scalar  $T_{i,j}$  and vector  $\mathbf{T}_{i,j}$  decompositions of the lattice-spin interaction tensor. They are, however, assumed to be the same for all nearest neighbouring ions (and zero for all other ions):  $T_{j,j+\delta} = T$  and  $\mathbf{T}_{j,j+\delta} = \mathbf{T}$ . The phonon polarization is restricted to one direction, implying that there is only one phonon mode number:  $\lambda = 1$ . Moreover, 30 000 lattice sites were used in each numerical computation, except for figure 3.10 whose computation used 3 000 lattice sites. The constant parameters used in the script are chosen as follows:  $\mathbf{a} = (1, 1, 0)$ ,  $m = 1$ ,  $K_1 = 100$ ,  $\boldsymbol{\xi}_{\mathbf{k},1} = (\sin(\mathbf{k} \cdot \mathbf{a}), 0, 0)$ ,  $S = 1/2$ ,  $J_{\parallel} = \sqrt{2}$ ,  $J_{\perp} = 1/\sqrt{2}$ ,  $\mathbf{D}_{j,j+\delta} = (1, i, 0)$  and  $\gamma = 1$ . They are to be regarded as scaling parameters, not necessarily corresponding to any experimental values. We can note that the restriction of one phonon polarization implies that  $E_{\mathbf{k},1,1}^{(-)} = 0$  and a square lattice implies that  $\epsilon_{\mathbf{k}} = \epsilon_{-\mathbf{k}}$ . Thus, as discussed in section 3.2, the frequencies of the coupled system are  $x_{1\mathbf{k},1}$  and  $x_{2\mathbf{k},1}$ , with the corresponding decay widths  $y_{1\mathbf{k},1}$  and  $y_{2\mathbf{k},1}$ , respectively.

In the frequency spectrum plots below are the free magnon and phonon frequencies represented by dashed red and blue lines, respectively. Figure 3.1 only shows the frequencies of free magnons and phonons, while all other frequency spectrums also show the frequencies of coupled magnons and phonons. The frequencies of the physical solutions to equation (3.21) are represented by cyan and magenta lines. The particle with a frequency represented by the cyan line has a decay width that is represented by the shaded cyan area. Similarly, the shaded magenta area represents the decay width of the particle with a frequency represented by the magenta line.

The x-axis of the frequency spectrum plots shows the crystal momentum within the first Brillouin zone, displayed by figure 3.2. It starts at  $\Gamma = (0, 0, 0)$ , and increases linearly in the  $x$ -direction to  $X = (\pi/a_x, 0, 0)$ . Then, it increases linearly in the  $y$ -direction to  $M = (\pi/a_x, \pi/a_y, 0)$ . Finally, it increases linearly in the  $(x + y)$ -direction to  $\Gamma = (2\pi/a_x, 2\pi/a_y, 0)$ . Due to the periodicity of the Brillouin zone and the symmetry of the square lattice, the last path is identical to the path

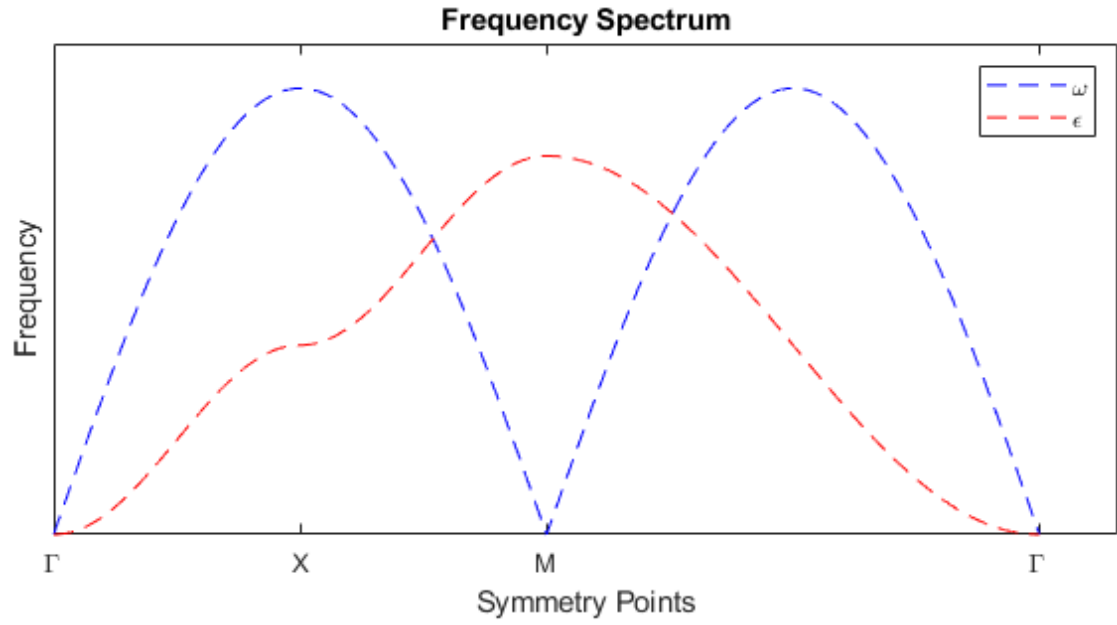


Figure 3.1: Frequency spectrum of free magnons and phonons.

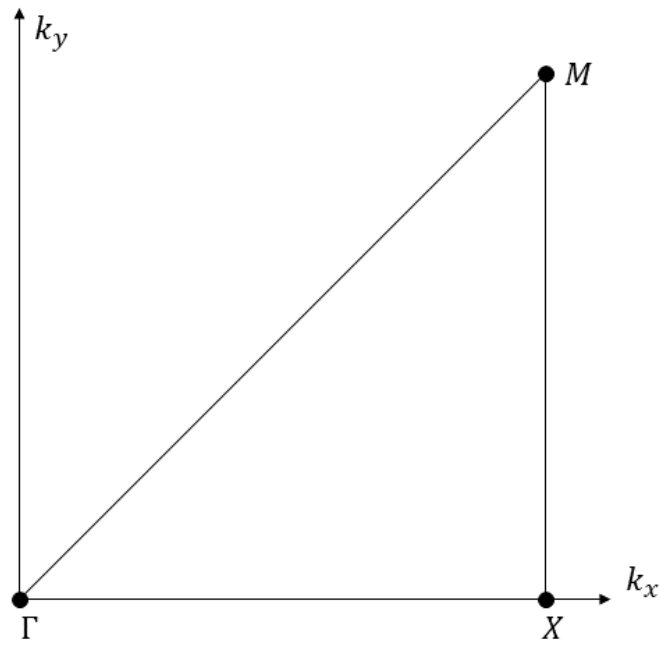


Figure 3.2: First Brillouin zone of a square lattice, showing lines of crystal momentum corresponding to the x-axis in the frequency spectrum plots.

that starts at  $(\pi/a_x, \pi/a_y, 0)$  and linearly decreases in the  $(x + y)$ -direction to  $\Gamma = (0, 0, 0)$ . The  $y$ -axis starts at 0 and increases linearly to 22 (the maximal value of any computed line is 20). The lines show the real parts of the solutions and the upper (lower) outer bounds of the shaded areas show the real parts plus (minus) the absolute values of the corresponding imaginary parts.

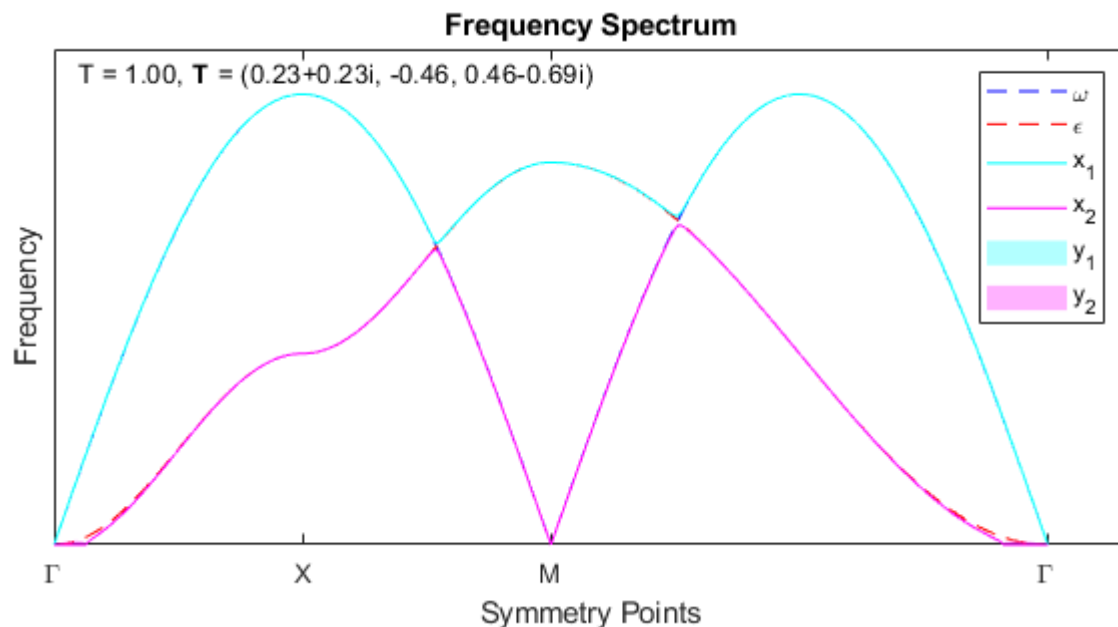


Figure 3.3: Frequency spectrum of magnons and phonons with a weak coupling:  $T = 1$  and  $\mathbf{T} = (1 + i, -2, 2 - 3i) / \sqrt{19}$ .

In figure 3.3 are the lattice-spin scalar and vector decompositions equal to 1 and  $(1 + i, -2, 2 - 3i) / \sqrt{19}$ , respectively, where  $\|(1 + i, -2, 2 - 3i) / \sqrt{19}\| = 1$ . I call this a *weak coupling*. We can see that the lines of the solutions to equation (3.21) are almost identical to the lines of the free magnons and phonons, except close to the  $\Gamma$ -point. Nevertheless, the two solutions do not consistently follow the free magnon or phonon frequencies when the crystal momentum increase; they switch between the two. The cyan line, corresponding to equation (3.23), follows the free phonon frequency at the start. When the free magnon and phonon frequencies are equal, between symmetry points  $X$  and  $M$ , it switches to the free magnon frequency. Then, the next time the free magnon and phonon frequencies are equal, between symmetry points  $M$  and  $\Gamma$ , the cyan lines switches back to being almost identical to the free phonon frequency. The magenta line, corresponding to equation (3.24), does the opposite: it starts by following the free magnon frequency, then the free phonon frequency and finally back to the free magnon frequency. We can also note that the magenta line is always below or equal to the cyan line.

Hence, we can interpret the magenta and cyan lines as a lower and higher energy states, respectively.

If we look closely at and around the  $\Gamma$ -point of figure 3.3, we can see that the magenta line is zero and that there is a small magenta-shaded area. I call this the *area of uncertainty*. The causes and implications of this area is unknown and will have to be investigated by future studies. One possibility is that the ground state is not stable in the frame of reference specified by equation (2.26). An example of phonon instabilities is discussed in the following reference [15]. Another possibility is that the assumption of small spin-fluctuations from the ground state is not valid and the model breaks down. It is also possible that the magnons are in a Bose-Einstein condensate. The existence of Bose-Einstein condensed magnons is supported by experiments in  $\text{TlCuCl}_3$  [16] and  $\text{Cs}_2\text{CuCl}_4$  [17]. Nevertheless, we don't know if that is what is observed here.

To summarize, the coupled states of magnons and phonons can be divided into a lower and a higher energy state. These states have a similar behaviour to either the free magnon or the free phonon state, depending on their crystal momentum. The lower energy state, however, has a distinct difference from the states of free magnons and phonons. It has a region, close to the  $\Gamma$ -point, wherein its frequency is uncertain.

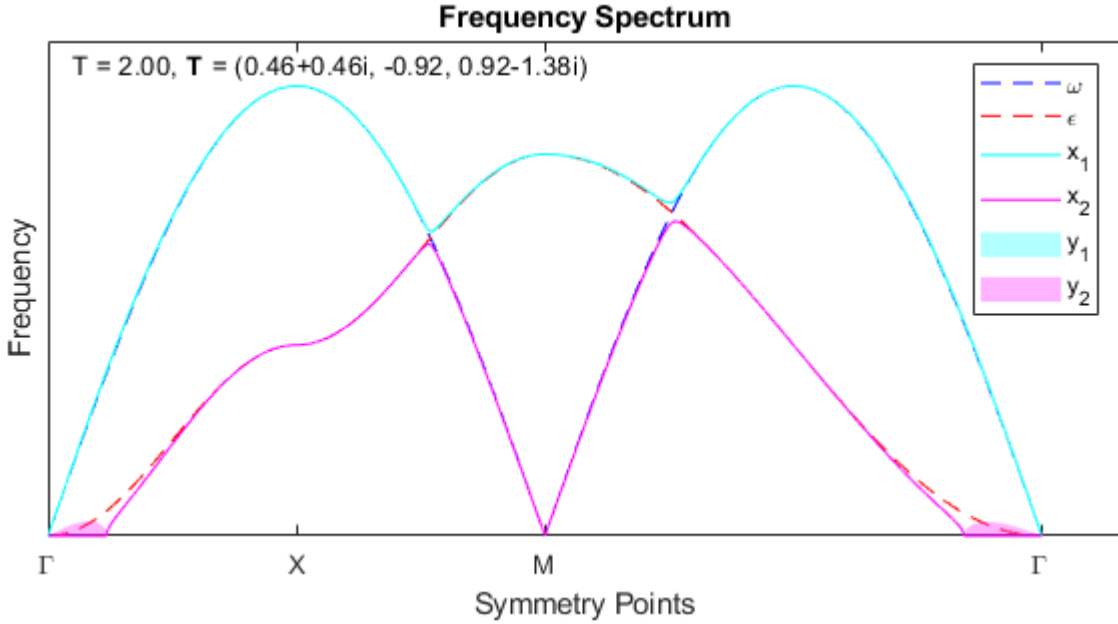


Figure 3.4: Frequency spectrum of magnons and phonons with a moderate coupling:  $T = 2$  and  $\mathbf{T} = 2(1 + i, -2, 2 - 3i)/\sqrt{19}$ .

Figure 3.4 shows the frequency spectrum of magnons and phonons with a coupling twice as strong as the one in figure 3.3. I call this coupling *moderate*. If we compare this with the weakly coupled magnons and phonons shown in figure 3.3, we can see that the discrepancy between the solid and the dashed lines are bigger. This is to be expected: the frequencies of the magnons and phonons should change when we change the strength of the coupling. The largest discrepancies seem to be around the  $\Gamma$ -point: the area of uncertainty is both wider and higher. This could mean that the model breaks down for larger crystal momentums, or that the hypothetical ground state instabilities or Bose-Einstein condensate covers a wider range of frequencies within a larger interval of crystal momentum. It could also mean something else, something that we have not thought of.

We can also note that the magenta line that precedes and follows from the area of uncertainty is lower in figure 3.4 than in figure 3.3. That is, for small crystal momentums, the frequencies of the lower energy state decrease when the strength of the coupling increase. Additionally, the discrepancies between the solid and the dashed lines are bigger close to the points where the free magnon and phonon frequencies are equal, compared to the weakly coupled magnons and phonons. Further, we can note that the discrepancy between the coupled states and the free phonon is small compared to the discrepancy between the coupled states and the free magnon. It seems that the phonons are more robust towards the coupled interactions than the magnons.

In summary, the frequencies of magnons and phonons change if the strength of the coupling increase. The area of uncertainty becomes bigger and the frequencies of the lower energy state becomes lower for low crystal momentums. Moreover, the magnons are more sensitive to changes in the coupling strength than the phonons.

Figure 3.5 shows the frequency spectrums of magnons and phonons with a strong (top) and a very strong (bottom) coupling: three and five times as strong as the coupling in figure 3.3, respectively. Here, we can see that the changes observed in figure 3.4 becomes more significant. The frequencies of the coupled phonons and magnons change even more, when the strength of the coupling increase. The area of uncertainty becomes bigger and the frequencies close to the area of uncertainty becomes even lower than in the cases of weak and moderate coupling. We can also observe that the magnons are more sensitive to the increasing coupling strength than the phonons. In conclusion, figure 3.5 establish a pattern of the effects of coupled interactions, discussed in connection with figure 3.4 and figure 3.3.

Figure 3.6 shows the frequency spectrum of magnons and phonons with a weak scalar coupling and no vector coupling. This figure looks almost identical to figure 3.4. That is, the frequency spectrum with a pure scalar coupling strength of one and no vector coupling, is almost identical to the frequency spectrum with both a scalar and vector coupling strength of two. Thus, in some cases, is the composition of the coupled interaction more important than its strength: how the

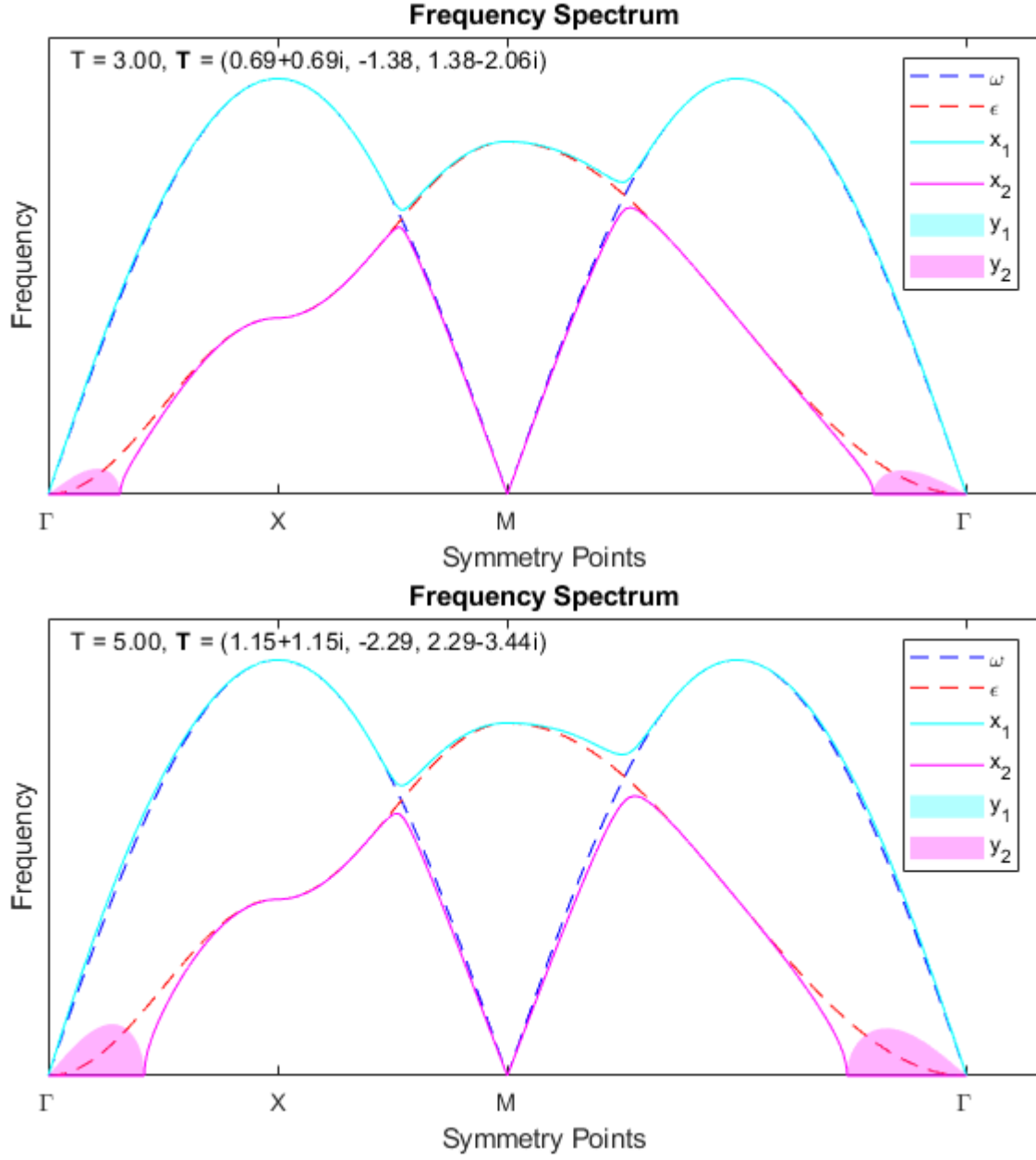


Figure 3.5: Frequency spectrums of magnons and phonons. The plot at the top has a strong coupling:  $T = 5$  and  $\mathbf{T} = 5(1+i, -2, 2-3i)/\sqrt{19}$ . The plot at the bottom has a very strong coupling:  $T = 5$  and  $\mathbf{T} = 5(1+i, -2, 2-3i)/\sqrt{19}$ .

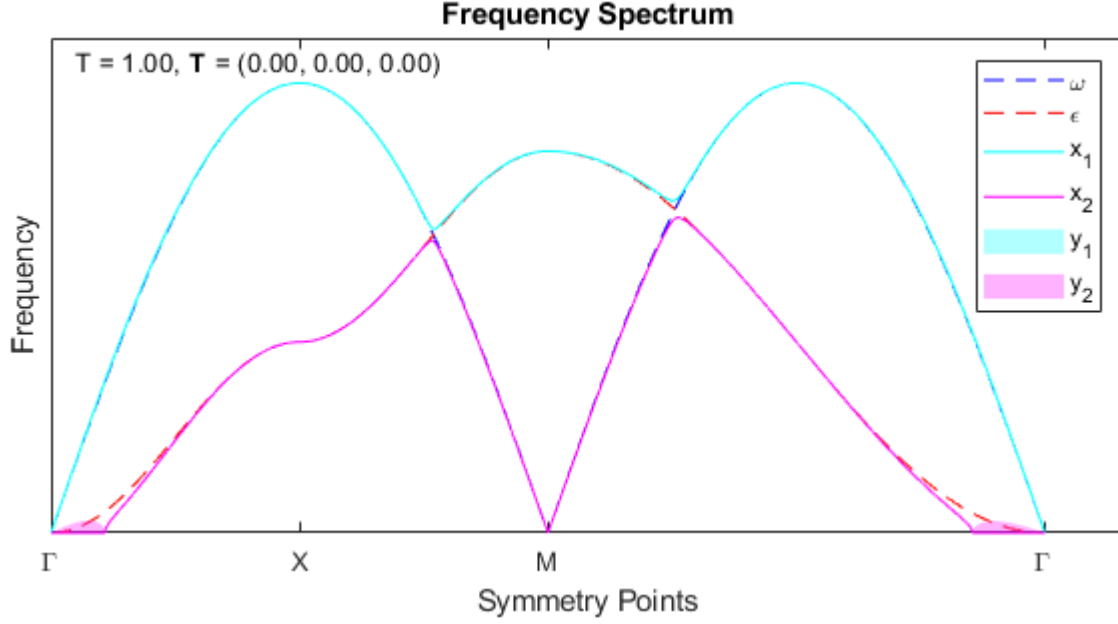


Figure 3.6: Frequency spectrum of magnons and phonons with a pure scalar coupling:  $T = 1$  and  $\mathbf{T} = \mathbf{0}$ .

coupled interaction is mediated may affect the frequencies of magnons and phonons more than the strength of the interaction. This conclusion is supported by figure 3.7, which shows the frequency spectrum with a vector coupling strength of one and no scalar coupling. This frequency spectrum, with a pure vector coupling, is slightly different from the one with a pure scalar coupling. The frequencies close the  $\Gamma$ -point are slightly less uncertain for the pure vector coupling compared to the case of pure scalar coupling. Figure 3.8 further supports this conclusion. It shows the frequency spectrum with a pure vector coupling of different distribution than all other plots:  $\mathbf{T} = (5i, -3, 1)/\sqrt{35}$ , where  $||\mathbf{T}|| = 1$ . In this case are the deviations from the frequency spectrum of free magnons and phonons very small. One has to look close at the either of the points where the free magnon and phonon frequencies are equal (including the  $\Gamma$ -point), to be able to see any difference. Conclusively, the composition of the interactions between magnons and phonons is, in some cases, more important than its strength.

Figure 3.9 shows the frequency spectrum with a scalar coupling strength of one hundredth compared to the weak coupling in figure 3.3 and no vector coupling. I call this a *very weak scalar* coupling. Here, we can see a shaded magenta area close to the  $\Gamma$ -point as well as a deviation between the solid magenta line and the dashed red line. This indicates that there is no critical coupling strength above zero, that completely removes the area of uncertainty. Nor is there any indication of a scalar

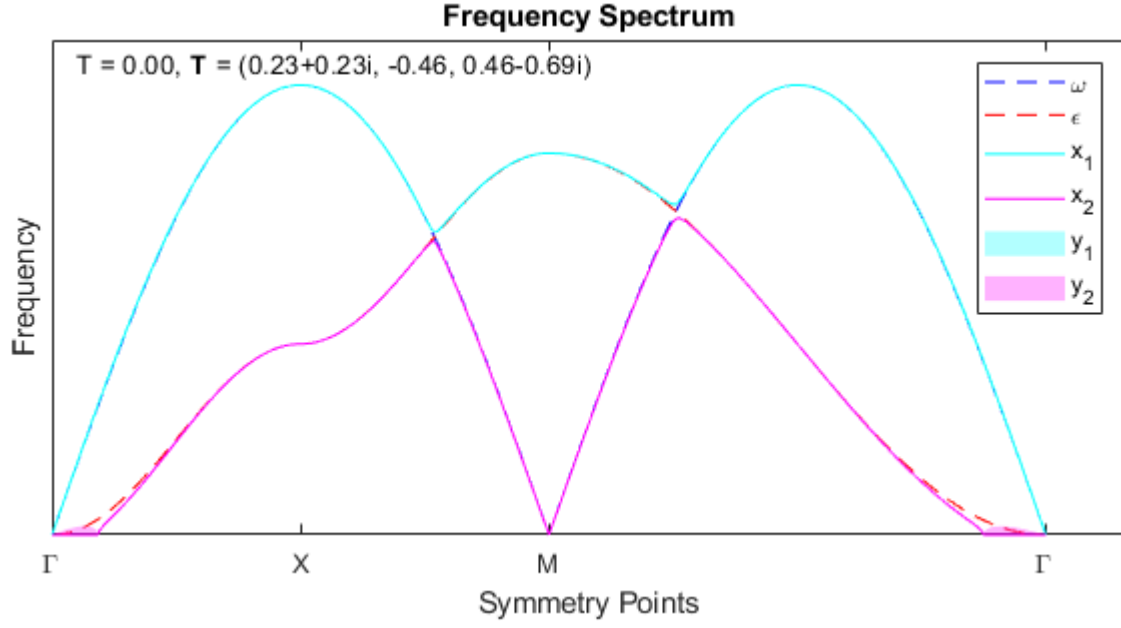


Figure 3.7: Frequency spectrum of magnons and phonons with a pure vector coupling:  $T = 0$  and  $\mathbf{T} = (1 + i, -2, 2 - 3i) / \sqrt{19}$ .

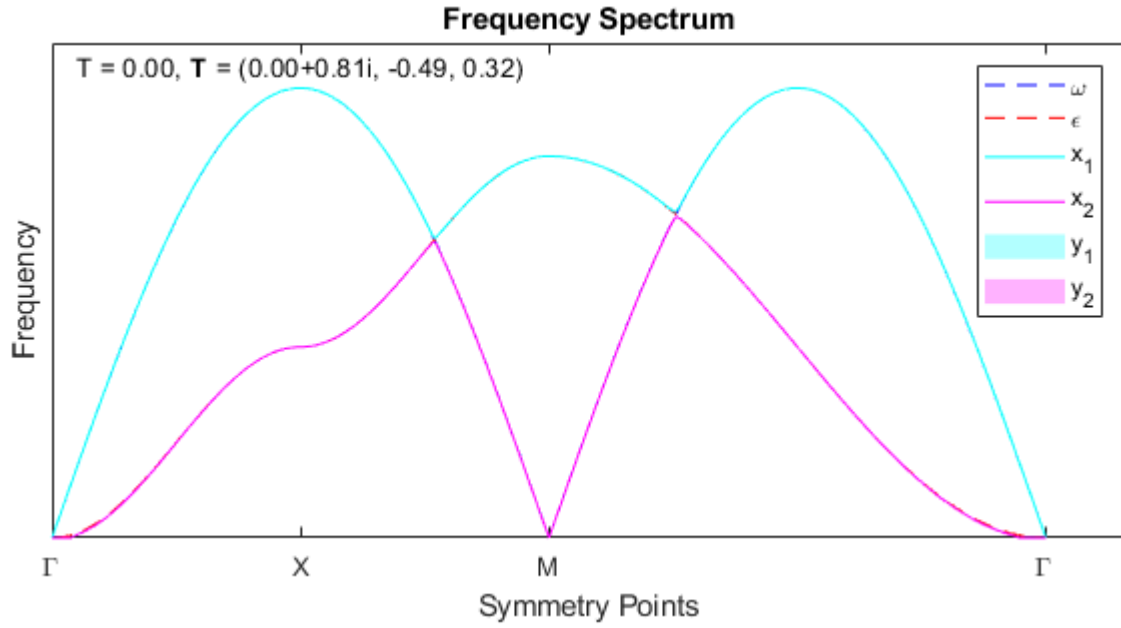


Figure 3.8: Frequency spectrum of magnons and phonons with a pure vector coupling of different distribution:  $T = 0$  and  $\mathbf{T} = (5i, -3, 1) / \sqrt{35}$ .

coupling strength different from zero whose frequency spectrum is identical to the one of free magnons or phonons. It seems that the behavioural changes of coupled compared to free magnons and phonons are independent of the strength of the coupled interactions; they are only dependent on the existence or absence of coupled interactions.

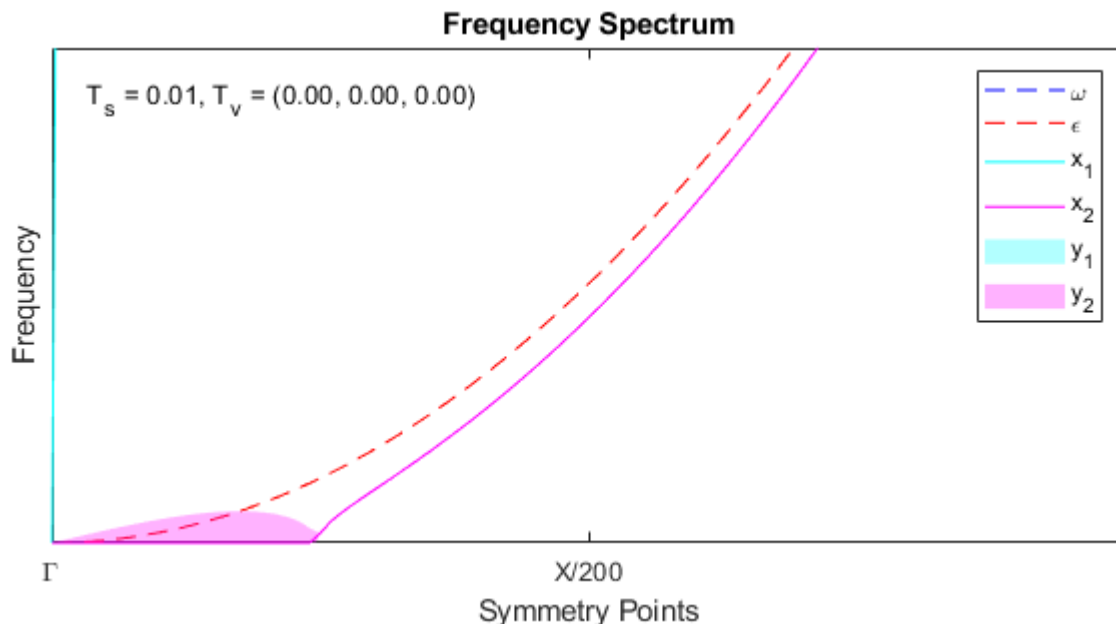


Figure 3.9: Frequency spectrum of magnons and phonons, close to the  $\Gamma$ -point, with a very weak scalar coupling:  $T = 0.01$  and  $\mathbf{T} = \mathbf{0}$ .

Figure 3.10 shows the solutions to equation (A.61) with a weak coupling (cf. figure 3.3). The solutions are solved with the Matlab function *fsolve* [14]. As is seen in the figure, equation (A.61) is not well-behaved numerically, at least not with my script (see appendix B). I have not analysed the numerical error; thus, we can only use figure 3.10 for general hints about the behaviour of coupled magnons and phonons. At some irregular intervals of crystal momentum, it switches solution or end up at arbitrary frequencies. Besides these irregularities, figure 3.10 looks like the bottom plot of figure 3.5. That is, the frequency spectrum from equation (A.61) is similar to the frequency spectrum from equation (3.21) with a coupling five times as strong. This is not to be expected since they are derived from the same equations of motion (3.1)-(3.4).

Additionally, the frequencies of the lower energy state are indecisive (they do not have a continuous dependence on the crystal momentum) close to the  $\Gamma$ -point. This region of indecision overlaps the area of uncertainty in the very strongly coupled frequency spectrum. This does not rule out any of the three hypotheses

regarding the area of uncertainty. The indecision might be because of an instable ground state, an invalid assumption of small spin-fluctuations from the ground state or a Bose-Einstein condensation of the magnons. Although, in the last case we would expect a more confined region of indecision, comparable to the area of uncertainty in figure 3.3. The discontinuous region of frequencies might also be a consequence of something we have not considered. In summary, figure 3.10 does not give us any new insight.

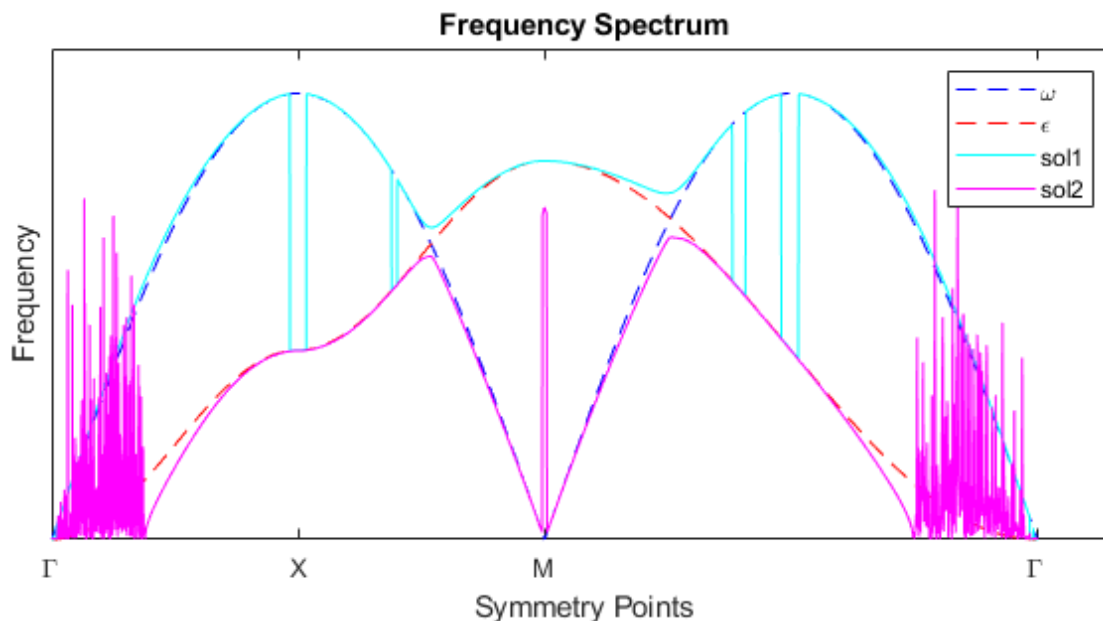


Figure 3.10: Frequency spectrum of magnons and phonons with a weak coupling:  $T = 1$  and  $\mathbf{T} = (1 + i, -2, 2 - 3i) / \sqrt{19}$ . sol1 and sol2 are solutions to equation (A.61), solved with the Matlab function *fsolve*. 3000 lattice sites are used for these solutions.

The propagated numerical floating point error of the numerical computations is at the order of  $10^{-8}$  (see appendix B). Each line in the plots connect 30 000 lattice points, except for figures 3.9 and 3.10 whose lines connect between 150 to 300 and 3 000 points, respectively. Further, each plot is 560 pixels wide and 312 pixels high. Therefore, any numerical error is at least two orders of magnitude smaller than the resolution of the plots, except for figures 3.9 and 3.10. The numerical error in figure 3.9 is of the same order of magnitude or smaller than the resolution. The numerical error in figure 3.10 is unknown. In conclusion, everything derived from figures 3.3-3.9 are within the margin of numerical error, and figure 3.10 might have visible errors.

## 4. Conclusions

A model is derived by expressing ionic spin and displacement in terms of magnon and phonon operators, respectively, and by evaluating their interactions in reciprocal space. The model is found to contain mixed terms of magnon and phonon operators. Some of these terms' mixes destruction and creation operators and preserve the harmonic oscillatory behaviour of the magnons and phonons. However, the model also has terms with two destruction or two creation operators. These terms indicate a non-harmonic behaviour of the model. To gain more insight, the frequency spectrum of coupled magnons and phonons is derived. This is initiated by using Heisenberg's equation of motion and with the introduction of Green's functions. The frequencies are then extracted through the poles of Green's function. Finally, frequency spectrums are plotted in a numerical computing environment.

Based on these plots, we can make multiple observations and conclusions. Firstly, the states of coupled magnons and phonons can be divided into a lower and a higher energy state. Each of these states have a similar behaviour to either the free magnon or the free phonon states, depending on their crystal momentum. Secondly, the magnons are more sensitive to changes in the strength of the coupled interactions than the phonons are. Thirdly, there is a region around the center of the Brillouin zone wherein the frequencies of the lower energy state are unknown. This region seems to appear for any strength of the coupled interaction, and it becomes larger with increasing strength. The causes and implications of this region is unknown. One hypothesis is that the ground state is instable. Another hypothesis is that the assumption of small spin-fluctuations from the ground state is not valid, causing the model to break down. A third hypothesis is that the magnons are in a Bose-Einstein condensate. Finally, the composition of the coupled interactions between magnons and phonons are, in some cases, more important than their strength.

A recommendation for future work is to compare this study with experimental results. The frequencies of magnons can be measured by inelastic neutron scattering, for example in chromium(III) bromide [18]. To do this one might have to start by changing the parameters in appendix B to fit the experimental setup. Other important work for future studies is to investigate the frequencies of the lower energy state around the center of the Brillouin zone, theoretically and experimentally.

## References

- [1] Melcom, *Kubisches Kristallsystem*, Wikimedia Foundation, Inc. (2014).  
URL: [https://commons.wikimedia.org/wiki/File:Kubisches\\_Kristallsystem.jpg](https://commons.wikimedia.org/wiki/File:Kubisches_Kristallsystem.jpg) (Acc. 2018-11-24).
- [2] R. Simmon, *Orbital Variations*, NASA Earth Observatory, (2000).  
URL: [https://earthobservatory.nasa.gov/features/Milankovitch/milankovitch\\_2.php](https://earthobservatory.nasa.gov/features/Milankovitch/milankovitch_2.php) (Acc. 2018-11-28).
- [3] G. D. Mahan, *Many-Particle Physics*, Third Edition, Kluwer Academic/-Plenum Publisher, New York (2000).  
ISBN: 0-306-46338-5.
- [4] D. Perera, D. M. Nicholson, M. Eisenbach, G. M. Stocks and D. P. Landau, *Phys. Rev. B* **95**, 014431 (2017).
- [5] F. Körmann, B. Grabowski, B. Dutta, T. Hickel, L. Mauger, B. Fultz and J. Neugebauer, *Phys. Rev. Lett.* **113**, 165503 (2014).
- [6] R. Pradip, P. Piekarz, A. Bosak, D. G. Merkel, O. Waller, A. Seiler, A. I. Chumakov, R. Rüffer, A. M. Oleś, K. Parlinski, M. Krisch, T. Baumbach and S. Stankov, *Phys. Rev. Lett.* **116**, 185501 (2016).
- [7] J. Fransson, D. Thonig, P. F. Bessarab, S. Bhattacharjee, J. Hellsvik and L. Nordström, *Phys. Rev. Materials* **1**, 074404 (2018).
- [8] T. Holstein and H. Primakoff, *Phys. Rev.* **58**, 1098 (1940).
- [9] L. Råde and B. Westergren, *Mathematics Handbook for Science and Engineering*, Edition 5:12, Studentlitteratur AB, Lund (2004). p. 297.  
ISBN: 978-91-44-03109-5.
- [10] T. Moriya, *Phys. Rev.* **120**, 91 (1960).
- [11] J. J. Sakurai and J. Napolitano, *Modern Quantum Mechanics*, Second Edition, Pearson Education, Inc., San Francisco (2011). p. 82-84, 500, 501.  
ISBN: 0-8053-8291-7.
- [12] *Quartic function*, Wikimedia Foundation, Inc. (2018).  
URL: [https://en.wikipedia.org/wiki/Quartic\\_function](https://en.wikipedia.org/wiki/Quartic_function) (Acc. 2018-11-13).

- [13] J. J. O'Connor and E. F. Robertson, *Quadratic, cubic and quartic equations*, MacTutor History of Mathematics archive, University of St Andrews, Scotland (1996).  
URL: [http://www-history.mcs.st-andrews.ac.uk/HistTopics/Quadratic\\_etc\\_equations.html](http://www-history.mcs.st-andrews.ac.uk/HistTopics/Quadratic_etc_equations.html) (Acc. 2018-11-13).
- [14] *Matlab R2018b*, Version 9.5.0.944444, The MathWorks, Inc. (1994-2018).  
URL: <https://se.mathworks.com/products/matlab.html> (Acc. 2018-09-20).
- [15] K. Einarsdotter, B. Sadigh, G. Grimvall and V. Ozoliņš, *Phys. Rev. Lett.* **79**, 5188 (1997).
- [16] T. Nikuni, M. Oshikawa, A. Oosawa and H. Tanaka, *Phys. Rev. Lett.* **84**, 5868 (2000).
- [17] T. Radu, H. Wilhelm, V. Yushankhai, D. Kovrizhin, R. Coldea, Z. Tylczynski, T. Lühmann and F. Steglich, *Phys. Rev. Lett.* **95**, 127202 (2005).
- [18] E. J. Samuelsen, Richard Silberglitt, G. Shirane and J. P. Remeika, *Phys. Rev. B* **3**, 157 (1971).

## Appendix A - Derivations

### A.1. Heisenberg Hamiltonian

The expression for the anisotropic Heisenberg Hamiltonian in reciprocal space with magnon operators, is derived by inserting the Holstein Primakoff transformations for small fluctuations (2.10) into original expression for the Heisenberg Hamiltonian (2.5). Finally, I use the Fourier transformed magnon operators (2.11) and carry out the calculations:

$$\begin{aligned}
H_{he} &= -J_{\parallel} \sum_{j,\delta} S_j^z S_{j+\delta}^z - J_{\perp} \sum_{j,\delta} S_j^- S_{j+\delta}^+ \\
&= -J_{\parallel} \sum_{j,\delta} \left( S - b_j^{\dagger} b_j \right) \left( S - b_{j+\delta}^{\dagger} b_{j+\delta} \right) - 2J_{\perp} S \sum_{j,\delta} b_j^{\dagger} b_{j+\delta} \\
&= -J_{\parallel} \sum_{j,\delta} \left( S - \frac{1}{N} \sum_{\mathbf{k},\mathbf{k}'} e^{i(\mathbf{k}-\mathbf{k}') \cdot \mathbf{R}_j} b_{\mathbf{k}}^{\dagger} b_{\mathbf{k}'} \right) \left( S - \frac{1}{N} \sum_{\mathbf{p},\mathbf{p}'} e^{i(\mathbf{p}-\mathbf{p}') \cdot (\mathbf{R}_j + \mathbf{R}_{\delta})} b_{\mathbf{p}}^{\dagger} b_{\mathbf{p}'} \right) \\
&\quad - 2J_{\perp} S \sum_{i\delta} \frac{1}{N} \sum_{\mathbf{k},\mathbf{k}'} e^{i\mathbf{k} \cdot \mathbf{R}_j} b_{\mathbf{k}}^{\dagger} e^{-i\mathbf{k}' \cdot (\mathbf{R}_j + \mathbf{R}_{\delta})} b_{\mathbf{k}'} \\
&= -J_{\parallel} \left( NS^2 Z - \frac{S}{N} \sum_{\delta,\mathbf{p},\mathbf{p}'} N\delta(\mathbf{p}-\mathbf{p}') e^{i(\mathbf{p}-\mathbf{p}') \cdot \mathbf{R}_{\delta}} b_{\mathbf{p}}^{\dagger} b_{\mathbf{p}'} - \frac{S}{N} \sum_{\delta,\mathbf{k},\mathbf{k}'} N\delta(\mathbf{k}-\mathbf{k}') b_{\mathbf{k}}^{\dagger} b_{\mathbf{k}'} \right. \\
&\quad \left. + \frac{1}{N^2} \sum_{\delta,\mathbf{k},\mathbf{k}',\mathbf{p},\mathbf{p}'} N\delta(\mathbf{k}-\mathbf{k}'+\mathbf{p}-\mathbf{p}') e^{i(\mathbf{p}-\mathbf{p}') \cdot \mathbf{R}_{\delta}} b_{\mathbf{k}}^{\dagger} b_{\mathbf{k}'} b_{\mathbf{p}}^{\dagger} b_{\mathbf{p}'} \right) \\
&\quad - 2J_{\perp} \frac{S}{N} \sum_{\delta\mathbf{k},\mathbf{k}'} N\delta(\mathbf{k}-\mathbf{k}') e^{-i\mathbf{k}' \cdot \mathbf{R}_{\delta}} b_{\mathbf{k}}^{\dagger} b_{\mathbf{k}'} \\
&= -J_{\parallel} NS^2 Z + 2J_{\parallel} SZ \sum_{\mathbf{k}} b_{\mathbf{k}}^{\dagger} b_{\mathbf{k}} - 2J_{\perp} S \sum_{\mathbf{k}} C_{\mathbf{k}} b_{\mathbf{k}} b_{\mathbf{k}}^{\dagger} - \frac{J_{\parallel}}{N} \sum_{\mathbf{k},\mathbf{k}',\mathbf{p}} C_{\mathbf{k}-\mathbf{k}'} b_{\mathbf{k}}^{\dagger} b_{\mathbf{k}'} b_{\mathbf{p}}^{\dagger} b_{\mathbf{k}-\mathbf{k}'+\mathbf{p}} \\
&= -J_{\parallel} NS^2 Z + 2S \sum_{\mathbf{k}} (J_{\parallel} Z - J_{\perp} C_{\mathbf{k}}) b_{\mathbf{k}}^{\dagger} b_{\mathbf{k}} - \frac{J_{\parallel}}{N} \sum_{\mathbf{k},\mathbf{k}',\mathbf{k}''} C_{\mathbf{k}-\mathbf{k}'} b_{\mathbf{k}}^{\dagger} b_{\mathbf{k}'} b_{\mathbf{k}''}^{\dagger} b_{\mathbf{k}-\mathbf{k}'+\mathbf{k}''},
\end{aligned} \tag{A.1}$$

where the structure constant is defined by  $C_{\mathbf{k}} = \sum_{\delta} e^{-i\mathbf{k} \cdot \mathbf{R}_{\delta}}$ .

## A.2. Dzyaloshinskii-Moriya Hamiltonian

The Hamiltonian for the anisotropic Dzyaloshinskii-Moriya interaction is given by equation (2.13). This is expressed in terms of magnon operators by using the Holstein-Primakoff transformations for small spin fluctuations (2.10):

$$\begin{aligned}
H_{DM} &= \sum_{j,\delta} \mathbf{D}_{j,j+\delta} \cdot (\mathbf{S}_j \times \mathbf{S}_{j+\delta}) \\
&= \sum_{j,\delta} \mathbf{D}_{j,j+\delta} \cdot \left( S_j^{(y)} S_{j+\delta}^{(z)} - S_j^{(z)} S_{j+\delta}^{(y)}, S_j^{(z)} S_{j+\delta}^{(x)} - S_j^{(x)} S_{j+\delta}^{(z)}, S_j^{(x)} S_{j+\delta}^{(y)} - S_j^{(y)} S_{j+\delta}^{(x)} \right) \\
&= \sum_{j,\delta} \left( -i\sqrt{\frac{S}{2}} D_{j,j+\delta}^{(x)} \left[ (b_j - b_j^\dagger) (S - b_{j+\delta}^\dagger b_{j+\delta}) - (S - b_j^\dagger b_j) (b_{j+\delta} - b_{j+\delta}^\dagger) \right] \right. \\
&\quad + \sqrt{\frac{S}{2}} D_{j,j+\delta}^{(y)} \left[ (S - b_j^\dagger b_j) (b_{j+\delta} + b_{j+\delta}^\dagger) - (b_j + b_j^\dagger) (S - b_{j+\delta}^\dagger b_{j+\delta}) \right] \\
&\quad \left. - i\frac{S}{2} D_{j,j+\delta}^{(z)} \left[ (b_j + b_j^\dagger) (b_{j+\delta} - b_{j+\delta}^\dagger) - (b_j - b_j^\dagger) (b_{j+\delta} + b_{j+\delta}^\dagger) \right] \right) \\
&= \sum_{j,\delta} \left( -i\sqrt{\frac{S}{2}} D_{j,j+\delta}^{(x)} \left[ S (b_j - b_j^\dagger - b_{j+\delta} + b_{j+\delta}^\dagger) \right. \right. \\
&\quad \left. \left. - b_j b_{j+\delta}^\dagger b_{j+\delta} + b_j^\dagger b_{j+\delta}^\dagger b_{j+\delta} + b_j^\dagger b_j b_{j+\delta} - b_j^\dagger b_j b_{j+\delta}^\dagger \right] \right. \\
&\quad + \sqrt{\frac{S}{2}} D_{j,j+\delta}^{(y)} \left[ S (-b_j - b_j^\dagger + b_{j+\delta} + b_{j+\delta}^\dagger) \right. \\
&\quad \left. + b_j b_{j+\delta}^\dagger b_{j+\delta} + b_j^\dagger b_{j+\delta}^\dagger b_{j+\delta} - b_j^\dagger b_j b_{j+\delta} - b_j^\dagger b_j b_{j+\delta}^\dagger \right] \\
&\quad \left. - iS D_{j,j+\delta}^{(z)} [b_j^\dagger b_{j+\delta} - b_j b_{j+\delta}^\dagger] \right) \\
&= \sqrt{\frac{S}{2}} \sum_{j,\delta} \left[ (iD_{j,j+\delta}^{(x)} + D_{j,j+\delta}^{(y)}) (-2Sb_j + b_j b_{j+\delta}^\dagger b_{j+\delta} - b_j^\dagger b_j b_{j+\delta}) \right. \\
&\quad + (-iD_{j,j+\delta}^{(x)} + D_{j,j+\delta}^{(y)}) (-2Sb_j^\dagger + b_j^\dagger b_{j+\delta}^\dagger b_{j+\delta} - b_j^\dagger b_j b_{j+\delta}^\dagger) \\
&\quad \left. - i\sqrt{2S} D_{j,j+\delta}^{(z)} b_j^\dagger b_{j+\delta} \right], \tag{A.2}
\end{aligned}$$

where I used that  $D_{j,j+\delta}$  is antisymmetric in the second last equality:  $D_{j,j+\delta} = -D_{j+\delta,j}$ . In the last equality I used that magnons are bosons:  $[b_j, b_{j+\delta}] = 0$ .

This is expressed in reciprocal space by using the Fourier transformed magnon

operators (2.11):

$$\begin{aligned}
H_{DM} &= \sqrt{\frac{S}{2}} \sum_{j,\delta} \left[ \left( iD_{j,j+\delta}^{(x)} + D_{j,j+\delta}^{(y)} \right) \left( -2Sb_j + b_j b_{j+\delta}^\dagger b_{j+\delta} - b_j^\dagger b_j b_{j+\delta} \right) \right. \\
&\quad + \left( -iD_{j,j+\delta}^{(x)} + D_{j,j+\delta}^{(y)} \right) \left( -2Sb_j^\dagger + b_j^\dagger b_{j+\delta}^\dagger b_{j+\delta} - b_j^\dagger b_j b_{j+\delta}^\dagger \right) \\
&\quad \left. - i\sqrt{2S} D_{j,j+\delta}^{(z)} b_j^\dagger b_{j+\delta} \right] \\
&= \sqrt{\frac{S}{2}} \sum_{j,\delta} \left[ \left( iD_{j,j+\delta}^{(x)} + D_{j,j+\delta}^{(y)} \right) \left( -\frac{2S}{\sqrt{N}} \sum_{\mathbf{k}} e^{-i\mathbf{k} \cdot \mathbf{R}_j} b_{\mathbf{k}} \right. \right. \\
&\quad + \frac{1}{N\sqrt{N}} \sum_{\mathbf{k},\mathbf{k}',\mathbf{k}''} e^{i(-\mathbf{k}+\mathbf{k}'-\mathbf{k}'') \cdot \mathbf{R}_j} e^{i(\mathbf{k}'-\mathbf{k}'') \cdot \mathbf{R}_\delta} b_{\mathbf{k}} b_{\mathbf{k}'}^\dagger b_{\mathbf{k}''} \\
&\quad \left. - \frac{1}{N\sqrt{N}} \sum_{\mathbf{k},\mathbf{k}',\mathbf{k}''} e^{i(\mathbf{k}-\mathbf{k}'-\mathbf{k}'') \cdot \mathbf{R}_j} e^{-i\mathbf{k}'' \cdot \mathbf{R}_\delta} b_{\mathbf{k}}^\dagger b_{\mathbf{k}'} b_{\mathbf{k}''} \right) \\
&\quad + \left( -iD_{j,j+\delta}^{(x)} + D_{j,j+\delta}^{(y)} \right) \left( -\frac{2S}{\sqrt{N}} \sum_{\mathbf{k}} e^{i\mathbf{k} \cdot \mathbf{R}_j} b_{\mathbf{k}}^\dagger \right. \\
&\quad + \frac{1}{N\sqrt{N}} \sum_{\mathbf{k},\mathbf{k}',\mathbf{k}''} e^{i(\mathbf{k}+\mathbf{k}'-\mathbf{k}'') \cdot \mathbf{R}_j} e^{i(\mathbf{k}'-\mathbf{k}'') \cdot \mathbf{R}_\delta} b_{\mathbf{k}}^\dagger b_{\mathbf{k}'}^\dagger b_{\mathbf{k}''} \\
&\quad \left. - \frac{1}{N\sqrt{N}} \sum_{\mathbf{k},\mathbf{k}',\mathbf{k}''} e^{i(\mathbf{k}-\mathbf{k}'+\mathbf{k}'') \cdot \mathbf{R}_j} e^{i\mathbf{k}'' \cdot \mathbf{R}_\delta} b_{\mathbf{k}}^\dagger b_{\mathbf{k}'} b_{\mathbf{k}''}^\dagger \right) \\
&\quad \left. - i\sqrt{2S} D_{j,j+\delta}^{(z)} \sum_{\mathbf{k},\mathbf{k}'} e^{i(\mathbf{k}-\mathbf{k}') \cdot \mathbf{R}_j} e^{-\mathbf{k}' \cdot \mathbf{R}_\delta} b_{\mathbf{k}}^\dagger b_{\mathbf{k}'} \right] \\
&= -\sqrt{\frac{2S^3}{N}} Z \sum_{j,\mathbf{k}} \left( iD_0^{(x)} + D_0^{(y)} \right) e^{-i\mathbf{k} \cdot \mathbf{R}_j} b_{\mathbf{k}} + \left( -iD_0^{(x)} + D_0^{(y)} \right) e^{i\mathbf{k} \cdot \mathbf{R}_j} b_{\mathbf{k}}^\dagger \\
&\quad + \sqrt{\frac{S}{2N^3}} Z \sum_{j,\mathbf{k},\mathbf{k}',\mathbf{k}''} \left( iD_{-\mathbf{k}'+\mathbf{k}''}^{(x)} + D_{-\mathbf{k}'+\mathbf{k}''}^{(y)} \right) e^{i(-\mathbf{k}+\mathbf{k}'-\mathbf{k}'') \cdot \mathbf{R}_j} b_{\mathbf{k}} b_{\mathbf{k}'}^\dagger b_{\mathbf{k}''} \\
&\quad - \left( iD_{\mathbf{k}''}^{(x)} + D_{\mathbf{k}''}^{(y)} \right) e^{i(\mathbf{k}-\mathbf{k}'-\mathbf{k}'') \cdot \mathbf{R}_j} b_{\mathbf{k}}^\dagger b_{\mathbf{k}'} b_{\mathbf{k}''} \\
&\quad + \left( -iD_{-\mathbf{k}'+\mathbf{k}''}^{(x)} + D_{-\mathbf{k}'+\mathbf{k}''}^{(y)} \right) e^{i(\mathbf{k}+\mathbf{k}'-\mathbf{k}'') \cdot \mathbf{R}_j} b_{\mathbf{k}}^\dagger b_{\mathbf{k}'}^\dagger b_{\mathbf{k}''} \\
&\quad - \left( -iD_{-\mathbf{k}''}^{(x)} + D_{-\mathbf{k}''}^{(y)} \right) e^{i(\mathbf{k}-\mathbf{k}'+\mathbf{k}'') \cdot \mathbf{R}_j} b_{\mathbf{k}}^\dagger b_{\mathbf{k}'} b_{\mathbf{k}''}^\dagger \\
&\quad - \sqrt{2i} \frac{SZ}{N} \sum_{\mathbf{k},\mathbf{k}'} D_{\mathbf{k}'}^{(z)} e^{i(\mathbf{k}-\mathbf{k}') \cdot \mathbf{R}_j} b_{\mathbf{k}}^\dagger b_{\mathbf{k}'}
\end{aligned}$$

$$\begin{aligned}
&= -\sqrt{2S^3NZ} \left[ \left( iD_0^{(x)} + D_0^{(y)} \right) b_0 + \left( -iD_0^{(x)} + D_0^{(y)} \right) b_0^\dagger \right] - \sqrt{2}iSZ \sum_{\mathbf{k}} D_{\mathbf{k}}^{(z)} b_{\mathbf{k}}^\dagger b_{\mathbf{k}} \\
&+ \sqrt{\frac{S}{2N}} Z \sum_{\mathbf{k}, \mathbf{k}'} \left[ \left( iD_{-\mathbf{k}}^{(x)} + D_{-\mathbf{k}}^{(y)} \right) b_{\mathbf{k}} b_{\mathbf{k}'}^\dagger b_{-\mathbf{k}+\mathbf{k}'} - \left( iD_{\mathbf{k}-\mathbf{k}'}^{(x)} + D_{\mathbf{k}-\mathbf{k}'}^{(y)} \right) b_{\mathbf{k}}^\dagger b_{\mathbf{k}'} b_{\mathbf{k}-\mathbf{k}'} \right. \\
&\quad \left. + \left( -iD_{\mathbf{k}}^{(x)} + D_{\mathbf{k}}^{(y)} \right) b_{\mathbf{k}}^\dagger b_{\mathbf{k}'}^\dagger b_{\mathbf{k}+\mathbf{k}'} - \left( -iD_{\mathbf{k}-\mathbf{k}'}^{(x)} + D_{\mathbf{k}-\mathbf{k}'}^{(y)} \right) b_{\mathbf{k}}^\dagger b_{\mathbf{k}'} b_{-\mathbf{k}+\mathbf{k}'} \right].
\end{aligned} \tag{A.3}$$

with  $D_{\mathbf{k}} = \frac{1}{Z} \sum_{\delta} D_{j,j+\delta} e^{-i\mathbf{k} \cdot \mathbf{R}_{\delta}}$  and  $D_0 = \frac{1}{Z} \sum_{\delta} D_{j,j+\delta}$ .

### A.3. Scalar Contribution

The scalar decomposition of the Hamiltonian (2.16) is expressed in terms of phonon and magnon operators in reciprocal space by inserting the Fourier transformed expression for displacement (2.17) and spin (2.11), respectively. The relation between spin and magnetic moment  $\mathbf{M}_j = \gamma \mathbf{S}_j$  is also used:

$$\begin{aligned}
H^{(S)} &= - \sum_{j,\delta} T_{j,j+\delta} \mathbf{Q}_j \cdot \mathbf{M}_{j+\delta} \\
&= - \sum_{j,\delta} T_{j,j+\delta} i \sum_{\mathbf{k},\lambda} \sqrt{\frac{1}{2mN\omega_{\mathbf{k},\lambda}}} \boldsymbol{\xi}_{\mathbf{k},\lambda} \left( a_{\mathbf{k},\lambda} + a_{-\mathbf{k},\lambda}^\dagger \right) e^{i\mathbf{k} \cdot \mathbf{R}_j} \cdot \gamma \mathbf{S}_{j+\delta} \\
&= -i \sum_{j,\delta,\mathbf{k},\lambda} \frac{\gamma}{\sqrt{2mN\omega_{\mathbf{k},\lambda}}} T_{j,j+\delta} \left( a_{\mathbf{k},\lambda} + a_{-\mathbf{k},\lambda}^\dagger \right) e^{i\mathbf{k} \cdot \mathbf{R}_j} \boldsymbol{\xi}_{\mathbf{k},\lambda} \\
&\quad \cdot \left( \sqrt{\frac{S}{2N}} \sum_{\mathbf{k}'} e^{-i\mathbf{k}' \cdot (\mathbf{R}_j + \mathbf{R}_{\delta})} \left( b_{\mathbf{k}'} + b_{-\mathbf{k}'}^\dagger \right), -i \sqrt{\frac{S}{2N}} \sum_{\mathbf{k}'} e^{-i\mathbf{k}' \cdot (\mathbf{R}_j + \mathbf{R}_{\delta})} \left( b_{\mathbf{k}'} - b_{-\mathbf{k}'}^\dagger \right) \right. \\
&\quad \left. , S - \frac{1}{N} \sum_{\mathbf{k}', \mathbf{k}''} e^{i(\mathbf{k}' - \mathbf{k}'') \cdot (\mathbf{R}_j + \mathbf{R}_{\delta})} b_{\mathbf{k}'}^\dagger b_{\mathbf{k}''} \right) \\
&= \frac{-i\gamma}{\sqrt{2mN}} \sum_{j,\delta,\mathbf{k},\lambda} \frac{1}{\sqrt{\omega_{\mathbf{k},\lambda}}} T_{j,j+\delta} \left( a_{\mathbf{k},\lambda} + a_{-\mathbf{k},\lambda}^\dagger \right) e^{i\mathbf{k} \cdot \mathbf{R}_j} \\
&\quad \times \left\{ S \boldsymbol{\xi}_{\mathbf{k},\lambda}^{(z)} + \sqrt{\frac{S}{2N}} \sum_{\mathbf{k}'} e^{-i\mathbf{k}' \cdot \mathbf{R}_j} e^{-i\mathbf{k}' \cdot \mathbf{R}_{\delta}} \left[ \boldsymbol{\xi}_{\mathbf{k},\lambda}^{(x)} \left( b_{\mathbf{k}'} + b_{-\mathbf{k}'}^\dagger \right) - i \boldsymbol{\xi}_{\mathbf{k},\lambda}^{(y)} \left( b_{\mathbf{k}'} - b_{-\mathbf{k}'}^\dagger \right) \right] \right. \\
&\quad \left. - \frac{1}{N} \boldsymbol{\xi}_{\mathbf{k},\lambda}^{(z)} \sum_{\mathbf{k}', \mathbf{k}''} e^{i(\mathbf{k}' - \mathbf{k}'') \cdot \mathbf{R}_j} e^{i(\mathbf{k}' - \mathbf{k}'') \cdot \mathbf{R}_{\delta}} b_{\mathbf{k}'}^\dagger b_{\mathbf{k}''} \right\}
\end{aligned}$$

$$\begin{aligned}
&= \frac{-i\gamma Z}{\sqrt{2mN}} \sum_{j,\mathbf{k},\lambda} \frac{1}{\sqrt{\omega_{\mathbf{k},\lambda}}} \left( a_{\mathbf{k},\lambda} + a_{-\mathbf{k},\lambda}^\dagger \right) e^{i\mathbf{k} \cdot \mathbf{R}_j} \times \left\{ S \xi_{\mathbf{k},\lambda}^{(z)} T_0 \right. \\
&\quad \left. + \sqrt{\frac{S}{2N}} \sum_{\mathbf{k}'} T_{\mathbf{k}'} e^{-i\mathbf{k}' \cdot \mathbf{R}_j} \left[ \xi_{\mathbf{k},\lambda}^{(x)} \left( b_{\mathbf{k}'} + b_{-\mathbf{k}'}^\dagger \right) - i \xi_{\mathbf{k},\lambda}^{(y)} \left( b_{\mathbf{k}'} - b_{-\mathbf{k}'}^\dagger \right) \right] \right. \\
&\quad \left. - \frac{1}{N} \xi_{\mathbf{k},\lambda}^{(z)} \sum_{\mathbf{k}',\mathbf{k}''} T_{-\mathbf{k}'+\mathbf{k}''} e^{i(\mathbf{k}'-\mathbf{k}'') \cdot \mathbf{R}_j} b_{\mathbf{k}'}^\dagger b_{\mathbf{k}''} \right\} \\
&= -\frac{i\gamma Z}{\sqrt{2m}} \sum_{\mathbf{k},\lambda} \frac{T_{\mathbf{k}}}{\sqrt{\omega_{\mathbf{k},\lambda}}} \left( a_{\mathbf{k},\lambda} + a_{-\mathbf{k},\lambda}^\dagger \right) \\
&\quad \times \left\{ \sqrt{\frac{S}{2}} \left[ \xi_{\mathbf{k},\lambda}^{(x)} \left( b_{\mathbf{k}} + b_{-\mathbf{k}}^\dagger \right) - i \xi_{\mathbf{k},\lambda}^{(y)} \left( b_{\mathbf{k}} - b_{-\mathbf{k}}^\dagger \right) \right] - \frac{1}{\sqrt{N}} \sum_{\mathbf{k}'} \xi_{\mathbf{k},\lambda}^{(z)} b_{\mathbf{k}'}^\dagger b_{\mathbf{k}+\mathbf{k}'} \right\} \\
&= \frac{\gamma Z}{\sqrt{2m}} \left( \sum_{\mathbf{k},\lambda} \frac{T_{\mathbf{k}}}{\sqrt{\omega_{\mathbf{k},\lambda}}} \left( a_{\mathbf{k},\lambda} + a_{-\mathbf{k},\lambda}^\dagger \right) \left\{ \sqrt{\frac{S}{2}} \left[ -i \xi_{\mathbf{k},\lambda}^{(x)} \left( b_{\mathbf{k}} + b_{-\mathbf{k}}^\dagger \right) \right. \right. \right. \\
&\quad \left. \left. + \xi_{\mathbf{k},\lambda}^{(y)} \left( b_{\mathbf{k}} - b_{-\mathbf{k}}^\dagger \right) \right] + \frac{i}{\sqrt{N}} \sum_{\mathbf{k}'} \xi_{\mathbf{k},\lambda}^{(z)} b_{\mathbf{k}'}^\dagger b_{\mathbf{k}+\mathbf{k}'} \right\} \right), \tag{A.4}
\end{aligned}$$

with  $T_{\mathbf{k}} = \frac{1}{Z} \sum_{\delta} T_{j,j+\delta} e^{-i\mathbf{k} \cdot \mathbf{R}_{\delta}}$  and  $T_0 = \frac{1}{Z} \sum_{\delta} T_{j,j+\delta}$ . In the second last equation I used that the phonon polarization approaches zero faster than the square root of the free phonon frequency when the crystal momentum approaches zero, see equation (2.18).

#### A.4. Vector Contribution

Similarly to the scalar contribution, the vector decomposition of the Hamiltonian given by equation (2.16) is expressed in terms of magnon and phonon operators in reciprocal space by inserting the Fourier transformed expression for spin (2.10) and displacement (2.17), respectively. The relation between spin and magnetic moment  $\mathbf{M}_j = \gamma \mathbf{S}_j$  is also used:

$$\begin{aligned}
H^{(V)} &= - \sum_{j,\delta} \mathbf{T}_{j,j+\delta} \cdot (\mathbf{Q}_j \times \mathbf{M}_{j+\delta}) \\
&= -\gamma \sum_{j,\delta} \left[ T_{j,j+\delta}^{(x)} \left( Q_j^{(y)} S_{j+\delta}^{(z)} - Q_j^{(z)} S_{j+\delta}^{(y)} \right) + T_{j,j+\delta}^{(y)} \left( Q_j^{(z)} S_{j+\delta}^{(x)} - Q_j^{(x)} S_{j+\delta}^{(z)} \right) \right. \\
&\quad \left. + T_{j,j+\delta}^{(z)} \left( Q_j^{(x)} S_{j+\delta}^{(y)} - Q_j^{(y)} S_{j+\delta}^{(x)} \right) \right]
\end{aligned}$$

$$\begin{aligned}
&= -\gamma \sum_{j,\delta} i \sum_{\mathbf{k},\lambda} \frac{1}{\sqrt{2mN\omega_{\mathbf{k},\lambda}}} \left( a_{\mathbf{k},\lambda} + a_{-\mathbf{k},\lambda}^\dagger \right) e^{i\mathbf{k}\cdot\mathbf{R}_j} \\
&\quad \times \left\{ T_{j,j+\delta}^{(x)} \left[ \xi_{\mathbf{k},\lambda}^{(y)} \left( S - \frac{1}{N} \sum_{\mathbf{k}',\mathbf{k}''} e^{i(\mathbf{k}'-\mathbf{k}'')\cdot\mathbf{R}_j} e^{i(\mathbf{k}'-\mathbf{k}'')\cdot\mathbf{R}_\delta} b_{\mathbf{k}'}^\dagger b_{\mathbf{k}''} \right) \right. \right. \\
&\quad \left. \left. + i\sqrt{\frac{S}{2N}} \xi_{\mathbf{k},\lambda}^{(z)} \sum_{\mathbf{k}'} e^{-i\mathbf{k}'\cdot\mathbf{R}_j} e^{-i\mathbf{k}'\cdot\mathbf{R}_\delta} \left( b_{\mathbf{k}'} - b_{-\mathbf{k}'}^\dagger \right) \right] \right. \\
&\quad \left. + T_{j,j+\delta}^{(y)} \left[ \sqrt{\frac{S}{2N}} \xi_{\mathbf{k},\lambda}^{(z)} \sum_{\mathbf{k}'} e^{-i\mathbf{k}'\cdot\mathbf{R}_j} e^{-i\mathbf{k}'\cdot\mathbf{R}_\delta} \left( b_{\mathbf{k}'} + b_{-\mathbf{k}'}^\dagger \right) \right. \right. \\
&\quad \left. \left. - \xi_{\mathbf{k},\lambda}^{(x)} \left( S - \frac{1}{N} \sum_{\mathbf{k}',\mathbf{k}''} e^{i(\mathbf{k}'-\mathbf{k}'')\cdot\mathbf{R}_j} e^{i(\mathbf{k}'-\mathbf{k}'')\cdot\mathbf{R}_\delta} b_{\mathbf{k}'}^\dagger b_{\mathbf{k}''} \right) \right] \right. \\
&\quad \left. - T_{j,j+\delta}^{(z)} \left[ i\sqrt{\frac{S}{2N}} \xi_{\mathbf{k},\lambda}^{(x)} \sum_{\mathbf{k}'} e^{-i\mathbf{k}'\cdot\mathbf{R}_j} e^{-i\mathbf{k}'\cdot\mathbf{R}_\delta} \left( b_{\mathbf{k}'} - b_{-\mathbf{k}'}^\dagger \right) \right. \right. \\
&\quad \left. \left. + \sqrt{\frac{S}{2N}} \xi_{\mathbf{k},\lambda}^{(y)} \sum_{\mathbf{k}'} e^{-i\mathbf{k}'\cdot\mathbf{R}_j} e^{-i\mathbf{k}'\cdot\mathbf{R}_\delta} \left( b_{\mathbf{k}'} + b_{-\mathbf{k}'}^\dagger \right) \right] \right\} \\
&= \frac{-i\gamma Z}{\sqrt{2m}} \sum_{\lambda,\mathbf{k}} \frac{1}{\sqrt{\omega_{\mathbf{k},\lambda}}} \left( a_{\mathbf{k},\lambda} + a_{-\mathbf{k},\lambda}^\dagger \right) \\
&\quad \times \left\{ \sqrt{\frac{S}{2}} \left[ iT_{\mathbf{k}}^{(x)} \xi_{\mathbf{k},\lambda}^{(z)} \left( b_{\mathbf{k}} - b_{-\mathbf{k}}^\dagger \right) + T_{\mathbf{k}}^{(y)} \xi_{\mathbf{k},\lambda}^{(z)} \left( b_{\mathbf{k}} + b_{-\mathbf{k}}^\dagger \right) \right. \right. \\
&\quad \left. \left. - iT_{\mathbf{k}}^{(z)} \xi_{\mathbf{k},\lambda}^{(x)} \left( b_{\mathbf{k}} - b_{-\mathbf{k}}^\dagger \right) - T_{\mathbf{k}}^{(z)} \xi_{\mathbf{k},\lambda}^{(y)} \left( b_{\mathbf{k}} + b_{-\mathbf{k}}^\dagger \right) \right] \right. \\
&\quad \left. - \frac{1}{\sqrt{N}} \sum_{\mathbf{k}'} \left( T_{\mathbf{k}}^{(x)} \xi_{\mathbf{k},\lambda}^{(y)} b_{\mathbf{k}'}^\dagger b_{\mathbf{k}+\mathbf{k}'} - T_{\mathbf{k}}^{(y)} \xi_{\mathbf{k},\lambda}^{(x)} b_{\mathbf{k}'}^\dagger b_{\mathbf{k}+\mathbf{k}'} \right) \right\} \\
&= \frac{\gamma Z}{\sqrt{2m}} \sum_{\lambda,\mathbf{k}} \frac{1}{\sqrt{\omega_{\mathbf{k},\lambda}}} \left( a_{\mathbf{k},\lambda} + a_{-\mathbf{k},\lambda}^\dagger \right) \\
&\quad \times \left\{ \sqrt{\frac{S}{2}} \left[ T_{\mathbf{k}}^{(x)} \xi_{\mathbf{k},\lambda}^{(z)} \left( b_{\mathbf{k}} - b_{-\mathbf{k}}^\dagger \right) - iT_{\mathbf{k}}^{(y)} \xi_{\mathbf{k},\lambda}^{(z)} \left( b_{\mathbf{k}} + b_{-\mathbf{k}}^\dagger \right) \right. \right. \\
&\quad \left. \left. - T_{\mathbf{k}}^{(z)} \xi_{\mathbf{k},\lambda}^{(x)} \left( b_{\mathbf{k}} - b_{-\mathbf{k}}^\dagger \right) + iT_{\mathbf{k}}^{(z)} \xi_{\mathbf{k},\lambda}^{(y)} \left( b_{\mathbf{k}} + b_{-\mathbf{k}}^\dagger \right) \right] \right. \\
&\quad \left. + \frac{i}{\sqrt{N}} \sum_{\mathbf{k}'} \left( T_{\mathbf{k}}^{(x)} \xi_{\mathbf{k},\lambda}^{(y)} b_{\mathbf{k}'}^\dagger b_{\mathbf{k}+\mathbf{k}'} - T_{\mathbf{k}}^{(y)} \xi_{\mathbf{k},\lambda}^{(x)} b_{\mathbf{k}'}^\dagger b_{\mathbf{k}+\mathbf{k}'} \right) \right\} \tag{A.5}
\end{aligned}$$

with  $\mathbf{T}_{\mathbf{k}} = \frac{1}{Z} \sum_{\delta} \mathbf{T}_{j,j+\delta} e^{-i\mathbf{k}\cdot\mathbf{R}_\delta}$  and  $\mathbf{T}_0 = \frac{1}{Z} \sum_{\delta} \mathbf{T}_{j,j+\delta}$ . In the second last equation

I used that the phonon polarization approaches zero faster than the square root of the free phonon frequency when the crystal momentum approaches zero, see equation (2.18).

## A.5. Coupled Hamiltonian

If  $\sqrt{N} \gg \sum_{\mathbf{k}} b_{\mathbf{k}}^\dagger b_{\mathbf{k}}$ , the Hamiltonian from equation (2.21) becomes

$$\begin{aligned}
H_T &= H_p + H_{he} + H_{DM} + H_{SQ}^{(S)} + H_{SQ}^{(V)} \\
&= -J_{\parallel} N S^2 Z + \sum_{\mathbf{k}, \lambda} \frac{\omega_{\mathbf{k}, \lambda}}{2} + \sum_{\mathbf{k}, \lambda} F'_{\mathbf{k}, \lambda} (a_{\mathbf{k}, \lambda} + a_{-\mathbf{k}, \lambda}^\dagger) + \sum_{\mathbf{k}} (G_{\mathbf{k}} b_{\mathbf{k}} + G_{-\mathbf{k}}^* b_{-\mathbf{k}}^\dagger) \\
&\quad + \sum_{\mathbf{k}, \lambda} \omega_{\mathbf{k}, \lambda} a_{\mathbf{k}, \lambda}^\dagger a_{\mathbf{k}, \lambda} + \sum_{\mathbf{k}} \epsilon_{\mathbf{k}} b_{\mathbf{k}}^\dagger b_{\mathbf{k}} + \sum_{\mathbf{k}, \lambda} (a_{\mathbf{k}, \lambda} + a_{-\mathbf{k}, \lambda}^\dagger) (E_{\mathbf{k}, \lambda} b_{\mathbf{k}} + E_{-\mathbf{k}, \lambda}^* b_{-\mathbf{k}}^\dagger).
\end{aligned} \tag{A.6}$$

Let  $\alpha_{\mathbf{k}, \lambda} = a_{\mathbf{k}, \lambda} + I_{\mathbf{k}, \lambda}$  and  $\beta_{\mathbf{k}, \lambda} = b_{\mathbf{k}} + J_{\mathbf{k}, \lambda}$  where  $I_{\mathbf{k}, \lambda} = I_{-\mathbf{k}, \lambda}^*$  and assume that the Hamiltonian can be written as follows:

$$\begin{aligned}
H &= \sum_{\mathbf{k}, \lambda} \omega_{\mathbf{k}, \lambda} \alpha_{\mathbf{k}, \lambda}^\dagger \alpha_{\mathbf{k}, \lambda} + \epsilon_{\mathbf{k}, \lambda} \beta_{\mathbf{k}, \lambda}^\dagger \beta_{\mathbf{k}, \lambda} \\
&\quad + (\alpha_{\mathbf{k}, \lambda} + \alpha_{-\mathbf{k}, \lambda}^\dagger) (E_{\mathbf{k}, \lambda} \beta_{\mathbf{k}, \lambda} + E_{-\mathbf{k}, \lambda}^* \beta_{-\mathbf{k}, \lambda}^\dagger) + K_{\mathbf{k}, \lambda} \\
&= \sum_{\mathbf{k}, \lambda} \omega_{\mathbf{k}, \lambda} (a_{\mathbf{k}, \lambda}^\dagger + I_{\mathbf{k}, \lambda}^*) (a_{\mathbf{k}, \lambda} + I_{\mathbf{k}, \lambda}) + \epsilon_{\mathbf{k}, \lambda} (b_{\mathbf{k}}^\dagger + J_{\mathbf{k}, \lambda}^*) (b_{\mathbf{k}} + J_{\mathbf{k}, \lambda}) \\
&\quad + (a_{\mathbf{k}, \lambda} + a_{-\mathbf{k}, \lambda}^\dagger + I_{\mathbf{k}, \lambda} + I_{-\mathbf{k}, \lambda}^*) \\
&\quad \times (E_{\mathbf{k}, \lambda} [b_{\mathbf{k}} + J_{\mathbf{k}, \lambda}] + E_{-\mathbf{k}, \lambda}^* [b_{-\mathbf{k}}^\dagger + J_{-\mathbf{k}, \lambda}^*]) + K_{\mathbf{k}, \lambda} \\
&= \sum_{\mathbf{k}, \lambda} \omega_{\mathbf{k}, \lambda} a_{\mathbf{k}, \lambda}^\dagger a_{\mathbf{k}, \lambda} + \omega_{\mathbf{k}, \lambda} I_{\mathbf{k}, \lambda}^* (a_{\mathbf{k}, \lambda} + a_{-\mathbf{k}, \lambda}^\dagger) + \omega_{\mathbf{k}, \lambda} |I_{\mathbf{k}, \lambda}|^2 + \epsilon_{\mathbf{k}, \lambda} b_{\mathbf{k}}^\dagger b_{\mathbf{k}} \\
&\quad + (\epsilon_{\mathbf{k}, \lambda} J_{\mathbf{k}, \lambda}^* b_{\mathbf{k}} + \epsilon_{-\mathbf{k}, \lambda} J_{-\mathbf{k}, \lambda} b_{-\mathbf{k}}^\dagger) + \epsilon_{\mathbf{k}, \lambda} |J_{\mathbf{k}, \lambda}|^2 + (a_{\mathbf{k}, \lambda} + a_{-\mathbf{k}, \lambda}^\dagger) \\
&\quad \times (E_{\mathbf{k}, \lambda} b_{\mathbf{k}} + E_{-\mathbf{k}, \lambda}^* b_{-\mathbf{k}}^\dagger) + (E_{\mathbf{k}, \lambda} J_{\mathbf{k}, \lambda} + E_{-\mathbf{k}, \lambda}^* J_{-\mathbf{k}, \lambda}^*) (a_{\mathbf{k}, \lambda} + a_{-\mathbf{k}, \lambda}^\dagger) \\
&\quad + 2I_{\mathbf{k}, \lambda} (E_{\mathbf{k}, \lambda} b_{\mathbf{k}} + E_{-\mathbf{k}, \lambda}^* b_{-\mathbf{k}}^\dagger) + 2I_{\mathbf{k}, \lambda} (E_{\mathbf{k}, \lambda} J_{\mathbf{k}, \lambda} + E_{-\mathbf{k}, \lambda}^* J_{-\mathbf{k}, \lambda}^*) + K_{\mathbf{k}, \lambda}.
\end{aligned} \tag{A.7}$$

The Hamiltonian in equation (A.7) should be that same as in equation (A.6). Thus, the coefficients in both equations should be equal:

$$\begin{aligned}
-J_{\parallel} N S^2 Z + \sum_{\mathbf{k}, \lambda} \frac{\omega_{\mathbf{k}, \lambda}}{2} &= \sum_{\mathbf{k}, \lambda} \omega_{\mathbf{k}, \lambda} |I_{\mathbf{k}, \lambda}|^2 + \epsilon_{\mathbf{k}, \lambda} |J_{\mathbf{k}, \lambda}|^2 \\
&\quad + 2I_{\mathbf{k}, \lambda} (E_{\mathbf{k}, \lambda} J_{\mathbf{k}, \lambda} + E_{-\mathbf{k}, \lambda}^* J_{-\mathbf{k}, \lambda}^*) + K_{\mathbf{k}, \lambda},
\end{aligned} \tag{A.8}$$

$$F'_{\mathbf{k},\lambda} = \omega_{\mathbf{k},\lambda} I_{\mathbf{k},\lambda}^* + E_{\mathbf{k},\lambda} J_{\mathbf{k},\lambda} + E_{-\mathbf{k},\lambda}^* J_{-\mathbf{k},\lambda}^*, \quad (\text{A.9})$$

$$G_{\mathbf{k}} = \sum_{\lambda} \epsilon_{\mathbf{k},\lambda} J_{\mathbf{k},\lambda}^* + 2I_{\mathbf{k},\lambda} E_{\mathbf{k},\lambda}, \quad (\text{A.10})$$

$$\sum_{\lambda} \epsilon_{\mathbf{k},\lambda} = \epsilon_{\mathbf{k}}. \quad (\text{A.11})$$

Note that equation (A.9) only holds if  $F'_{\mathbf{k},\lambda} = F'_{-\mathbf{k},\lambda}^*$ , since  $I_{\mathbf{k},\lambda} = I_{-\mathbf{k},\lambda}^*$ . Equations (A.8) and (A.11) can be solved by letting

$$K_{\mathbf{k},\lambda} = -\frac{J_{\parallel} S^2 Z}{L} + \omega_{\mathbf{k},\lambda} \left( \frac{1}{2} - |I_{\mathbf{k},\lambda}|^2 \right) - \epsilon_{\mathbf{k},\lambda} |J_{\mathbf{k},\lambda}|^2 - 2I_{\mathbf{k}} (E_{\mathbf{k},\lambda} J_{\mathbf{k},\lambda} + E_{-\mathbf{k},\lambda}^* J_{-\mathbf{k},\lambda}^*) \quad (\text{A.12})$$

and

$$\epsilon_{\mathbf{k},\lambda} = \frac{\epsilon_{\mathbf{k}}}{L}, \quad (\text{A.13})$$

respectively.

Applying equation (2.18) to the definition of  $F_{\mathbf{k},\lambda}$  found in reference [3] as well as to equations (2.23) and (2.25) gives

$$\lim_{\mathbf{k} \rightarrow \mathbf{0}} F_{\mathbf{k},\lambda}(\mathbf{r}_j) = 0, \quad (\text{A.14})$$

$$\lim_{\mathbf{k} \rightarrow \mathbf{0}} F'_{\mathbf{k},\lambda} = \lim_{\mathbf{k} \rightarrow \mathbf{0}} \sum_j F_{\mathbf{k},\lambda}(\mathbf{r}_j) e^{i\mathbf{k} \cdot \mathbf{r}_j} = 0 \quad (\text{A.15})$$

and

$$\lim_{\mathbf{k} \rightarrow \mathbf{0}} E_{\mathbf{k},\lambda} = 0, \quad (\text{A.16})$$

respectively. From equation (A.9) and the limits above, it follows that  $\lim_{\mathbf{k} \rightarrow \mathbf{0}} I_{\mathbf{k},\lambda} = 0$ . Additionally, in the limit of zero crystal momentum, equation (A.10) becomes

$$\lim_{\mathbf{k} \rightarrow \mathbf{0}} J_{\mathbf{k},\lambda} = \lim_{\mathbf{k} \rightarrow \mathbf{0}} \frac{\sqrt{2N S^3 Z}}{\epsilon_{\mathbf{k}}} \left( iD_0^{(x)} - D_0^{(y)} \right) \delta_{\mathbf{k},\mathbf{0}}. \quad (\text{A.17})$$

In the case of  $\mathbf{k} \neq \mathbf{0}$ , equation (A.10) can be rewritten as follows

$$I_{\mathbf{k},\lambda} = -\frac{\epsilon_{\mathbf{k},\lambda} J_{\mathbf{k},\lambda}^*}{2E_{\mathbf{k},\lambda}}. \quad (\text{A.18})$$

Since  $I_{\mathbf{k},\lambda} = I_{-\mathbf{k},\lambda}^*$  it follows that

$$-\frac{\epsilon_{\mathbf{k},\lambda} J_{\mathbf{k},\lambda}^*}{2E_{\mathbf{k},\lambda}} = -\frac{\epsilon_{-\mathbf{k},\lambda}^* J_{-\mathbf{k},\lambda}}{2E_{-\mathbf{k},\lambda}^*}. \quad (\text{A.19})$$

Inserting the two equations just above into equation (A.9) gives

$$\begin{aligned}
F'_{\mathbf{k},\lambda} &= \omega_{\mathbf{k},\lambda} I_{\mathbf{k},\lambda}^* + E_{\mathbf{k},\lambda} J_{\mathbf{k},\lambda} + E_{-\mathbf{k},\lambda}^* J_{-\mathbf{k},\lambda}^* \\
&= -\omega_{\mathbf{k},\lambda} \frac{\epsilon_{\mathbf{k},\lambda} J_{\mathbf{k},\lambda}}{2E_{\mathbf{k},\lambda}^*} + E_{\mathbf{k},\lambda} J_{\mathbf{k},\lambda} + E_{-\mathbf{k},\lambda}^* J_{\mathbf{k},\lambda} \frac{\epsilon_{\mathbf{k},\lambda} E_{-\mathbf{k},\lambda}}{\epsilon_{-\mathbf{k},\lambda} E_{\mathbf{k},\lambda}^*} \\
&= \frac{-\omega_{\mathbf{k},\lambda} \epsilon_{\mathbf{k},\lambda} \epsilon_{-\mathbf{k},\lambda} + 2E_{\mathbf{k},\lambda}^2 (\epsilon_{-\mathbf{k},\lambda} - \epsilon_{\mathbf{k},\lambda})}{2\epsilon_{-\mathbf{k},\lambda} E_{\mathbf{k},\lambda}} J_{\mathbf{k},\lambda},
\end{aligned} \tag{A.20}$$

implying that

$$J_{\mathbf{k},\lambda} = \frac{2F'_{\mathbf{k},\lambda} \epsilon_{-\mathbf{k},\lambda} E_{\mathbf{k},\lambda}}{-\omega_{\mathbf{k},\lambda} \epsilon_{\mathbf{k},\lambda} \epsilon_{-\mathbf{k},\lambda} + 2E_{\mathbf{k},\lambda}^2 (\epsilon_{-\mathbf{k},\lambda} - \epsilon_{\mathbf{k},\lambda})}. \tag{A.21}$$

Inserting this into equation (A.18) yields

$$I_{\mathbf{k},\lambda} = \frac{-F_{\mathbf{k},\lambda}'^* \epsilon_{\mathbf{k},\lambda} \epsilon_{-\mathbf{k},\lambda} E_{\mathbf{k},\lambda}^*}{-\omega_{\mathbf{k},\lambda} \epsilon_{\mathbf{k},\lambda} \epsilon_{-\mathbf{k},\lambda} E_{\mathbf{k},\lambda} + 2E_{\mathbf{k},\lambda}^* |E_{\mathbf{k},\lambda}|^2 (\epsilon_{-\mathbf{k},\lambda} - \epsilon_{\mathbf{k},\lambda})}. \tag{A.22}$$

## A.6. Green's Functions

Acting with the partial derivative with respect to time at Green's function of the shifted phonon destruction operator  $\alpha_{\mathbf{k},\lambda}$  (3.5) yields:

$$\begin{aligned}
&i\partial_t g_{\alpha_{\mathbf{k},\lambda}}(t-t') \\
&= \partial_t \left\langle T_t \alpha_{\mathbf{k},\lambda}(t) \alpha_{\mathbf{k},\lambda}^\dagger(t') \right\rangle \\
&= \partial_t \left[ \theta(t-t') \left\langle \alpha_{\mathbf{k},\lambda}(t) \alpha_{\mathbf{k},\lambda}^\dagger(t') \right\rangle + \theta(t'-t) \left\langle \alpha_{\mathbf{k},\lambda}^\dagger(t') \alpha_{\mathbf{k},\lambda}(t) \right\rangle \right] \\
&= \delta(t-t') \left\langle \alpha_{\mathbf{k},\lambda}(t) \alpha_{\mathbf{k},\lambda}^\dagger(t') \right\rangle + \theta(t-t') \left\langle \partial_t \alpha_{\mathbf{k},\lambda}(t) \alpha_{\mathbf{k},\lambda}^\dagger(t') \right\rangle \\
&\quad - \delta(t'-t) \left\langle \alpha_{\mathbf{k},\lambda}^\dagger(t') \alpha_{\mathbf{k},\lambda}(t) \right\rangle + \theta(t'-t) \left\langle \alpha_{\mathbf{k},\lambda}^\dagger(t') \partial_t \alpha_{\mathbf{k},\lambda}(t) \right\rangle \\
&= \delta(t-t') \left\langle \left[ \alpha_{\mathbf{k},\lambda}(t), \alpha_{\mathbf{k},\lambda}^\dagger(t') \right] \right\rangle + \left\langle T_t \partial_t \alpha_{\mathbf{k},\lambda}(t) \alpha_{\mathbf{k},\lambda}^\dagger(t') \right\rangle \\
&= \delta(t-t') \left\langle \left[ \alpha_{\mathbf{k},\lambda}(t), \alpha_{\mathbf{k},\lambda}^\dagger(t') \right] \right\rangle - i \left\langle T_t [\alpha_{\mathbf{k},\lambda}(t), H] \alpha_{\mathbf{k},\lambda}^\dagger(t') \right\rangle \\
&= \delta(t-t') + \omega_{\mathbf{k},\lambda} g_{\alpha_{\mathbf{k},\lambda}}(t, t') - i \left\langle T_t \left( E_{-\mathbf{k},\lambda} \beta_{-\mathbf{k},\lambda}(t) + E_{\mathbf{k},\lambda}^* \beta_{\mathbf{k},\lambda}^\dagger(t) \right) \alpha_{\mathbf{k},\lambda}^\dagger(t') \right\rangle,
\end{aligned} \tag{A.23}$$

where  $\theta(x) = \begin{cases} 1 & \text{if } x > 0 \\ 0 & \text{if } x < 0 \\ \frac{1}{2} & \text{if } x = 0 \end{cases}$  [3]. In the second last equality of equation (A.23),

Heisenberg's equation of motion was used [11]. In reciprocal space  $i\partial_t$  corresponds

to a frequency  $z$ . Equation (A.23) should hold in the case of no coupling:

$$g_{\alpha \mathbf{k}, \lambda; z} = \frac{1}{z - \omega_{\mathbf{k}, \lambda}}. \quad (\text{A.24})$$

Similarly, for Greens function of  $\alpha_{\mathbf{k}, \lambda}^\dagger$  I get

$$\begin{aligned} & i\partial_t g_{\alpha^\dagger \mathbf{k}, \lambda}(t - t') \\ &= \delta(t - t') \left\langle \left[ \alpha_{\mathbf{k}, \lambda}^\dagger(t), \alpha_{\mathbf{k}, \lambda}(t') \right] \right\rangle - i \left\langle T_t \left[ \alpha_{\mathbf{k}, \lambda}^\dagger(t), H \right] \alpha_{\mathbf{k}, \lambda}(t') \right\rangle. \end{aligned} \quad (\text{A.25})$$

This should hold independently of the strength of the coupling. Thus, I can evaluate in the case of no coupling  $E_{\mathbf{k}, \lambda} = 0$ :

$$i\partial_t g_{\alpha^\dagger \mathbf{k}, \lambda}(t - t') = -\delta(t - t') - \omega_{\mathbf{k}, \lambda} g_{\alpha^\dagger \mathbf{k}, \lambda}(t, t'). \quad (\text{A.26})$$

In reciprocal space this can be written as

$$g_{\alpha^\dagger \mathbf{k}, \lambda; z} = \frac{1}{z + \omega_{\mathbf{k}, \lambda}}. \quad (\text{A.27})$$

Green's function for the  $\beta_{\mathbf{k}, \lambda}$  operator is defined by equation (3.7). Similarly to the shifted phonon operators, I can act with  $i\partial_t$ :

$$\begin{aligned} & i\partial_t g_{\beta \mathbf{k}, \lambda}(t - t') \\ &= \frac{1}{L} \sum_{\lambda'} \partial_t \left\langle T_t \beta_{\mathbf{k}, \lambda}(t) \beta_{\mathbf{k}, \lambda'}^\dagger(t') \right\rangle \\ &= \delta(t - t') \frac{1}{L} \sum_{\lambda'} \left\langle \left[ \beta_{\mathbf{k}, \lambda}(t), \beta_{\mathbf{k}, \lambda'}^\dagger(t') \right] \right\rangle - \frac{i}{L} \sum_{\lambda'} \left\langle T_t [\beta_{\mathbf{k}, \lambda}(t), H] \beta_{\mathbf{k}, \lambda'}^\dagger(t') \right\rangle \\ &= \delta(t - t') - \frac{i}{L} \sum_{\lambda', \lambda''} \left\langle T_t \left[ \epsilon_{\mathbf{k}, \lambda''} \beta_{\mathbf{k}, \lambda''}(t) + E_{\mathbf{k}, \lambda''}^* \alpha_{-\mathbf{k}, \lambda''}(t) + E_{\mathbf{k}, \lambda''}^* \alpha_{\mathbf{k}, \lambda''}^\dagger(t) \right] \beta_{\mathbf{k}, \lambda'}^\dagger(t') \right\rangle \end{aligned} \quad (\text{A.28})$$

In the case of no coupling  $\beta_{\mathbf{k}, \lambda} = b_{\mathbf{k}} = \beta_{\mathbf{k}, \lambda'}$  for any  $\lambda$  and  $\lambda'$ ; because  $J_{\mathbf{k}, \lambda} = 0$  if  $E_{\mathbf{k}, \lambda} = 0$ . Equation (A.28) should hold in the case of no coupling:

$$i\partial_t g_{\beta \mathbf{k}, \lambda}(t, t') = \delta(t - t') + \epsilon_{\mathbf{k}} g_{\beta \mathbf{k}, \lambda}(t - t'). \quad (\text{A.29})$$

In reciprocal space this can be written as

$$g_{\beta \mathbf{k}, \lambda; z} = \frac{1}{z - \epsilon_{\mathbf{k}}}. \quad (\text{A.30})$$

Similarly, Green's function for  $\beta_{\mathbf{k}, \lambda}^\dagger$  is

$$g_{\beta^\dagger \mathbf{k}, \lambda; z} = \frac{1}{z + \epsilon_{\mathbf{k}}}. \quad (\text{A.31})$$

## A.7. Coupled Phonons

Acting with  $g_{\alpha_{\mathbf{k},\lambda};z}^{-1}$  at equation (3.10) and using the equations of motion for  $\beta_{\mathbf{k},\lambda}$  (3.12) and  $\beta_{\mathbf{k},\lambda}^\dagger$  (3.13) gives:

$$\begin{aligned}
& g_{\alpha_{\mathbf{k},\lambda};z}^{-1} \alpha_{\mathbf{k},\lambda} \\
&= E_{-\mathbf{k},\lambda} \beta_{-\mathbf{k},\lambda} + E_{\mathbf{k},\lambda}^* \beta_{\mathbf{k},\lambda}^\dagger \\
&= E_{-\mathbf{k},\lambda} g_{\beta_{-\mathbf{k},\lambda};z} \left[ \sum_{\lambda' \neq \lambda} (\epsilon_{-\mathbf{k},\lambda'} J_{-\mathbf{k},\lambda'}) + \sum_{\lambda'} \left( E_{-\mathbf{k},\lambda'}^* \alpha_{\mathbf{k},\lambda'} + E_{-\mathbf{k},\lambda'}^* \alpha_{-\mathbf{k},\lambda'}^\dagger \right) \right] \\
&\quad - E_{\mathbf{k},\lambda}^* g_{\beta_{\mathbf{k},\lambda};z}^\dagger \left[ \sum_{\lambda' \neq \lambda} (\epsilon_{\mathbf{k},\lambda'} J_{\mathbf{k},\lambda'}^*) + \sum_{\lambda'} \left( E_{\mathbf{k},\lambda'} \alpha_{\mathbf{k},\lambda'} + E_{\mathbf{k},\lambda'} \alpha_{-\mathbf{k},\lambda'}^\dagger \right) \right] \\
&= \sum_{\lambda'} \left( \left[ g_{\beta_{-\mathbf{k},\lambda};z} E_{\mathbf{k},\lambda} E_{\mathbf{k},\lambda'}^* - g_{\beta_{\mathbf{k},\lambda};z}^\dagger E_{\mathbf{k},\lambda}^* E_{\mathbf{k},\lambda'} \right] [\alpha_{\mathbf{k},\lambda'} + \alpha_{-\mathbf{k},\lambda'}^\dagger] \right) + J'_{\mathbf{k},\lambda} \\
&= \sum_{\lambda'} A_{\mathbf{k},\lambda,\lambda';z} \left( \alpha_{\mathbf{k},\lambda'} + \alpha_{-\mathbf{k},\lambda'}^\dagger \right) + J'_{\mathbf{k},\lambda} \tag{A.32}
\end{aligned}$$

and

$$g_{\alpha_{-\mathbf{k},\lambda};z}^{-1} \alpha_{-\mathbf{k},\lambda}^\dagger = \sum_{\lambda'} A_{\mathbf{k},\lambda,\lambda';z} \left( \alpha_{\mathbf{k},\lambda'} + \alpha_{-\mathbf{k},\lambda'}^\dagger \right) + J'_{\mathbf{k},\lambda}, \tag{A.33}$$

with

$$\begin{aligned}
A_{\mathbf{k},\lambda,\lambda';z} &= g_{\beta_{-\mathbf{k},\lambda};z} E_{\mathbf{k},\lambda} E_{\mathbf{k},\lambda'}^* - g_{\beta_{\mathbf{k},\lambda};z}^\dagger E_{\mathbf{k},\lambda}^* E_{\mathbf{k},\lambda'} \\
&= \frac{E_{\mathbf{k},\lambda} E_{\mathbf{k},\lambda'}^*}{z - \epsilon_{-\mathbf{k}}} - \frac{E_{\mathbf{k},\lambda}^* E_{\mathbf{k},\lambda'}}{z + \epsilon_{\mathbf{k}}} \\
&= \frac{E_{\mathbf{k},\lambda} E_{\mathbf{k},\lambda'}^* (z + \epsilon_{\mathbf{k}}) - E_{\mathbf{k},\lambda}^* E_{\mathbf{k},\lambda'} (z - \epsilon_{-\mathbf{k}})}{(z - \epsilon_{-\mathbf{k}})(z + \epsilon_{\mathbf{k}})} \\
&= \frac{(E_{\mathbf{k},\lambda} E_{\mathbf{k},\lambda'}^* - E_{\mathbf{k},\lambda}^* E_{\mathbf{k},\lambda'}) z + E_{\mathbf{k},\lambda} E_{\mathbf{k},\lambda'}^* \epsilon_{\mathbf{k}} + E_{\mathbf{k},\lambda}^* E_{\mathbf{k},\lambda'} \epsilon_{-\mathbf{k}}}{(z - \epsilon_{-\mathbf{k}})(z + \epsilon_{\mathbf{k}})} \\
&= \frac{E_{\mathbf{k},\lambda,\lambda'}^{(-)} z + E_{\mathbf{k},\lambda,\lambda'}^{(\epsilon)}}{(z - \epsilon_{-\mathbf{k}})(z + \epsilon_{\mathbf{k}})} \tag{A.34}
\end{aligned}$$

and

$$J'_{\mathbf{k},\lambda} = E_{-\mathbf{k},\lambda} g_{\beta_{-\mathbf{k},\lambda};z} \sum_{\lambda' \neq \lambda} (\epsilon_{-\mathbf{k},\lambda'} J_{-\mathbf{k},\lambda'}) - E_{\mathbf{k},\lambda}^* g_{\beta_{\mathbf{k},\lambda};z}^\dagger \sum_{\lambda' \neq \lambda} (\epsilon_{\mathbf{k},\lambda'} J_{\mathbf{k},\lambda'}^*), \tag{A.35}$$

where I made the following definitions

$$E_{\mathbf{k},\lambda,\lambda'}^{(-)} = E_{\mathbf{k},\lambda} E_{\mathbf{k},\lambda'}^* - E_{\mathbf{k},\lambda}^* E_{\mathbf{k},\lambda'} \tag{A.36}$$

and

$$E_{\mathbf{k},\lambda,\lambda'}^{(\epsilon)} = E_{\mathbf{k},\lambda} E_{\mathbf{k},\lambda'}^* \epsilon_{\mathbf{k}} + E_{\mathbf{k},\lambda}^* E_{\mathbf{k},\lambda'} \epsilon_{-\mathbf{k}}. \quad (\text{A.37})$$

Writing equations (A.32) and (A.33) in one matrix equation:

$$\sum_{\lambda'} \begin{pmatrix} g_{\alpha}^{-1} \mathbf{k}, \lambda; z \delta_{\lambda, \lambda'} - A_{\mathbf{k}, \lambda, \lambda'; z} & -A_{\mathbf{k}, \lambda, \lambda'; z} \\ -A_{\mathbf{k}, \lambda, \lambda'; z} & g_{\alpha^\dagger}^{-1} -\mathbf{k}, \lambda; z \delta_{\lambda, \lambda'} - A_{\mathbf{k}, \lambda, \lambda'; z} \end{pmatrix} \begin{pmatrix} \alpha_{\mathbf{k}, \lambda'} \\ \alpha_{-\mathbf{k}, \lambda'}^\dagger \end{pmatrix} = \begin{pmatrix} J'_{\mathbf{k}, \lambda} \\ J'_{\mathbf{k}, \lambda} \end{pmatrix}. \quad (\text{A.38})$$

Green's function for coupled phonons is given by equation (3.19) and it is repeated here:

$$\mathbb{G}_{A\mathbf{k}, \lambda; z} = \left\langle \left\langle \begin{pmatrix} \alpha_{\mathbf{k}, \lambda} \alpha_{\mathbf{k}, \lambda}^\dagger & \alpha_{\mathbf{k}, \lambda} \alpha_{-\mathbf{k}, \lambda} \\ \alpha_{\mathbf{k}, \lambda}^\dagger \alpha_{-\mathbf{k}, \lambda}^\dagger & \alpha_{-\mathbf{k}, \lambda}^\dagger \alpha_{-\mathbf{k}, \lambda} \end{pmatrix} \right\rangle \right\rangle (z). \quad (\text{A.39})$$

In the limit of no coupling ( $E_{\mathbf{k}, \lambda} \rightarrow 0$ ),  $\mathbb{G}_{A\mathbf{k}, \lambda; z}$  reduces to

$$\mathbb{G}_{A\mathbf{k}, \lambda; z} = \begin{pmatrix} g_{\alpha\mathbf{k}, \lambda; z} & 0 \\ 0 & g_{\alpha^\dagger -\mathbf{k}, \lambda; z} \end{pmatrix}. \quad (\text{A.40})$$

Therefore, the following equation should hold:

$$\sum_{\lambda'} \begin{pmatrix} g_{\alpha}^{-1} \mathbf{k}, \lambda; z \delta_{\lambda, \lambda'} - A_{\mathbf{k}, \lambda, \lambda'; z} & -A_{\mathbf{k}, \lambda, \lambda'; z} \\ -A_{\mathbf{k}, \lambda, \lambda'; z} & g_{\alpha^\dagger}^{-1} -\mathbf{k}, \lambda; z \delta_{\lambda, \lambda'} - A_{\mathbf{k}, \lambda, \lambda'; z} \end{pmatrix} \mathbb{G}_{A\mathbf{k}, \lambda; z} = \begin{pmatrix} 1 & 0 \\ 0 & -1 \end{pmatrix}. \quad (\text{A.41})$$

Solving equation (A.41):

$$\begin{aligned} \mathbb{G}_{A\mathbf{k}, \lambda; z} &= \sum_{\lambda', \lambda''} \left\{ \left( g_{\alpha}^{-1} \mathbf{k}, \lambda; z \delta_{\lambda, \lambda'} - A_{\mathbf{k}, \lambda, \lambda'; z} \right) \left( g_{\alpha^\dagger}^{-1} -\mathbf{k}, \lambda; z \delta_{\lambda, \lambda''} - A_{\mathbf{k}, \lambda, \lambda''; z} \right) \right. \\ &\quad \left. - A_{\mathbf{k}, \lambda, \lambda'} A_{\mathbf{k}, \lambda, \lambda''; z} \right\}^{-1} \\ &\quad \times \sum_{\lambda'''} \begin{pmatrix} g_{\alpha^\dagger}^{-1} -\mathbf{k}, \lambda \delta_{\lambda, \lambda'''} - A_{\mathbf{k}, \lambda, \lambda'''; z} & A_{\mathbf{k}, \lambda, \lambda'''; z} \\ A_{\mathbf{k}, \lambda, \lambda'''; z} & g_{\alpha}^{-1} \mathbf{k}, \lambda; z \delta_{\lambda, \lambda'''} - A_{\mathbf{k}, \lambda, \lambda'''; z} \end{pmatrix} \begin{pmatrix} 1 & 0 \\ 0 & -1 \end{pmatrix} \\ &= \sum_{\lambda', \lambda''} \left\{ ([z - \omega_{\mathbf{k}, \lambda}] \delta_{\lambda, \lambda'} - A_{\mathbf{k}, \lambda, \lambda'; z}) (-[z + \omega_{-\mathbf{k}, \lambda}] \delta_{\lambda, \lambda''} - A_{\mathbf{k}, \lambda, \lambda''; z}) \right. \\ &\quad \left. - A_{\mathbf{k}, \lambda, \lambda'} A_{\mathbf{k}, \lambda, \lambda''; z} \right\}^{-1} \\ &\quad \times \sum_{\lambda'''} \begin{pmatrix} -[z + \omega_{-\mathbf{k}, \lambda}] \delta_{\lambda, \lambda'''} - A_{\mathbf{k}, \lambda, \lambda'''; z} & A_{\mathbf{k}, \lambda, \lambda'''; z} \\ A_{\mathbf{k}, \lambda, \lambda'''; z} & [z - \omega_{\mathbf{k}, \lambda}] \delta_{\lambda, \lambda'''} - A_{\mathbf{k}, \lambda, \lambda'''; z} \end{pmatrix} \\ &\quad \times \begin{pmatrix} 1 & 0 \\ 0 & -1 \end{pmatrix} \end{aligned}$$

$$\begin{aligned}
&= \frac{1}{-z^2 + \omega_{\mathbf{k},\lambda}^2 + 2\omega_{\mathbf{k},\lambda} \sum_{\lambda'} A_{\mathbf{k},\lambda,\lambda';z}} \\
&\quad \times \begin{pmatrix} -z - \omega_{\mathbf{k},\lambda} - \sum_{\lambda''} A_{\mathbf{k},\lambda,\lambda'';z} & -\sum_{\lambda''} A_{\mathbf{k},\lambda,\lambda'';z} \\ \sum_{\lambda''} A_{\mathbf{k},\lambda,\lambda'';z} & -z + \omega_{\mathbf{k},\lambda} + \sum_{\lambda''} A_{\mathbf{k},\lambda,\lambda'';z} \end{pmatrix} \\
&= \frac{1}{z^2 - \omega_{\mathbf{k},\lambda}^2 - 2\omega_{\mathbf{k},\lambda} \sum_{\lambda'} A_{\mathbf{k},\lambda,\lambda';z}} \\
&\quad \times \begin{pmatrix} z + \omega_{\mathbf{k},\lambda} + \sum_{\lambda''} A_{\mathbf{k},\lambda,\lambda'';z} & \sum_{\lambda''} A_{\mathbf{k},\lambda,\lambda'';z} \\ -\sum_{\lambda''} A_{\mathbf{k},\lambda,\lambda'';z} & z - \omega_{\mathbf{k},\lambda} - \sum_{\lambda''} A_{\mathbf{k},\lambda,\lambda'';z} \end{pmatrix}. \quad (\text{A.42})
\end{aligned}$$

Taking the trace:

$$\begin{aligned}
\text{tr} \mathbb{G}_{A\mathbf{k},\lambda;z} &= \frac{2z}{z^2 - \omega_{\mathbf{k},\lambda}^2 - 2\omega_{\mathbf{k},\lambda} \sum_{\lambda'} A_{\mathbf{k},\lambda,\lambda';z}} \\
&= \frac{2z}{z^2 - \omega_{\mathbf{k},\lambda}^2 - 2\omega_{\mathbf{k},\lambda} \sum_{\lambda'} \frac{E_{\mathbf{k},\lambda,\lambda'}^{(-)} z + E_{\mathbf{k},\lambda,\lambda'}^{(\epsilon)}}{(z - \epsilon_{-\mathbf{k}})(z + \epsilon_{\mathbf{k}})}} \\
&= \frac{2z(z - \epsilon_{-\mathbf{k}})(z + \epsilon_{\mathbf{k}})}{(z^2 - \omega_{\mathbf{k},\lambda}^2)(z - \epsilon_{-\mathbf{k}})(z + \epsilon_{\mathbf{k}}) - 2\omega_{\mathbf{k},\lambda} \left( \sum_{\lambda'} E_{\mathbf{k},\lambda,\lambda'}^{(-)} z + E_{\mathbf{k},\lambda,\lambda'}^{(\epsilon)} \right)}. \quad (\text{A.43})
\end{aligned}$$

## A.8. Coupled Magnons

Equations (3.10)-(3.13), may also be rewritten in terms of the new magnon operators:

$$\begin{aligned}
&g_{\beta}^{-1}{}_{\mathbf{k},\lambda;z} \beta_{\mathbf{k},\lambda} \\
&= \sum_{\lambda'} \left( E_{\mathbf{k},\lambda'}^* \alpha_{-\mathbf{k},\lambda'} + E_{\mathbf{k},\lambda'}^* \alpha_{\mathbf{k},\lambda'}^\dagger \right) + \sum_{\lambda' \neq \lambda} \epsilon_{\mathbf{k},\lambda'} J_{\mathbf{k},\lambda'} \\
&= \sum_{\lambda'} E_{\mathbf{k},\lambda'}^* g_{\alpha_{-\mathbf{k},\lambda';z}} \left( E_{\mathbf{k},\lambda'} \beta_{\mathbf{k},\lambda'} + E_{-\mathbf{k},\lambda'}^* \beta_{-\mathbf{k},\lambda'}^\dagger \right) \\
&\quad - \sum_{\lambda'} E_{\mathbf{k},\lambda'}^* g_{\alpha_{\mathbf{k},\lambda';z}} \left( E_{\mathbf{k},\lambda'} \beta_{\mathbf{k},\lambda'} + E_{-\mathbf{k},\lambda'}^* \beta_{-\mathbf{k},\lambda'}^\dagger \right) + \sum_{\lambda' \neq \lambda} \epsilon_{\mathbf{k},\lambda'} J_{\mathbf{k},\lambda'} \\
&= \sum_{\lambda'} E_{\mathbf{k},\lambda'}^* (g_{\alpha_{-\mathbf{k},\lambda';z}} - g_{\alpha_{\mathbf{k},\lambda';z}}) \left( E_{\mathbf{k},\lambda'} \beta_{\mathbf{k},\lambda'} + E_{-\mathbf{k},\lambda'}^* \beta_{-\mathbf{k},\lambda'}^\dagger \right) + \epsilon_{\mathbf{k},\lambda'} J_{\mathbf{k},\lambda'} (1 - \delta_{\lambda,\lambda'}) \\
&= \sum_{\lambda'} B_{\mathbf{k},\lambda'} \left( E_{\mathbf{k},\lambda'} \beta_{\mathbf{k},\lambda'} + E_{-\mathbf{k},\lambda'}^* \beta_{-\mathbf{k},\lambda'}^\dagger \right) + \epsilon_{\mathbf{k},\lambda'} J_{\mathbf{k},\lambda'} (1 - \delta_{\lambda,\lambda'}), \quad (\text{A.44})
\end{aligned}$$

and

$$g_{\beta^\dagger - \mathbf{k}, \lambda; z}^{-1} \beta_{-\mathbf{k}, \lambda}^\dagger = \sum_{\lambda'} B_{-\mathbf{k}, \lambda'}^* \left( E_{\mathbf{k}, \lambda'} \beta_{\mathbf{k}, \lambda'} + E_{-\mathbf{k}, \lambda'}^* \beta_{-\mathbf{k}, \lambda'}^\dagger \right) + \epsilon_{-\mathbf{k}, \lambda'} J_{-\mathbf{k}, \lambda'}^* (1 - \delta_{\lambda, \lambda'}) \quad (\text{A.45})$$

with

$$B_{\mathbf{k}, \lambda} = E_{\mathbf{k}, \lambda}^* (g_{\alpha - \mathbf{k}, \lambda} - g_{\alpha^\dagger \mathbf{k}, \lambda; z}). \quad (\text{A.46})$$

Combining equations (A.44) and (A.45) into one matrix equations:

$$\begin{aligned} & \sum_{\lambda'} \begin{pmatrix} g_{\beta^{-1} \mathbf{k}, \lambda; z}^{-1} \delta_{\lambda, \lambda'} - B_{\mathbf{k}, \lambda'} E_{\mathbf{k}, \lambda'} & -B_{\mathbf{k}, \lambda'} E_{-\mathbf{k}, \lambda'}^* \\ -B_{-\mathbf{k}, \lambda'}^* E_{\mathbf{k}, \lambda'} & g_{\beta^\dagger - \mathbf{k}, \lambda; z}^{-1} \delta_{\lambda, \lambda'} - B_{-\mathbf{k}, \lambda'}^* E_{-\mathbf{k}, \lambda'}^* \end{pmatrix} \begin{pmatrix} \beta_{\mathbf{k}, \lambda'} \\ \beta_{-\mathbf{k}, \lambda'}^\dagger \end{pmatrix} \\ &= \sum_{\lambda'} \begin{pmatrix} \epsilon_{\mathbf{k}, \lambda'} J_{\mathbf{k}, \lambda'} (1 - \delta_{\lambda, \lambda'}) \\ \epsilon_{-\mathbf{k}, \lambda'} J_{-\mathbf{k}, \lambda'}^* (1 - \delta_{\lambda, \lambda'}) \end{pmatrix}. \end{aligned} \quad (\text{A.47})$$

Let us now introduce Green's function for coupled magnons:

$$\mathbb{G}_{B\mathbf{k}, \lambda; z} = \left\langle \left\langle \begin{pmatrix} \beta_{\mathbf{k}, \lambda} \beta_{\mathbf{k}, \lambda}^\dagger & \beta_{\mathbf{k}, \lambda} \beta_{-\mathbf{k}, \lambda} \\ \beta_{\mathbf{k}, \lambda}^\dagger \beta_{-\mathbf{k}, \lambda}^\dagger & \beta_{-\mathbf{k}, \lambda}^\dagger \beta_{-\mathbf{k}, \lambda} \end{pmatrix} \right\rangle \right\rangle (z). \quad (\text{A.48})$$

In the limit of no coupling ( $E_{\mathbf{k}, \lambda} \rightarrow 0$ ),  $\mathbb{G}_{B\mathbf{k}, \lambda; z}$  reduces to

$$\mathbb{G}_{A\mathbf{k}, \lambda; z} = \begin{pmatrix} g_{\beta \mathbf{k}, \lambda; z} & 0 \\ 0 & g_{\beta^\dagger - \mathbf{k}, \lambda; z} \end{pmatrix}. \quad (\text{A.49})$$

Therefore, the following equation should hold:

$$\sum_{\lambda'} \begin{pmatrix} g_{\beta^{-1} \mathbf{k}, \lambda; z}^{-1} \delta_{\lambda, \lambda'} - B_{\mathbf{k}, \lambda'} E_{\mathbf{k}, \lambda'} & -B_{\mathbf{k}, \lambda'} E_{-\mathbf{k}, \lambda'}^* \\ -B_{-\mathbf{k}, \lambda'}^* E_{\mathbf{k}, \lambda'} & g_{\beta^\dagger - \mathbf{k}, \lambda; z}^{-1} \delta_{\lambda, \lambda'} - B_{-\mathbf{k}, \lambda'}^* E_{-\mathbf{k}, \lambda'}^* \end{pmatrix} \mathbb{G}_{B\mathbf{k}, \lambda; z} = \begin{pmatrix} 1 & 0 \\ 0 & -1 \end{pmatrix}. \quad (\text{A.50})$$

Solving this equation:

$$\begin{aligned} \mathbb{G}_{B\mathbf{k}, \lambda; z} &= \sum_{\lambda', \lambda''} \left\{ \left( g_{\beta^{-1} \mathbf{k}, \lambda; z}^{-1} \delta_{\lambda, \lambda'} - B_{\mathbf{k}, \lambda'} E_{\mathbf{k}, \lambda'} \right) \left( g_{\beta^\dagger - \mathbf{k}, \lambda; z}^{-1} \delta_{\lambda, \lambda''} - B_{-\mathbf{k}, \lambda''}^* E_{-\mathbf{k}, \lambda''}^* \right) \right. \\ &\quad \left. - B_{\mathbf{k}, \lambda'} E_{-\mathbf{k}, \lambda'}^* B_{-\mathbf{k}, \lambda''}^* E_{\mathbf{k}, \lambda''} \right\}^{-1} \\ &\times \sum_{\lambda'''} \begin{pmatrix} g_{\beta^{-1} - \mathbf{k}, \lambda; z}^{-1} \delta_{\lambda, \lambda'''} - B_{-\mathbf{k}, \lambda'''}^* E_{-\mathbf{k}, \lambda'''}^* & B_{-\mathbf{k}, \lambda'''}^* E_{\mathbf{k}, \lambda'''} \\ B_{\mathbf{k}, \lambda'''} E_{-\mathbf{k}, \lambda'''}^* & g_{\beta^{-1} \mathbf{k}, \lambda; z}^{-1} \delta_{\lambda, \lambda'''} - B_{\mathbf{k}, \lambda'''} E_{\mathbf{k}, \lambda'''} \end{pmatrix} \\ &\times \begin{pmatrix} 1 & 0 \\ 0 & -1 \end{pmatrix} \end{aligned} \quad (\text{A.51})$$

$$= \sum_{\lambda', \lambda''} \{ ([z - \epsilon_{\mathbf{k}}] \delta_{\lambda, \lambda'} - B_{\mathbf{k}, \lambda'} E_{\mathbf{k}, \lambda'}) (-[z + \epsilon_{-\mathbf{k}}] \delta_{\lambda, \lambda''} - B_{-\mathbf{k}, \lambda''}^* E_{-\mathbf{k}, \lambda''}^*) \} \quad (\text{A.52})$$

$$- B_{\mathbf{k}, \lambda'} E_{-\mathbf{k}, \lambda'}^* B_{-\mathbf{k}, \lambda''}^* E_{\mathbf{k}, \lambda''} \}^{-1} \quad (\text{A.53})$$

$$\times \begin{pmatrix} -z - \epsilon_{-\mathbf{k}} - \sum_{\lambda'''} B_{-\mathbf{k}, \lambda'''}^* E_{-\mathbf{k}, \lambda'''}^* & - \sum_{\lambda'''} B_{-\mathbf{k}, \lambda'''}^* E_{\mathbf{k}, \lambda'''} \\ \sum_{\lambda'''} B_{\mathbf{k}, \lambda'''} E_{-\mathbf{k}, \lambda'''}^* & -z + \epsilon_{\mathbf{k}} + \sum_{\lambda'''} B_{\mathbf{k}, \lambda'''} E_{\mathbf{k}, \lambda'''} \end{pmatrix} \quad (\text{A.54})$$

$$= \left\{ z^2 - (\epsilon_{\mathbf{k}} - \epsilon_{-\mathbf{k}}) z - \epsilon_{\mathbf{k}} \epsilon_{-\mathbf{k}} - \sum_{\lambda'} (B_{\mathbf{k}, \lambda'} E_{\mathbf{k}, \lambda'} - B_{-\mathbf{k}, \lambda'}^* E_{-\mathbf{k}, \lambda'}^*) z \right. \quad (\text{A.55})$$

$$\left. - \sum_{\lambda'} (B_{\mathbf{k}, \lambda'} E_{\mathbf{k}, \lambda'} \epsilon_{-\mathbf{k}} + B_{-\mathbf{k}, \lambda'}^* E_{-\mathbf{k}, \lambda'}^* \epsilon_{\mathbf{k}}) \right\}^{-1} \quad (\text{A.56})$$

$$\times \begin{pmatrix} z + \epsilon_{-\mathbf{k}} + \sum_{\lambda''} B_{-\mathbf{k}, \lambda''}^* E_{-\mathbf{k}, \lambda''}^* & \sum_{\lambda''} B_{-\mathbf{k}, \lambda''}^* E_{\mathbf{k}, \lambda''} \\ - \sum_{\lambda''} B_{\mathbf{k}, \lambda''} E_{-\mathbf{k}, \lambda''}^* & z - \epsilon_{\mathbf{k}} - \sum_{\lambda''} B_{\mathbf{k}, \lambda''} E_{\mathbf{k}, \lambda''} \end{pmatrix}. \quad (\text{A.57})$$

Evaluating  $B_{\mathbf{k}, \lambda'}$ :

$$\begin{aligned} B_{\mathbf{k}, \lambda} &= E_{\mathbf{k}, \lambda}^* (g_{\alpha - \mathbf{k}, \lambda} - g_{\alpha^\dagger \mathbf{k}, \lambda; z}) \\ &= E_{\mathbf{k}, \lambda}^* \left( \frac{1}{z - \omega_{-\mathbf{k}, \lambda}} - \frac{1}{z + \omega_{\mathbf{k}, \lambda}} \right) \\ &= \frac{2\omega_{\mathbf{k}, \lambda} E_{\mathbf{k}, \lambda}^*}{z^2 - \omega_{\mathbf{k}, \lambda}^2}. \end{aligned} \quad (\text{A.58})$$

The trace of Green's function of coupled magnons is

$$\begin{aligned}
& \text{tr} (\mathbb{G}_{B\mathbf{k},\lambda;z}) \\
&= \left\{ z^2 - (\epsilon_{\mathbf{k}} - \epsilon_{-\mathbf{k}}) z - \epsilon_{\mathbf{k}} \epsilon_{-\mathbf{k}} - \sum_{\lambda'} (B_{\mathbf{k},\lambda'} E_{\mathbf{k},\lambda'} - B_{-\mathbf{k},\lambda'}^* E_{-\mathbf{k},\lambda'}^*) z \right. \\
&\quad \left. - \sum_{\lambda'} (B_{\mathbf{k},\lambda'} E_{\mathbf{k},\lambda'} \epsilon_{-\mathbf{k}} + B_{-\mathbf{k},\lambda'}^* E_{-\mathbf{k},\lambda'}^* \epsilon_{\mathbf{k}}) \right\}^{-1} \\
&\quad \times \begin{pmatrix} z + \epsilon_{-\mathbf{k}} + \sum_{\lambda''} B_{-\mathbf{k},\lambda''}^* E_{-\mathbf{k},\lambda''}^* & \sum_{\lambda''} B_{-\mathbf{k},\lambda''}^* E_{\mathbf{k},\lambda''} \\ - \sum_{\lambda''} B_{\mathbf{k},\lambda''} E_{-\mathbf{k},\lambda''}^* & z - \epsilon_{\mathbf{k}} - \sum_{\lambda''} B_{\mathbf{k},\lambda''} E_{\mathbf{k},\lambda''} \end{pmatrix} \\
&= \left\{ z^2 - (\epsilon_{\mathbf{k}} - \epsilon_{-\mathbf{k}}) z - \epsilon_{\mathbf{k}} \epsilon_{-\mathbf{k}} \right. \\
&\quad - \sum_{\lambda'} 4\omega_{\mathbf{k},\lambda'}^2 |E_{\mathbf{k},\lambda'}|^2 \left( \frac{1}{z^2 - \omega_{\mathbf{k},\lambda'}^2} - \frac{1}{(z^2)^* - \omega_{\mathbf{k},\lambda'}^2} \right) z \\
&\quad \left. - \sum_{\lambda'} 4\omega_{\mathbf{k},\lambda'}^2 |E_{\mathbf{k},\lambda'}|^2 \left( \frac{\epsilon_{-\mathbf{k}}}{z^2 - \omega_{\mathbf{k},\lambda'}^2} + \frac{\epsilon_{\mathbf{k}}}{(z^2)^* - \omega_{\mathbf{k},\lambda'}^2} \right) \right\}^{-1} \\
&\quad \times \left\{ 2z + \epsilon_{-\mathbf{k}} - \epsilon_{\mathbf{k}} - \sum_{\lambda'} 4\omega_{\mathbf{k},\lambda'}^2 |E_{\mathbf{k},\lambda'}|^2 \left( \frac{1}{z^2 - \omega_{\mathbf{k},\lambda'}^2} - \frac{1}{(z^2)^* - \omega_{\mathbf{k},\lambda'}^2} \right) \right\} \\
&= \left\{ z^2 - (\epsilon_{\mathbf{k}} - \epsilon_{-\mathbf{k}}) z - \epsilon_{\mathbf{k}} \epsilon_{-\mathbf{k}} \right. \\
&\quad - \sum_{\lambda'} 4\omega_{\mathbf{k},\lambda'}^2 |E_{\mathbf{k},\lambda'}|^2 \frac{-2\text{Im}(z^2)}{|z^2|^2 - 2\omega_{\mathbf{k},\lambda'} \text{Re}(z^2) + \omega_{\mathbf{k},\lambda'}^4} z \\
&\quad \left. - \sum_{\lambda'} 4\omega_{\mathbf{k},\lambda'}^2 |E_{\mathbf{k},\lambda'}|^2 \left( \frac{\epsilon_{\mathbf{k}} z^2 + \epsilon_{-\mathbf{k}} (z^2)^* - \omega_{\mathbf{k},\lambda'}^2 (\epsilon_{-\mathbf{k}} + \epsilon_{\mathbf{k}})}{|z^2|^2 - 2\omega_{\mathbf{k},\lambda'} \text{Re}(z^2) + \omega_{\mathbf{k},\lambda'}^4} \right) \right\}^{-1} \\
&\quad \times \left\{ 2z + \epsilon_{-\mathbf{k}} - \epsilon_{\mathbf{k}} - \sum_{\lambda'} 4\omega_{\mathbf{k},\lambda'}^2 |E_{\mathbf{k},\lambda'}|^2 \frac{-2\text{Im}(z^2)}{|z^2|^2 - 2\omega_{\mathbf{k},\lambda'} \text{Re}(z^2) + \omega_{\mathbf{k},\lambda'}^4} \right\}. \quad (\text{A.59})
\end{aligned}$$

Assuming that  $\epsilon_{\mathbf{k}} = \epsilon_{-\mathbf{k}}$  gives:

$$\begin{aligned}
& \text{tr} \left( \mathbb{G}_{B\mathbf{k},\lambda;z} \right) \\
&= \left\{ z^2 - (\epsilon_{\mathbf{k}} - \epsilon_{-\mathbf{k}}) z - \epsilon_{\mathbf{k}} \epsilon_{-\mathbf{k}} \right. \\
&\quad - \sum_{\lambda'} 4\omega_{\mathbf{k},\lambda'}^2 |E_{\mathbf{k},\lambda'}|^2 \frac{-2\text{Im}(z^2)}{|z^2|^2 - 2\omega_{\mathbf{k},\lambda'} \text{Re}(z^2) + \omega_{\mathbf{k},\lambda'}^4} z \\
&\quad \left. - \sum_{\lambda'} 4\omega_{\mathbf{k},\lambda'}^2 |E_{\mathbf{k},\lambda'}|^2 \left( \frac{\epsilon_{\mathbf{k}} z^2 + \epsilon_{-\mathbf{k}} (z^2)^* - \omega_{\mathbf{k},\lambda'}^2 (\epsilon_{-\mathbf{k}} + \epsilon_{\mathbf{k}})}{|z^2|^2 - 2\omega_{\mathbf{k},\lambda'} \text{Re}(z^2) + \omega_{\mathbf{k},\lambda'}^4} \right) \right\}^{-1} \\
&\quad \times \left\{ 2z + \epsilon_{-\mathbf{k}} - \epsilon_{\mathbf{k}} - \sum_{\lambda'} 4\omega_{\mathbf{k},\lambda'}^2 |E_{\mathbf{k},\lambda'}|^2 \frac{-2\text{Im}(z^2)}{|z^2|^2 - 2\omega_{\mathbf{k},\lambda'} \text{Re}(z^2) + \omega_{\mathbf{k},\lambda'}^4} \right\} \\
&= \left\{ z^2 - \epsilon_{\mathbf{k}}^2 - \sum_{\lambda'} 4\omega_{\mathbf{k},\lambda'}^2 |E_{\mathbf{k},\lambda'}|^2 \left( \frac{-2\text{Im}(z^2) z + 2\epsilon_{\mathbf{k}} \text{Re}(z^2) - 2\omega_{\mathbf{k},\lambda'}^2 \epsilon_{\mathbf{k}}}{|z^2|^2 - 2\omega_{\mathbf{k},\lambda'} \text{Re}(z^2) + \omega_{\mathbf{k},\lambda'}^4} \right) \right\}^{-1} \\
&\quad \times \left\{ 2z + \sum_{\lambda'} 4\omega_{\mathbf{k},\lambda'}^2 |E_{\mathbf{k},\lambda'}|^2 \frac{2\text{Im}(z^2)}{|z^2|^2 - 2\omega_{\mathbf{k},\lambda'} \text{Re}(z^2) + \omega_{\mathbf{k},\lambda'}^4} \right\}.
\end{aligned} \tag{A.60}$$

The poles of this function are the solutions to the following equation:

$$\begin{aligned}
0 &= (z^2 - \epsilon_{\mathbf{k}}^2) \prod_{\lambda'} |z^2 - \omega_{\mathbf{k},\lambda'}^2|^2 \\
&\quad + 8 \sum_{\lambda''} \omega_{\mathbf{k},\lambda''}^2 |E_{\mathbf{k},\lambda''}|^2 [\text{Im}(z^2) z - \epsilon_{\mathbf{k}} \text{Re}(z^2) + \omega_{\mathbf{k},\lambda''}^2 \epsilon_{\mathbf{k}}] \prod_{\lambda' \neq \lambda''} |z^2 - \omega_{\mathbf{k},\lambda'}^2|^2.
\end{aligned} \tag{A.61}$$

I cannot solve this equation analytically. It can, however, be solved numerically with the script in appendix B. Figure 3.10 shows the results.

## Appendix B - Numerical Script

The script below is written and executed in Matlab R2018b [14]. The value of  $T$  is determined by line number 29, and the composition and magnitude of  $\mathbf{T}$  are determined by line numbers 30 and 32, respectively. The propagated numerical floating point error is determined by executing the script as is, and comparing the results with those of the script executed with lines 46-51 uncommented. Figure 3.9 is obtained by uncommenting line numbers 195, 219, 220 and 241-244 (as well as choosing  $T = 0.01$  and  $\mathbf{T} = \mathbf{0}$ ). Figure 3.10 is obtained by uncommenting line numbers 183-190 and 247-258. The plot found on the title page is obtained by choosing  $T = 5$ ,  $\mathbf{T} = 5(1 + i, -2, 2 - 3i)$  and uncommenting line numbers 283-318.

```
1 %% Frequency_Calculations.m
2 %%
3 %% This script is a part of a degree project E in physics and it is
4 %% based upon the calculations in the thesis titled Magnon-Phonon
5 %% Coupling.
6 %%
7 %% Jacob Persson, Department of Physics and Astronomy, Uppsala
8 %% universitet, Uppsala, Sweden.
9 %%
10 %% 2018-11-14
11 %%
12 %%
13
14
15 % This is a calculation of the frequency spectrum of coupled magnons
16 % and phonons. A two-dimensional lattice with rectangular structure
17 % is assumed. The phonon polarization is restricted to one direction
18 % and only one ion at each lattice site is assumed. Further, the
19 % Dzyaloshinskii-Moriya coupling constant and the coupling constant
20 % of the interactions between magnons and phonons are assumed to be
21 % independent of the distance to the nearest neighbours. The phonon
22 % polarization is assumed to have a sinus dependence of the crystal
23 % momentum.
24
25 clear all
26 close all
27
28 % Parameters to vary:
29 T_s = 1; % Scalar coupling strength,
30 T_v = [1+1i, -2, 2-3*1i]; % Vector coupling composition,
31 %T_v = [5*1i, -3, 2];
```

```

32 T_v = 1*T_v/norm(T_v); % Vector coupling strength,
33
34 % Constants:
35 N = 10000; % 1/3 of the number of lattice sites,
36 a = [1, 1, 0]; % Lattice vector,
37 m = 1; % Ion mass,
38 K = 10^2*[1; 0; 0]; % K(lambda): Force constant of phonons;
39 xi_s = [1, 0, 0]; % xi(lambda): Phonon polarization strength;
40 L = nnz(xi_s); % Number of phonon modes,
41 S = 1/2; % Total spin of each ion,
42 J_para = sqrt(2); % Heisenberg coupling in the xy-plane,
43 J_perp = 1/sqrt(2); % Heisenberg coupling in the z-direction,
44 D_j = [1, 1i, 0]; % Strength of DM-interaction,
45 gamma = 1; % Gyromagnetic ratio of the ions.
46
47 %% Error analysis
48 % a(1) = a(1) + eps; a(2) = a(2) + eps; m = m + eps;
49 % K(1) = K(1) + eps; xi_s(1) = xi_s(1) + eps; S = S + eps;
50 % J_para = J_para + eps; J_perp = J_perp + eps; D_j(1) = D_j(1) + eps;
51 % gamma = gamma + eps; D_j(2) = D_j(2) + eps;
52
53 % Symmetry points
54 G1 = [0, 0, 0]; G2 = [2*pi/a(1), 2*pi/a(2), 0];
55 X = [pi/a(1), 0, 0]; M = X + [0, pi/a(2), 0];
56
57 % Momentum paths
58 G_M = [linspace(G1(1),X(1),N); ...
59         linspace(G1(2),X(2),N); linspace(G1(3),X(3),N)]';
60 X_M = [linspace(X(1),M(1),N); ...
61         linspace(X(2),M(2),N); linspace(X(3),M(3),N)]';
62 M_G = [linspace(M(1),G2(1),N); ...
63         linspace(M(2),G2(2),N); linspace(M(3),G2(3),N)]';
64
65 k = [G_M; X_M; M_G]; % Crystal momentum.
66 k_m = -k; % Negative crystal momentum
67
68 % R_delta(ion, r): Vector to all nearest neighbours, assuming that
69 % a(1) and a(2) are different from zero.
70 if a(1) == 0 || a(2) == 0
71     disp('First or second element of the lattice vector is zero')
72 end
73 R_delta = [a(1), a(2), a(3); a(1), a(2), 0; a(1), a(2), -a(3); ...
74            a(1), 0, a(3); a(1), 0, 0; a(1), 0, -a(3); ...
75            a(1), -a(2), a(3); a(1), -a(2), 0; a(1), -a(2), -a(3); ...
76            0, a(2), a(3); 0, a(2), 0; 0, a(2), -a(3); ...
77            0, 0, a(3); 0, 0, 0; 0, 0, -a(3); ...
78            0, -a(2), a(3); 0, -a(2), 0; 0, -a(2), -a(3); ...
79            -a(1), a(2), a(3); -a(1), a(2), 0; -a(1), a(2), -a(3); ...
80            -a(1), 0, a(3); -a(1), 0, 0; -a(1), 0, -a(3); ...

```

```

81     -a(1), -a(2), a(3); -a(1), -a(2), 0; -a(1), -a(2), -a(3)];
82 if a(3) == 0
83     R_delta(27,:) = []; R_delta(26,:) = []; R_delta(24,:) = [];
84     R_delta(23,:) = []; R_delta(21,:) = []; R_delta(20,:) = [];
85     R_delta(18,:) = []; R_delta(17,:) = []; R_delta(15,:) = [];
86     R_delta(14,:) = []; R_delta(13,:) = []; R_delta(12,:) = [];
87     R_delta(11,:) = []; R_delta(9,:) = []; R_delta(8,:) = [];
88     R_delta(6,:) = []; R_delta(5,:) = []; R_delta(3,:) = [];
89     R_delta(2,:) = [];
90 end
91 Z = numel(R_delta)/3; % Number of nearest neighbours.
92
93 % k-dependent coefficients
94 % Structure constants assuming 2 dimensional material:
95 C=0; C_m=0; % C(k) and C(-k), respectively.
96 for lambda=1:length(R_delta(:,1))
97     C = C + exp(-1i*k(:,1)*R_delta(lambda,1)) ...
98         + exp(-1i*k(:,2)*R_delta(lambda,2));
99     C_m = C_m + exp(-1i*k_m(:,1)*R_delta(lambda,1)) ...
100         + exp(-1i*k_m(:,2)*R_delta(lambda,2));
101 end
102 if max(imag(C)) > 1e-10 || max(imag(C_m)) > 1e-10
103     disp('Imaginary C')
104 end
105 C = real(C); C_m = real(C_m);
106 D = (1/Z)*D_j.*C; % D(k),
107 D_m = (1/Z)*D_j.*C_m; % D(-k),
108 T_sk = (1/Z)*T_s.*C; % Scalar-coefficient,
109 T_vk = (1/Z)*T_v.*C; % Vector-coefficient,
110 % assuming that D, T_s och T_v is independent of the displacement of
111 % the ions
112
113 % xi(k, xi): Phonon polarization, assuming sinus dependence.
114 xi = xi_s.*sin(sum(k.*a, 2));
115
116 % omega(k,lambda): Free phonon frequency.
117 omega = zeros(N*3,L);
118 for j=1:L
119     omega(:,j) = sqrt((4*K(j)/m)*sin(sum(k.*a, 2)/2).^2);
120 end
121
122 % epsilon(k): Free magnon frequency.
123 epsilon = 2*S*J_para*Z*ones(length(k(:,1)),1) ...
124     - 2*S*J_perp*C - sqrt(2)*1i*S*Z*D(:,3);
125 epsilon_m = 2*S*J_para*Z*ones(length(k_m(:,1)),1) ...
126     - 2*S*J_perp*C_m - sqrt(2)*1i*S*Z*D_m(:,3); % epsilon(-k).
127
128 % E(k, lambda): Mixed magnon-phonon frequency.
129 E = zeros(length(k),L);

```

```

130 for lambda=1:L
131     E(:,lambda) = gamma* sqrt(S)*Z./(2*sqrt(m)*sqrt(omega(:,1))) .*...
132     (T_sk.*(-1i*xi(:,1,1) + xi(:,2,1)) ...
133     + T_vk(:,1).*xi(:,3,1) - 1i*T_vk(:,2).*xi(:,3,1) ...
134     - T_vk(:,3).*xi(:,1,1) + 1i*T_vk(:,3).*xi(:,2,1));
135 end
136 E(isnan(E))=0; % Replace undefined values with zero
137
138 % E_epsilon(k, lambda, lambda') and E_-(k, lambda, lambda')
139 E_epsilon = zeros(length(k), L, L); E_minus = zeros(length(k), L, L);
140 for lambda=1:L
141     E_epsilon(:, :, lambda) = E.*conj(E(:, lambda)).*epsilon ...
142     + conj(E).*E(:, lambda).*epsilon_m;
143     E_minus(:, :, lambda) = E.*conj(E(:, lambda)) - conj(E).*E(:, lambda);
144 end
145
146 % a(k, lambda): Coefficients for the equation of the poles of Green's
147 % function
148 a_0 = omega.^2.*epsilon.*epsilon_m - 2*omega.*sum(E_epsilon,3);
149 a_1 = - omega.^2.*(epsilon-epsilon_m) - 2*omega.*sum(E_minus,3);
150 a_2 = - omega.^2 - epsilon.*epsilon_m;
151 a_3 = epsilon - epsilon_m;
152
153 % Parameters for the solution of the coupled frequencies
154 % p(k, lambda) and q(k, lambda)
155 p = a_2 - (3/8)*a_3.^2;
156 q = (1/8)*a_3.^3 - (1/2)*a_3.*a_2 + a_1;
157 % Delta_0(k, lambda) and Delta_1(k, lambda):
158 Delta_0 = a_2.^2 - 3*a_3.*a_1 + 12*a_0;
159 Delta_1 = 2.*a_2.^3 - 9*a_3.*a_2.*a_1 + 27*a_3.^2.*a_0 ...
160 + 27*a_1.^2 - 72*a_2.*a_0;
161 % Q(k, lambda) and S(k, lambda):
162 Q = ( (Delta_1 - sqrt(Delta_1.^2 - 4*Delta_0.^3))/2 ).^(1/3);
163 S = (1/2)*sqrt(-(2/3)*p + (1/3)*(Q + Delta_0./Q));
164
165 % Solutions
166 z_1 = -(1/4)*a_3 + S + (1/2)*sqrt(-4*S.^2 - 2*p - q./S);
167 z_2 = -(1/4)*a_3 + S - (1/2)*sqrt(-4*S.^2 - 2*p - q./S);
168 z_3 = -(1/4)*a_3 - S + (1/2)*sqrt(-4*S.^2 - 2*p + q./S);
169 z_4 = -(1/4)*a_3 - S - (1/2)*sqrt(-4*S.^2 - 2*p + q./S);
170
171 % If sum(E_minus)=0 and \epsilon_k = \epsilon_{-k} , it is enough to
172 % look at the absolute values of the real and the imaginary parts of
173 % solutions 1 and 3.
174 if sum(sum(max(E_minus))) > 1e-10
175     disp('E_minus is not 0')
176 elseif max(abs(epsilon-epsilon_m)) > 1e-10
177     disp('\epsilon_k - \epsilon_{-k} is not equal to 0')
178 end

```

```

179 | x_1 = abs(real(z_1)); y_1 = abs(imag(z_1));
180 | x_2 = abs(real(z_2)); y_2 = abs(imag(z_2));
181 |
182 | %% Magnon equation if epsilon=epsilon_m
183 | % fun = @(z)(magnons(z, omega, epsilon, E));
184 | % options = optimset('MaxFunEvals', 40000, 'TolFun', 1e-10);
185 | % x01 = x_1+0.1;
186 | % x02 = x_2-0.1;
187 | % zsol1 = fsolve(fun, x01);
188 | % zsol2 = fsolve(fun, x02);
189 | % xsol1 = abs(zsol1);
190 | % xsol2 = abs(zsol2);
191 |
192 | %% Plots for lambda = 1
193 | k_p = [sum(G_M,2); sum(X_M,2); sum(M_G,2)]; % Plotted momentum.
194 | ax = [ 0 k_p(end)+1 0 max(max(omega))+2]; % Axis
195 | %ax = [0 X(1)/100 0 0.001]; % Axis if Ts = 0.01 and Tv=0
196 | f1 = figure('Position', [1360, 560, 560, 420*0.745]);
197 | h3 = plot(k_p, omega(:,1), 'b—', k_p, epsilon(:,1), 'r—', ...
198 |         k_p, x_1(:,1), 'c', k_p, x_2(:,1), 'm'); % Real parts
199 | hold on
200 |
201 | % Imaginary parts
202 | tp = 0.3; % Transparency
203 | h1 = area(k_p, [x_1(:,1)-y_1(:,1), 2*y_1(:,1)]);
204 | h1(1).FaceColor = 'none'; h1(1).LineStyle = 'none';
205 | h1(2).EdgeColor = 'none'; h1(2).FaceColor = 'c';
206 | h1(2).FaceAlpha = tp;
207 | hold on
208 | h2 = area(k_p, [x_2(:,1)-y_2(:,1), 2*y_2(:,1)]);
209 | h2(1).FaceColor = 'none'; h2(1).LineStyle = 'none';
210 | h2(2).EdgeColor = 'none'; h2(2).FaceColor = 'm';
211 | h2(2).FaceAlpha = tp;
212 |
213 | % Title and axes
214 | title('Frequency Spectrum')
215 | xlabel('Symmetry Points')
216 | names = {'\Gamma'; 'X'; 'M'; '\Gamma'};
217 | set(gca, 'xtick', [sum(G1), sum(X), sum(M), sum(G2)], ...
218 |         'xticklabel', names)
219 | % names = {'\Gamma'; 'X/200'}; % at very small coupling
220 | % set(gca, 'xtick', [sum(G1), sum(X)/200], 'xticklabel', names)
221 | ylabel('Frequency')
222 | set(gca, 'ytick', [])
223 | axis(ax)
224 |
225 | % Legend
226 | [~, h_legend] = legend('\omega', '\epsilon', 'x_1', 'x_2', 'y_1', ...
227 |                       'y_2', 'Location', 'northeast');

```

```

228 PatchInLegend = findobj(h_legend, 'type', 'patch');
229 set(PatchInLegend(1), 'FaceColor', 'c');
230 set(PatchInLegend(2), 'FaceColor', 'm');
231 set(PatchInLegend(2), 'FaceAlpha', tp);
232 set(PatchInLegend(1), 'FaceAlpha', tp);
233
234 % Display values of the coupling strength
235 txt_T = [ 'T = ', num2str(T_s, '%.2f'), ', ', '\bfT = (', ...
236          num2str(T_v(1), '%.2f'), ', ', num2str(T_v(2), '%.2f'), ', ', ...
237          num2str(T_v(3), '%.2f'), ') '];
238 text(ax(1)+0.3, ax(4)-1, txt_T)
239
240 % % Display values of the coupling strength at very small coupling
241 % txt_T_s = [ 'T_s = ', num2str(T_s, '%.2f'), ', ', 'T_v = (', ...
242 % num2str(T_v(1), '%.2f'), ', ', num2str(T_v(2), '%.2f'), ', ', ...
243 % num2str(T_v(3), '%.2f'), ') '];
244 % text(ax(1)+0.001, ax(4)-0.0001, txt_T_s)
245
246 % % Magnons plot
247 % f2 = figure('Position', [1360, 560, 560, 420*0.745]);
248 % plot(k_p, omega(:,1), 'b--', k_p, epsilon(:,1), 'r--', ...
249 %      k_p, xsol1, 'c', k_p, xsol2, 'm')
250 % title('Frequency Spectrum')
251 % xlabel('Symmetry Points')
252 % names = {'\Gamma'; 'X'; 'M'; '\Gamma'};
253 % set(gca, 'xtick', [sum(G1), sum(X), sum(M), sum(G2)], ...
254 %      'xticklabel', names)
255 % legend('\omega', '\epsilon', 'sol1', 'sol2', 'Location', '
256 %         northeast');
257 % ylabel('Frequency')
258 % set(gca, 'ytick', [])
259 % axis(ax)
260
261 % Removing figure margin
262 ax2 = gca;
263 outerpos = ax2.OuterPosition;
264 ti = ax2.TightInset;
265 left = outerpos(1) + ti(1);
266 bottom = outerpos(2) + ti(2);
267 ax2_width = outerpos(3) - ti(1) - ti(3);
268 ax2_height = outerpos(4) - ti(2) - ti(4);
269 ax2.Position = [left bottom ax2_width ax2_height];
270
271 % Control plots of Q and S: the solutions might not be true if Q = 0
272 % or S = 0.
273 f3 = figure('Position', [1360, 60, 560, 420]);
274 plot(k_p, abs(Q(:,1)), k_p, 4*abs(S(:,1)).^2)
275 title('Q_x and 4S_x^2')
276 xlabel('Symmetry Points')

```

```

276 names = { '\Gamma'; 'X'; 'M'; '\Gamma' };
277     set(gca, 'xtick', [sum(G1), sum(X), sum(M), sum(G2)], ...
278         'xticklabel', names)
279 ylabel('Magnitude')
280 legend('Q_x', '4S_x^2')
281
282 %% Front page plot
283 %% figure
284 %% Real parts
285 % h4 = plot(k_p, omega(:,1), 'b--', k_p, epsilon(:,1), 'r--', ...
286 %     k_p, x_1(:,1), 'c', k_p, x_2(:,1), 'm', ...
287 %     k_p, zeros(length(k_p),1), 'w');
288 % hold on
289 %
290 %% Imaginary parts
291 % tp = 0.3; % Transperancy
292 % h5 = area(k_p, [x_1(:,1)-y_1(:,1), 2*y_1(:,1)]);
293 % h5(1).FaceColor = 'none'; h5(1).LineStyle = 'none';
294 % h5(2).EdgeColor = 'none'; h5(2).FaceColor = 'c';
295 % h5(2).FaceAlpha = tp;
296 % hold on
297 % h6 = area(k_p, [x_2(:,1)-y_2(:,1), 2*y_2(:,1)]);
298 % h6(1).FaceColor = 'none'; h6(1).LineStyle = 'none';
299 % h6(2).EdgeColor = 'none'; h6(2).FaceColor = 'm';
300 % h6(2).FaceAlpha = tp;
301 %
302 %% Removing figure margin
303 % ax4 = gca;
304 % outerpos = ax4.OuterPosition;
305 % ti = ax4.TightInset;
306 % left = outerpos(1) + ti(1);
307 % bottom = outerpos(2) + ti(2);
308 % ax4_width = outerpos(3) - ti(1) - ti(3);
309 % ax4_height = outerpos(4) - ti(2) - ti(4);
310 % ax4.Position = [left bottom ax4_width ax4_height];
311 %
312 % ax3 = [ 0 k_p(end) 0 max(max(x_1))]; % Axis
313 % axis(ax3)
314 % box off
315 % axis off
316 % set(gca, 'visible', 'off')
317 % set(gcf, 'color', [1 1 1])
318 %% axes('Color', 'none', 'XColor', 'none')

```